THE MINOR PLANET BULLETIN

BULLETIN OF THE MINOR PLANETS SECTION OF THE ASSOCIATION OF LUNAR AND PLANETARY OBSERVERS

VOLUME 50, NUMBER 2, A.D. 2023 APRIL-JUNE 114.

CALL FOR VOLUNTEER TO MAINTAIN THE LIGHTCURVE DATABASE

Frederick Pilcher
4438 Organ Mesa Loop
Las Cruces, NM 88011 USA
fpilcher35@gmail.com

Brian D. Warner
446 Sycamore Ave.
Eaton, CO 80615
brian@MinPlanObs.org

The Lightcurve Database (LCDB) is a valuable resource to the Minor Planet Community. The position of Lightcurve Database Manager is soon to be open. Volunteers for this position are encouraged to make known their interest and willingness to serve, so that the LCDB may continue to grow as a resource supporting new science on into the future. A summary description of the duties and requirements follow.

The ALPO Minor Planets Section is seeking a dedicated, long-term volunteer to assume the duties of maintaining the Lightcurve Database (LCDB; Warner et al., 2009, *Icarus* **202**, 134-146) since the current manager, Brian Warner, is retiring. The specific duties consist of monitoring those sources that publish, online or in print form, new rotational parameters of asteroids, including lightcurves, rotation periods, amplitudes, orbital as well as rotational data for binary and suspected binary asteroids, evidence of tumbling behavior, new or revised data on H, G, and when available G1 and G2. Also included are taxonomic classifications and, when available, color indexes. References to the sources of these data are required. At least one updated version of the each of the several files in the current LCDB each year should be produced, usually in February, for submission to the ITA, St. Petersburg, Russia, and to NASA's Planetary Data System.

LCDB co-authors Warner and Alan Harris have offered to assist the new manager during a transition period. Inquiries and indications of interest should be directed to: brian@MinPlanObs.org

REVISED SYNODIC ROTATION PERIOD FOR ASTEROID 2243 LONNROT

Alessandro Marchini, Leonardo Cavaglioni, Chiara A. Privitera
Astronomical Observatory, DSFTA - University of Siena (K54)
Via Roma 56, 53100 - Siena, ITALY
marchini@unisi.it

Riccardo Papini, Fabio Salvaggio
Wild Boar Remote Observatory (K49)
San Casciano in Val di Pesa (FI), ITALY

(Received: 2022 December 15)

Photometric observations of the asteroid 2243 Lonnrot were conducted in order to obtain a more accurate estimate of the synodic rotation period than the one published by the authors in 2021. During this more favorable apparition we found P = 3.681 ± 0.001 h, A = 0.10 ± 0.02 mag.

CCD photometric observations of the asteroid 2243 Lonnrot were carried out in October 2022 at the Astronomical Observatory of the University of Siena (K54), a facility inside the Department of Physical Sciences, Earth and Environment (DSFTA, 2022). We used a 0.30m *f*/5.6 Maksutov-Cassegrain telescope, SBIG STL-6303E NABG CCD camera, and clear filter; the pixel scale was 2.30 arcsec when binned at 2×2 pixels and all exposures were 300 seconds.

Data processing and analysis were done with *MPO Canopus* (Warner, 2018). All images were calibrated with dark and flat-field frames and the instrumental magnitudes converted to R magnitudes using solar-colored field stars from a version of the CMC-15 catalogue distributed with *MPO Canopus*. Table I shows the observing circumstances and results.

The authors had observed this asteroid in 2021 while it was crossing by serendipity the field where they were observing another target. Since those measurements were very few and the published solution not very precise (Marchini et al., 2021), we decided to observe the asteroid 2243 Lonnrot again during this much more favorable apparition of October 2022.

2243 Lonnrot (1941 SA1) was discovered on 1941 September 25 by Y. Vaisala at Turku and named after Elias Lonnrot (1802-1884), a physician in Kajaani and later professor of the Finnish language in Helsinki. [Ref: Minor Planet Circ. 7944] This main-belt asteroid is a member of the Flora dynamical family with a semi-major axis of 2.248 AU, eccentricity 0.197, inclination 6.845°, and an orbital period of 3.37 years. Its absolute magnitude is H = 12.59 (JPL, 2022). The WISE/NEOWISE satellite infrared radiometry survey (Masiero et al., 2014) found a diameter D = 8.628 ± 0.113 km using an absolute magnitude H = 12.8.

In this favorable apparition, observations were conducted over six nights and collected 336 data points. The period analysis shows a clear bimodal solution for the rotational period of P = 3.681 ± 0.001 h with an amplitude A = 0.10 ± 0.02 mag.

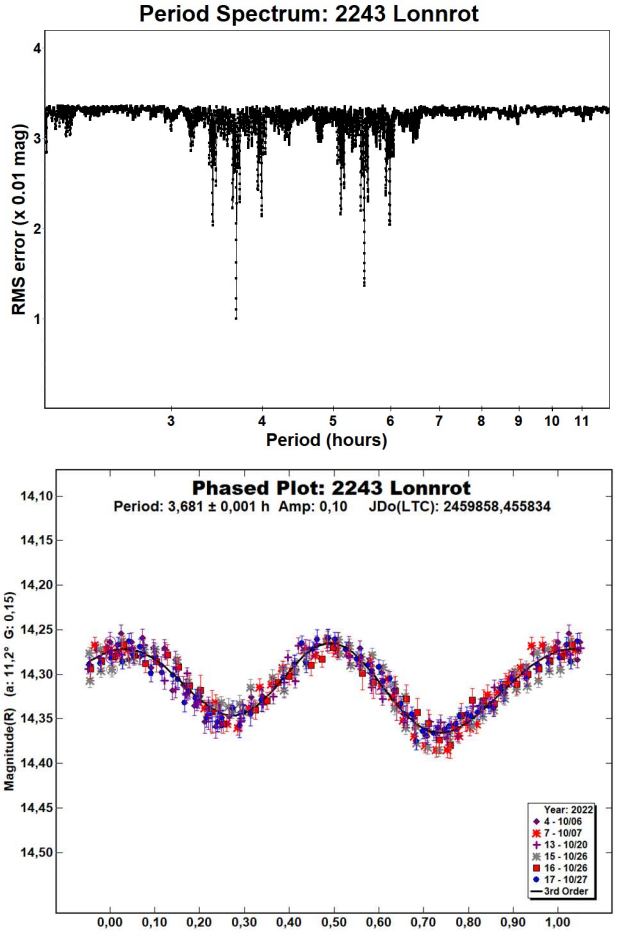

Acknowledgements

Leonardo Cavaglioni and Chiara Angelica Privitera, students of the course in Physics and Advanced Technologies at the University of Siena, observed the asteroid 2243 Lonnrot during their internship in 2021. Although they had already finished their training, they wanted to attend the observations in this apparition too. Minor Planet Circulars (MPCs) are published by the International Astronomical Union's Minor Planet Center.
https://www.minorplanetcenter.net/iau/ECS/MPCArchive/MPCArchive_TBL.html

References

DSFTA (2022). Dipartimento di Scienze Fisiche, della Terra e dell'Ambiente - Astronomical Observatory. *https://www.dsfta.unisi.it/en/research/labs/astronomical-observatory*

Harris, A.W.; Young, J.W.; Scaltriti, F.; Zappala, V. (1984). "Lightcurves and phase relations of the asteroids 82 Alkmene and 444 Gyptis." *Icarus* **57**, 251-258.

JPL (2022). Small-Body Database Browser. *http://ssd.jpl.nasa.gov/sbdb.cgi#top*

Marchini, A.; Cavaglioni, L.; Privitera, C.A.; Papini, R.; Salvaggio, F. (2021). "Rotation Period Determination for Asteroids 2243 Lonnrot, (10859) 1995 GJ7, (18640) 1998 EF9 and (49483) 1999 BP13." *Minor Planet Bulletin* **48**, 206-208.

Masiero, J.R.; Grav, T.; Mainzer, A.K.; Nugent, C.R.; Bauer, J.M.; Stevenson, R.; Sonnett, S. (2014). "Main-belt Asteroids with WISE/NEOWISE: Near-infrared Albedos." *Astrophys. J.* **791**, 121.

Warner, B.D.; Harris, A.W.; Pravec, P. (2009). "The Asteroid Lightcurve Database." *Icarus* **202**, 134-146. Updated 2022 Sep. *http://www.minorplanet.info/lightcurvedatabase.html*

Warner, B.D. (2018). MPO Software, MPO Canopus v10.7.7.0. Bdw Publishing. *http://minorplanetobserver.com*

Number	Name	2022/mm/dd	Phase	L_{PAB}	B_{PAB}	Period(h)	P.E.	Amp	A.E.	Grp
2243	Lonnrot	10/05-10/27	*11.3,2.7	30	1	3.681	0.001	0.10	0.02	FLOR

Table I. Observing circumstances and results. The first line gives the results for the primary of a binary system. The second line gives the orbital period of the satellite and the maximum attenuation. The phase angle is given for the first and last date. If preceded by an asterisk, the phase angle reached an extrema during the period. L_{PAB} and B_{PAB} are the approximate phase angle bisector longitude/latitude at mid-date range (see Harris et al., 1984). Grp is the asteroid family/group (Warner et al., 2009).

ROTATION PERIOD DETERMINATION FOR ASTEROID (11671) 1998 BG4

Alessandro Marchini, Riccardo Papini
Astronomical Observatory, DSFTA - University of Siena (K54)
Via Roma 56, 53100 - Siena, ITALY
marchini@unisi.it

(Received: 2023 January 9)

Photometric observations of the inner main-belt asteroid (11671) 1998 BG4 were conducted in order to determine its synodic rotation period. We found P = 4.630 ± 0.006 h, A = 0.83 ± 0.15 mag.

CCD photometric observations of the inner main-belt asteroid (11671) 1998 BG4 were carried out in October 2022 at the Astronomical Observatory of the University of Siena (K54), a facility inside the Department of Physical Sciences, Earth and Environment (DSFTA, 2023). We used a 0.30-m *f*/5.6 Maksutov-Cassegrain telescope, SBIG STL-6303E NABG CCD camera, and clear filter; the pixel scale was 2.30 arcsec when binned at 2×2 pixels and all exposures were 300 seconds.

Data processing and analysis were done with *MPO Canopus* (Warner, 2018). All images were calibrated with dark and flat-field frames and the instrumental magnitudes converted to R magnitudes using solar-colored field stars from a version of the CMC-15 catalogue distributed with *MPO Canopus*. Table I shows the observing circumstances and results.

A search through the asteroid lightcurve database (LCDB; Warner et al., 2009) indicates that our result may be the first reported lightcurve observations and results for this asteroid.

(11671) 1998 BG4 was discovered on 1998 January 21 at Nachi-Katsuura by Y. Shimizu and T. Urata. It is an inner main-belt asteroid with a semi-major axis of 2.392 AU, eccentricity 0.148, inclination 1.118°, and an orbital period of 3.70 years. Its absolute magnitude is H = 14.87 (JPL, 2023). On the asteroid lightcurve database (Warner et al., 2009) we found a diameter D = 3.35 km using an absolute magnitude H = 14.74.

Observations were conducted over two nights and collected 162 data points. In the first session we found (11671) 1998 BG4 by serendipity in the same field of another asteroid. It was quite faint for our instrumentation, but the large amplitude permitted us to perform a period analysis that shows a solution of P = 4.630 ± 0.006 h with an amplitude A = 0.83 ± 0.15 mag as the most likely bimodal solution for its rotational period.

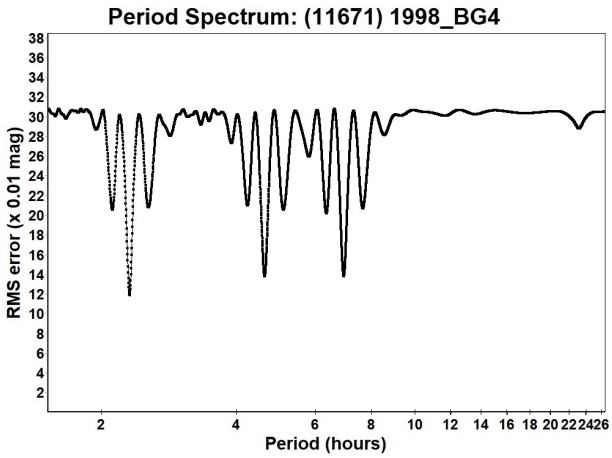

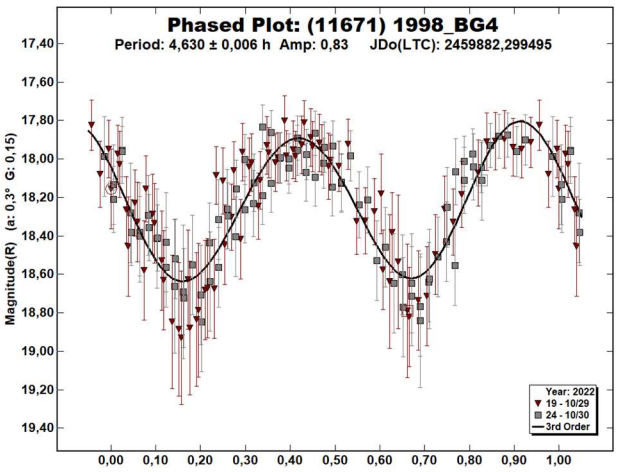

References

DSFTA (2023). Dipartimento di Scienze Fisiche, della Terra e dell'Ambiente - Astronomical Observatory. *https://www.dsfta.unisi.it/en/research/labs/astronomical-observatory*

Harris, A.W.; Young, J.W.; Scaltriti, F.; Zappala, V. (1984). "Lightcurves and phase relations of the asteroids 82 Alkmene and 444 Gyptis." *Icarus* **57**, 251-258.

JPL (2023). Small Body Database Search Engine. *https://ssd.jpl.nasa.gov*

Warner, B.D.; Harris, A.W.; Pravec, P. (2009). "The Asteroid Lightcurve Database." *Icarus* **202**, 134-146. Updated 2021 Dec. *https://minplanobs.org/mpinfo/php/lcdb.php*

Warner, B.D. (2018). MPO Software, MPO Canopus v10.7.7.0. Bdw Publishing. *http://bdwpublishing.com/*

Number	Name	2022/mm/dd	Phase	L_{PAB}	B_{PAB}	Period(h)	P.E.	Amp	A.E.	Grp
11671	1998 BG4	10/29-10/31	*0.4,0.2	37	0	4.630	0.006	0.83	0.15	MB-I

Table I. Observing circumstances and results. The phase angle is given for the first and last date. If preceded by an asterisk, the phase angle reached an extrema during the period. L_{PAB} and B_{PAB} are the approximate phase angle bisector longitude/latitude at mid-date range (see Harris et al., 1984). Grp is the asteroid family/group (Warner et al., 2009).

THE LIGHTCURVE AND ROTATION PERIOD OF 128 NEMESIS 2022 AUGUST THROUGH OCTOBER

Frederick Pilcher
Organ Mesa Observatory (G50)
4438 Organ Mesa Loop
Las Cruces, NM 88011 USA
fpilcher35@gmail.com

Julian Oey
Blue Mountains Observatory (Q68)
94 Rawson Pde. Leura, NSW, AUSTRALIA

(Received: 2022 November 19)

A synodic rotation period of 38.922 hours and amplitude 0.09 magnitudes with a somewhat irregular lightcurve is found for 128 Nemesis at its 2022 August-October apparition.

The first published lightcurve of 128 Nemesis was by Scaltriti et al. (1979), who found a period of 39 hours, amplitude 0.10 magnitudes, celestial longitude 78º, with a somewhat unsymmetric bimodal lightcurve.

This author (Pilcher, 2015) was unable to fit his observations from 2015 Jan. 5 - Apr 14, celestial longitude near 131º, to a period near 39 hours and published for that longitude a period of 77.81 hours, amplitude 0.08 magnitudes that had a good fit to a slightly unsymmetic bimodal lightcurve.

Colazo et al. (2022) found a period 38.907 hours, amplitude 0.14 magnitudes, celestial longitude near 245º, with a good fit to an unsymmetric bimodal lightcurve.

Vernazza et al. (2021) obtained disk resolved images of 128 Nemesis in the year 2018 with the SPHERE (Spectro-Polarimetric High contrast Exoplanet Research) instrument on the 8-meter VLT at the European Southern Observatory. They found a sidereal rotation period of 38.9325 ± 0.0001 hours and a rotational pole located at celestial longitude 313º, celestial latitude -19º.

Being now the only author who claimed a period twice as great as near 38.9 hours, this author (Pilcher, 2022) re-examined his data from the year 2015. By adjusting the zero points of many sessions a few x 0.01 magnitudes, he found a fit to period 38.91 hours, amplitude 0.05 magnitudes with one asymmetric maximum and minimum per rotational cycle that was almost as good as to the original 77.81 hours. The two halves of a split halves plot to 77.81 hours were nearly identical. While the data near celestial longitude 131º are ambiguous between 38.91 hours and 77.81 hours, the overlap of the split halves plot led the author to prefer the 38.91-hour period.

In the next issue of the *Minor Planet Bulletin,* Ferrais et al. (2022) published a rotation period of 38.904 hours, amplitude 0.17 magnitudes with a slightly unsymmetric bimodal lightcurve near celestial longitude 235º.

In 2022 September 128 Nemesis came to opposition at brightest magnitude 10.6, declination -12º near perihelion. First author Pilcher invited second author Oey, who kindly accepted his invitation, to collaborate from the southern hemisphere. The observing strategy was to sample the full double period near 77.8 hours. A good overlap, including small irregularities, of both halves of the split halves lightcurve would constitute a robust resolution of the ambiguity in favor of near 38.9 hours.

First author Pilcher used a 0.35m f/10 Meade LX200 GPS SCT, SBIG STL-1001E CCD, clear filter, exposure times limited to 20-30 seconds by the brightness of the target. Second author Oey used a 0.35m f/5.9 SCT, SBIG ST-8XME CCD, clear filter, 60 second exposure times. Both observers were hampered by an abundance of cloudy nights, but between them sampled the entire 38.9-hour lightcurve and all but one six-hour segment of the 77.8-hour lightcurve.

A total of 22 sessions were obtained in the interval 2022 Aug. 22 to Oct. 29 with the target near celestial longitude 354º. The data make an excellent fit to a somewhat irregular monomodal lightcurve with period 38.922 ± 0.003 hours, amplitude 0.09 ± 0.01 magnitudes. When phased to 77.850 hours, the split halves diagram shows that both halves of the lightcurve fit closely except for a missing 6-hour segment in the uniformly rising part of the lightcurve. Even without the other fully compatible results described in the next paragraph, the evidence in favor of the shorter period is strong.

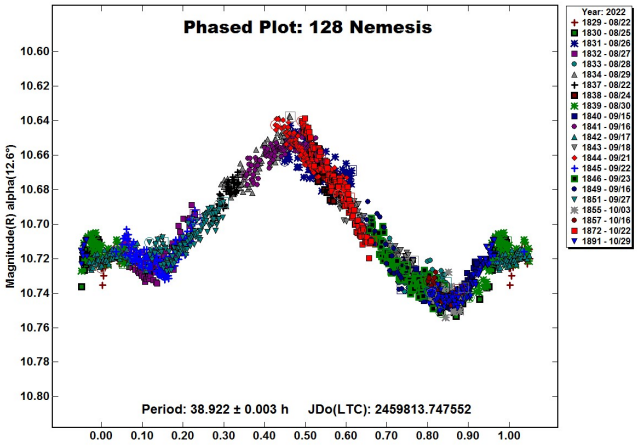

Number	Name	yyyy/mm/dd	Phase	L_{PAB}	B_{PAB}	Period(h)	P.E	Amp	A.E.
128	Nemesis	2022/08/22-10/29	*12.6 - 17.8	354	-8	38.922	0.003	0.09	0.01

Table I. Observing circumstances and results. The phase angle is given for the first and last date, where the * indicates that a minimum value was reached between these dates. L_{PAB} and B_{PAB} are the approximate phase angle bisector longitude and latitude at mid-date range (see Harris et al., 1984).

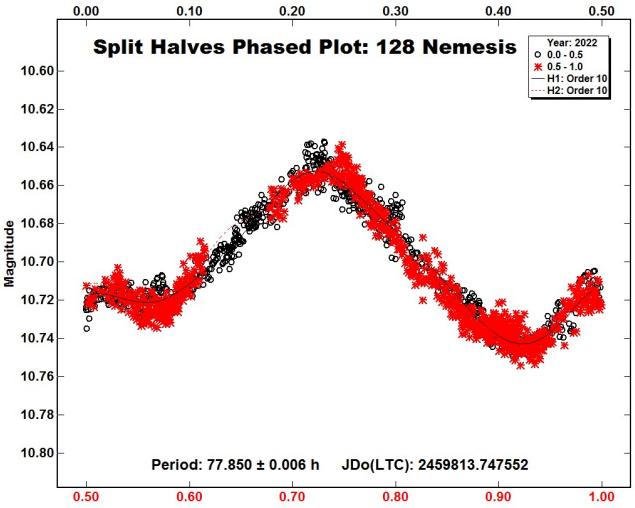

Five dense lightcurves well distributed around the sky, and disk resolved images from adaptive optics, are all compatible with a period very close to the 38.922 hours found in this study. The period ambiguity has been resolved and a period near 38.922 hours can be considered secure; bringing a match to the conclusions reached through independent techniques.

References

Colazo, M.; Morales, M.; Chapman, C.; Garcia, A.; Santos, F.; Melia, R.; Suarez, N.; Stechina, A.; Scotta, D.; Martini, M.; Santucho, M.; Moreschi, A.; Wilberger, A.; Mottino, A.; Bellocchio, E.; Quinones, C.; Speranza, T.; Llanos, R.; Altuna, L; Caballero, M.; Romero, F.; Galarza, C.; Colazo, C. (2022) "Photometry and light curve analysis of eight asteroids by GORA's observatories." *Minor Planet Bull.* **49**, 48-50.

Ferrais, M.; Vernazza, P.; Jorda, L; Jehin, E.; Porzuelos, F.J.; Manfroid, J.; Moulane, Y.; Barkaoui, K.; Benkhaldoun, Z. (2022). "Photometry of 25 large main-belt asteroids with Trappist-North and -South." *Minor Planet Bull.* **49**, 307-313.

Harris, A.W.; Young, J.W.; Scaltriti, F.; Zappala, V. (1984). "Lightcurves and phase relations of the asteroids 82 Alkmene and 444 Gyptis." *Icarus* **57**, 251-258.

Pilcher, F. (2015). "New photometric observations of 128 Nemesis, 249 Ilse, and 279 Thule." *Minor Planet Bull.* **42**, 190-192.

Pilcher, F. (2022). "The rotation period of 128 Nemesis is re-examined." *Minor Planet Bull.* **49**, 162-163.

Scaltriti, F.; Zappala, V.; Schober, H.J. (1979). "The rotations of 128 Nemesis and 393 Lampetia: The longest known periods to date." *Icarus* **37**, 133-141.

Vernazza, P. and 66 co-authors. (2021). "VLT/SPHERE imaging survey of the largest main-belt asteroids: Final results and synthesis." *Astron. Astrophys.* **A56**.

ROTATIONAL PERIOD DETERMINATION AND TAXONOMIC CLASSIFICATION FOR ASTEROID (1399) TENERIFFA

Massimiliano Mannucci, Nico Montigiani
Associazione Astrofili Fiorentini
Osservatorio Astronomico Margherita Hack (A57)
Florence, ITALY
info@astrofilifiorentini.it

Paolo Aldinucci
Associazione Astrofili Fiorentini
Osservatorio Astronomico Orciatico
Orciatico (PI), ITALY

(Received: 2022 December 20)

CCD photometric observations of one main-belt asteroid was obtained in order to measure its rotation period and define their taxonomic class. These measures were performed on October 2022 using the instrumentation available at the two observatories.

CCD photometric observations of (1399) Teneriffa were carried out in 2022 October at the Osservatorio Astronomico Margherita Hack (A57) and Osservatorio Astronomico Orciatico. The Osservatorio Astronomico Margherita Hack is equipped with a 0.35-m f/8.25 Schmidt-Cassegrain telescope, a SBIG ST10 XME ccd camera and Johnson-Cousins BVRc photometric filters. The pixel scale was 1 arcsec when binned at 2×2 pixels. The Osservatorio Astronomico Orciatico is equipped with a 0.35-m f/7.4 Schmidt-Cassegrain telescope and a SBIG ST1603 XME ccd camera with Johnson-Cousins BVRcIc photometric filters, having the pixel scale of 1.41 arcsec in bin 2×2. Data processing and analysis were done with *MPO Canopus* (Warner, 2021). All the images were calibrated with dark and flat field frames using *Astroart 6.0*. and Ricerca (Warner, 2006). Table I shows the observing circumstances and results.

1399 Teneriffa was discovered on 1936 Aug 23 at Heidelberg by the german astronomer Karl Wilhelm Reinmuth. The asteroid takes its name from the island of Tenerife, the largest of the Canary Islands. It was chosen from the list of lightcurve photometry opportunities on the *Minor Planet Bulletin* (Warner et al., 2022). It is a main-belt asteroid with a semi-major axis of 2.21576 AU, eccentricity 0.1663, inclination 6.507°, and an orbital period of 3.298 years. Its absolute magnitude is H = 13.62 (JPL, 2022; MPC, 2022). Our observations were conducted in two different steps. The first step consisted in collecting 209 data points during 4 nights across 18/10/2022 and 29/10/2022. The period analysis shows a bimodal solution for the rotational period with P = 2.69247 ± 0.00009h and an amplitude A = 0.15 mag, AE = 0.01 mag (Figure 1). The split-halves plot (Figure 2) let us solve the potential ambiguity between monomodal and bimodal solution by showing that the two halves of the 2.69247 h solution are not well superimposable even if very similar. This makes the bimodal solution much more probable. Moreover, we consulted the asteroid lightcurve database (LCDB; Warner et al., 2009) and we found one previous calculated period: P = 2.692 (Waszczak, 2015). The period we found seems to be in very good agreement with the previous mentioned period.

Number	Name	2022 mm/dd	Pts	Phase	L_{PAB}	B_{PAB}	Period(h)	P.E.	Amp	A.E.	Grp
1399	Teneriffa	10/18-10/29	209	5.87-7.53	28,9	-7.55	2.6925	±0.0001	0.15	0.01	MBA

Table I. Observing circumstances and results. Pts is the number of data points. The phase angle is given for the first and last date. L_{PAB} and B_{PAB} are the approximate phase angle bisector longitude and latitude at mid-date range (see Harris et al., 1984). Grp is the asteroid family/group (Warner et al., 2009).

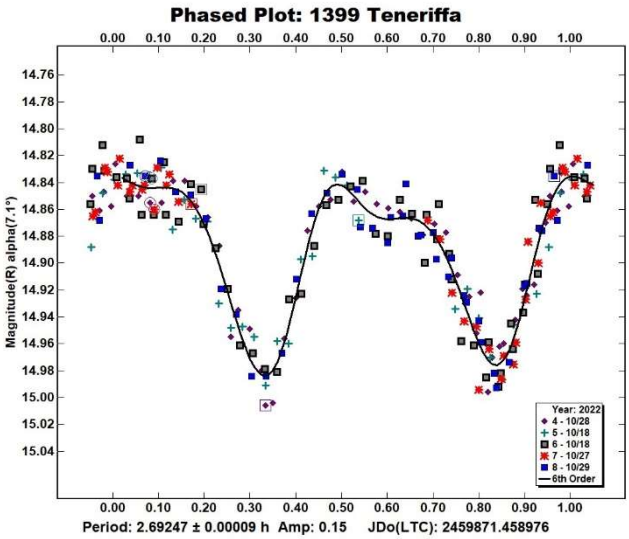

Figure 1. Phased lightcurve of 1399 Teneriffa.

In the second step we collected further 39 data points in one night using filters B, V, Rc and Ic. This allowed us to determine the color indexes (B-V) = 0.81 +/- 0.025, (V-Rc) = 0.495 +/- 0.015 and (Rc-Ic) = 0.405 +/- 0.015 (Figure 3). These values are consistent with a medium albedo S-type taxonomic class (Shevchenko and Lupishko, 1998), and the albedo value of 0.227 reported in the bibliography (JPL, 2022) is also consistent with a taxonomic class of type S (Shevchenko and Lupishko, 1998).

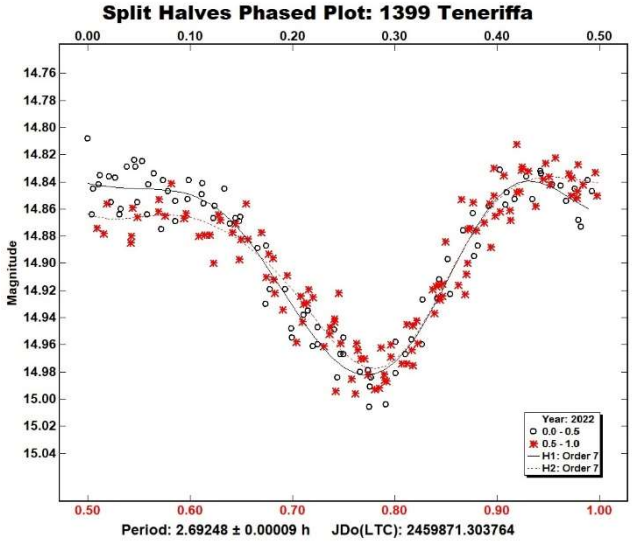

Figure 2. Split halves lightcurve of 1399 Teneriffa.

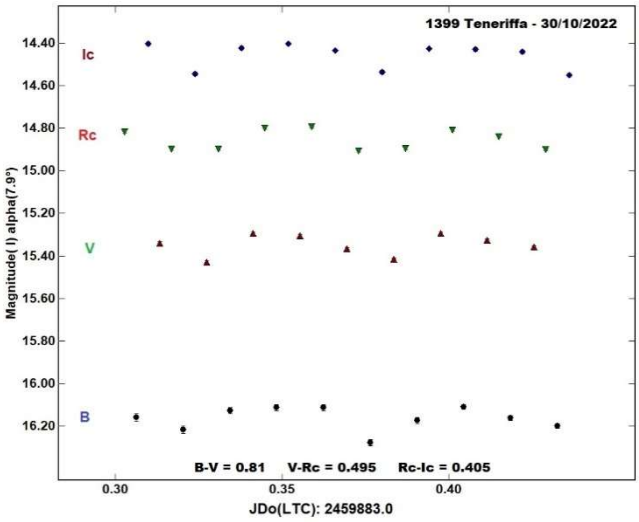

Figure 3. (B-V), (V-Rc) and (Rc-Ic) raw plot of 1399 Teneriffa

References

Harris, A.W.; Young, J.W.; Scaltriti, F.; Zappala, V. (1984). "Lightcurves and phase relations of the asteroids 82 Alkmene and 444 Gyptis." *Icarus* **57**, 251-258.

JPL (2022). Small-Body Database Browser. *http://ssd.jpl.nasa.gov/sbdb.cgi#top*

MPC (2022). MPC Database. *http://www.minorplanetcenter.net/db_search/*

Shevchenko, V.G.; Lupishko, D.F. (1998). "Optical Properties of Asteroids from Photometric Data." *Solar System Research* **32**, 220.

Warner, B.D. (2006). *A Practical Guide to Lightcurve Photometry and Analysis (2nd edition)*. Springer, New York.

Warner, B.D.; Harris, A.W.; Pravec, P. (2009). "The Asteroid Lightcurve Database." *Icarus* **202**, 134-146. Updated 2018 June. *http://www.minorplanet.info/lightcurvedatabase.html*

Warner, B.D. (2021). MPO Software, MPO Canopus v10.8.5.0. Bdw Publishing. *http://minorplanetobserver.com*

Warner, B.D.; Harris, A.W.; Ďurech, J.; Benner, L.A.M. (2022). "Lightcurve photometry opportunities: 2022 October-December." *Minor Planet Bull.* **49**, 350-354.

Waszczak, A.; Chang, C.-K.; Ofek, E.O.; Laher, R.; Masci, F.; Levitan, D.; Surace, J.; Cheng, Y.-C.; Ip, W.-H.; Kinoshita, D.; Helou, G.; Prince, T.A.; Kulkarni, S. (2015) "Asteroid Light Curves from the Palomar Transient Factory Survey: Rotation Periods and Phase Functions from Sparse Photometry" *Astronomical Journal* **150**, Issue **3**, article id. 75, 35 pp.

4376 SHIGEMORI: AN ASTEROID WITH AN EARTH COMMENSURATE ROTATION PERIOD

Alessandro Marchini, Riccardo Papini
Astronomical Observatory, DSFTA - University of Siena (K54)
Via Roma 56, 53100 - Siena, ITALY
marchini@unisi.it

Lorenzo Franco
Balzaretto Observatory (A81), Rome, ITALY

Frederick Pilcher
Organ Mesa Observatory (G50)
4438 Organ Mesa Loop
Las Cruces, NM 88011 USA

Julian Oey
Blue Mountains Observatory (Q68)
94 Rawson Pde. Leura, NSW, AUSTRALIA

(Received: 2022 December 30)

Multi-site photometric observations of the asteroid 4376 Shigemori were conducted in order to discern its synodic rotation period, which presented a challenge in being very close to that of Earth. In fact, we obtained P = 23.984 ± 0.004 h with an amplitude A = 0.21 ± 0.03 mag.

CCD photometric observations of the asteroid 4376 Shigemori were carried out in 2022 October-November from Italy by the Astronomical Observatory of the University of Siena (DSFTA, 2022), from New Mexico (USA) by the Organ Mesa Observatory, from Australia by the Blue Mountains Observatory. Equipment details are on Table I. Observations from different longitudes became indispensable when, after the first sessions from Italy, it was realized that the asteroid had a period very close to 24 h.

Data processing and analysis were done with *MPO Canopus* (Warner, 2018). All images were calibrated with dark and flat-field frames and the instrumental magnitudes converted to R magnitudes using solar-colored field stars from a version of the CMC-15 catalogue distributed with *MPO Canopus*. Table II shows the observing circumstances and results.

A search through the asteroid lightcurve database (LCDB; Warner et al., 2009) indicates that our result may be the first reported lightcurve observations and results for this asteroid.

4376 Shigemori (1987 FA) was discovered on 1987 March 20 at Ojima by T. Niijima and T. Urata and named for a Japanese military commander, Taira-no Shigemori (1138-1179), the eldest son of Taira-no Kiyomori. [Ref: Minor Planet Circ. 19696] It is an inner main-belt asteroid with a semi-major axis of 2.231 AU, eccentricity 0.158, inclination 0.876°, and an orbital period of 3.33 years. Its absolute magnitude is H = 13.69 (JPL, 2022). The WISE/NEOWISE satellite infrared radiometry survey (Masiero et al., 2014) found a diameter D = 4.967 ± 0.290 km using an absolute magnitude H = 13.6.

Observations were conducted over eight nights and collected 747 data points. The period analysis shows a bimodal solution for the rotational period of P = 23.984 ± 0.004 h with an amplitude A = 0.21 ± 0.03 mag.

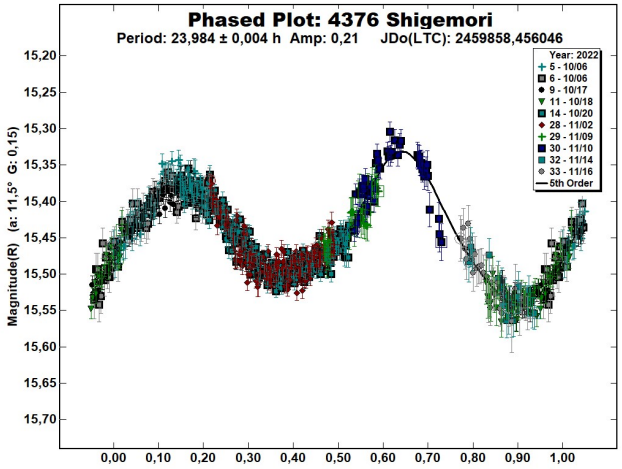

Observer Observatory	Telescope	CCD	Sessions (mm/dd)
Alessandro Marchini Astronomical Observatory University of Siena (K54)	0.30-m MCT f/5.6	SBIG STL-6303E	10/05, 10/06, 10/17, 10/18, 11/14, 11/16
Frederick Pilcher Organ Mesa Observatory (G50)	0.35-m SCT f/10.0	SBIG STL-1001E	10/20, 11/02
Julian Oey Blue Mountains Observatory (Q68)	0.35-m SCT f/5.9	SBIG ST-8XME	11/09, 11/10

Table I. Observing equipment. MCT: Maksutov-Cassegrain, SCT: Schmidt-Cassegrain.

Number	Name	2022/mm/dd	Phase	L_{PAB}	B_{PAB}	Period(h)	P.E.	Amp	A.E.	Grp
4376	Shigemori	10/05-11/16	*11.6,14.3	31	0	23.984	0.004	0.21	0.03	MB-I

Table II. Observing circumstances and results. The first line gives the results for the primary of a binary system. The second line gives the orbital period of the satellite and the maximum attenuation. The phase angle is given for the first and last date. If preceded by an asterisk, the phase angle reached an extrema during the period. L_{PAB} and B_{PAB} are the approximate phase angle bisector longitude/latitude at mid-date range (see Harris et al., 1984). Grp is the asteroid family/group (Warner et al., 2009).

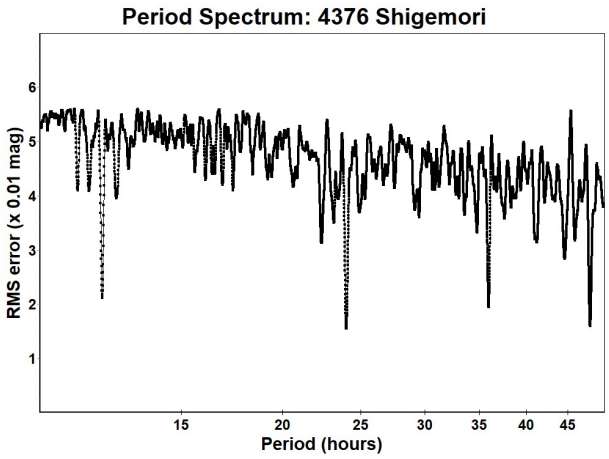

Acknowledgements

Minor Planet Circulars (MPCs) are published by the International Astronomical Union's Minor Planet Center. *https://www.minorplanetcenter.net/iau/ECS/MPCArchive/MPCArchive_TBL.html*

References

DSFTA (2022). Dipartimento di Scienze Fisiche, della Terra e dell'Ambiente - Astronomical Observatory. *https://www.dsfta.unisi.it/en/research/labs/astronomical-observatory*

Harris, A.W.; Young, J.W.; Scaltriti, F.; Zappala, V. (1984). "Lightcurves and phase relations of the asteroids 82 Alkmene and 444 Gyptis." *Icarus* **57**, 251-258.

JPL (2022). Small-Body Database Browser. *http://ssd.jpl.nasa.gov/sbdb.cgi#top*

Masiero, J.R.; Grav, T.; Mainzer, A.K.; Nugent, C.R.; Bauer, J.M.; Stevenson, R.; Sonnett, S. (2014). "Main-belt Asteroids with WISE/NEOWISE: Near-infrared Albedos." *Astrophys. J.* **791**, 121.

Warner, B.D.; Harris, A.W.; Pravec, P. (2009). "The Asteroid Lightcurve Database." *Icarus* **202**, 134-146. Updated 2022 Sep. *http://www.minorplanet.info/lightcurvedatabase.html*

Warner, B.D. (2018). MPO Software, MPO Canopus v10.7.7.0. Bdw Publishing. *http://minorplanetobserver.com*

A COMPREHENSIVE PHOTOMETRIC STUDY OF 603 TIMANDRA

Frederick Pilcher
Organ Mesa Observatory (G50)
4438 Organ Mesa Loop
Las Cruces, NM 88011 USA
fpilcher35@gmail.com

Lorenzo Franco
Balzaretto Observatory (A81), Rome, ITALY

Alessandro Marchini
Astronomical Observatory, DSFTA - University of Siena (K54)
Via Roma 56, 53100 - Siena, ITALY

Riccardo Papini
Wild Boar Remote Observatory (K49)
San Casciano in Val di Pesa (FI), ITALY

Paolo Bacci, Martina Maestripieri
GAMP - San Marcello Pistoiese (104), Pistoia, ITALY

Mauro Bachini, Giacomo Succi
BSCR Observatory (K47), Santa Maria a Monte (PI), ITALY

Gianni Galli
GiaGa Observatory (203), Pogliano Milanese, ITALY

Luca Bertagna
Tycho Observatory (M17), La Spezia, ITALY

Marco Iozzi, Alessio Squilloni, Maura Tombelli
Beppe Forti Observatory (K83), Montelupo Fiorentino, ITALY

Marco Iozzi
HOB Astronomical Observatory (L63)
Capraia Fiorentina, ITALY

Giulio Scarfi
Iota Scorpii Observatory (K78), La Spezia, ITALY

(Received: 2023 January 9)

Based on 65 sessions 2022 Sept. 24 - Dec. 28, we find for 603 Timandra a synodic rotation period of 330.1 ± 0.5 hours and amplitude 0.80 ± 0.05 magnitudes. There is also low-level tumbling with a possible second period of 273 hours, PAR -2. The period, amplitude, and epoch of lightcurve maximum all agree with a recent posting on the DAMIT website. Data obtained on 2022 Oct. 15 show that (B-V) = 0.80 ± 0.04 and (V-R) = 0.51 ± 0.02. At mid-light, H = 12.18 ± 0.14 in the V band, G = 0.20 ± 0.17.

The first author of this paper (Pilcher, 2011) obtained twelve photometric sessions of 9 to 11 hours each on 603 Timandra 2010 Nov. 13 - Dec. 24. These data were measured with uncalibrated comparison stars, that is, instrumental magnitudes only. The zero points of the individual lightcurves were adjusted up to several ×0.1 magnitudes to provide a fit to a rotation period of 41.79 hours, amplitude 0.1 magnitudes. The uncalibrated data have been posted onto *www.ALCDEF.org* with sharing allowed. The reader is invited to download them and perform his own investigation.

Durech (2020) posted onto the DAMIT website a LI inversion model based entirely on sparse data from ATLAS between 2016/02 and 2018/10. The dense lightcurves obtained in 2010 by this author were not utilized to prepare the LI model presented in DAMIT. A sidereal period of 330.2 hours with rotational pole at celestial longitude 223º, celestial latitude 72º was found. The model shows a long equatorial axis about twice the length of the short equatorial axis. With a rotational pole nearly at a right angle to the orbital plane, a rotational amplitude near 0.7 magnitudes is expected.

The CCD images have been lost in the twelve years since they were made, but the original uncalibrated measurement data are preserved. First author Pilcher re-examined the original data obtained in the year 2010. When a lightcurve was drawn with the period forced to 330.2 hours, it was immediately apparent that there were many large gaps. Therefore, the half period of 165.1 hours was used to adjust the zero points of the individual sessions up to a few ×0.1 magnitudes until a good fit was obtained. With a range of periods between 160 hours and 170 hours thereafter adopted, small additional zero-point adjustments were made to minimize the rms residual at 164.9 hours.

For an amplitude of 0.8 magnitudes, a period with only one maximum and minimum per cycle cannot be fit to any model shape and is definitively ruled out. Therefore, we do not present the half period lightcurve. The period is twice as great. The final step was to adjust a lightcurve for best fit within a range of 325 to 335 hours. A period 330.5 ± 0.1 hours (formal error) and amplitude 0.8 ± 0.1 magnitudes is found and presented (Fig. 1). The real period error is likely to be larger.

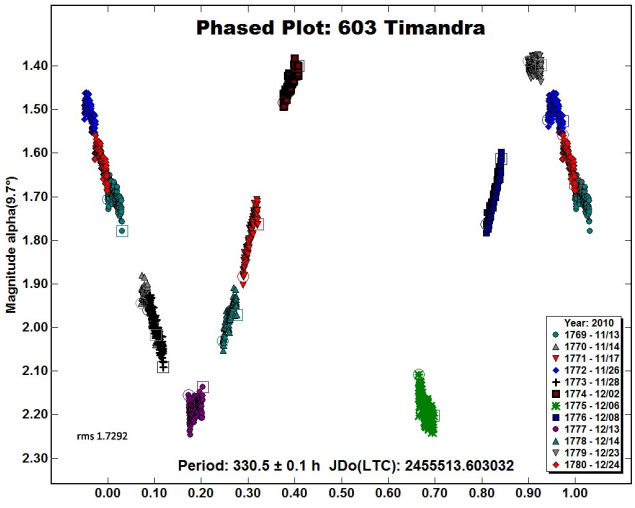

Fig. 1. The lightcurve of 603 Timandra phased to 330.5 hours drawn from year 2010 data.

A period spectrum between 100 hours and 400 hours shows deep minima only at 165 hours and at 330 hours (Fig. 2). Even with the data being uncalibrated, no period within this range except 330 hours can be allowed.

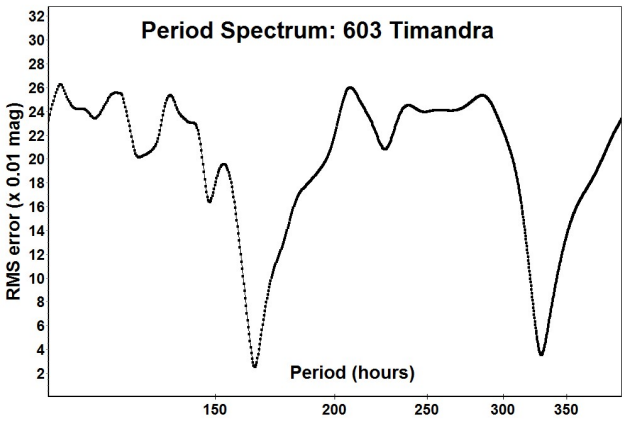

Fig. 2. The period spectrum of 603 Timandra for year 2010.

With another favorable opposition of 603 Timandra occurring in late 2022, first author Pilcher invited all the other authors of this paper to contribute photometric sessions. Observing circumstances and results are reported in table I. The full list of equipment of the several observers is provided below in table II. The target magnitudes in the R band for all sessions were calibrated with the r' magnitudes of solar colored stars in the CMC15 catalog, where R = r' - 0.22.

A total of 65 sessions, most of them less than 4 hours, were obtained by the several observers over the interval 2022 Sept. 24 to Dec. 28, including almost seven rotation cycles. Single period lightcurves were drawn with *MPO Canopus v. 10.7* software. Data from these sessions can be fit to a lightcurve with period 330.1 ± 0.1 hours (formal error), although we consider an error of ± 0.5 hours to be more realistic. The amplitude is 0.80 ± 0.05 magnitudes. Discordances in the plotted points for the several sessions suggest the presence of low-level tumbling. We present both a lightcurve phased to 330.1 hours (Fig. 3) and a raw lightcurve (Fig. 4), both including data from all sessions.

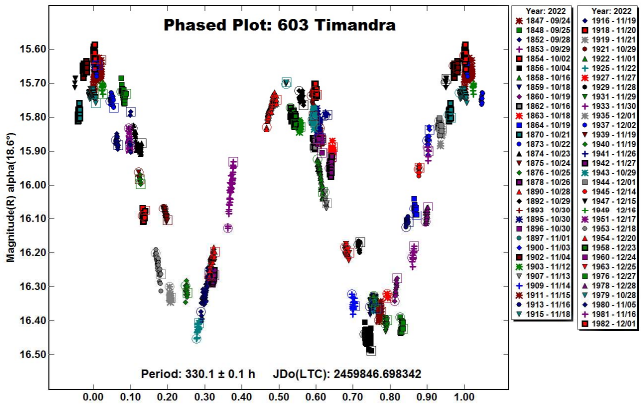

Fig. 3. The lightcurve of 603 Timandra phased to 330.1 hours drawn by single period software for year 2022 data.

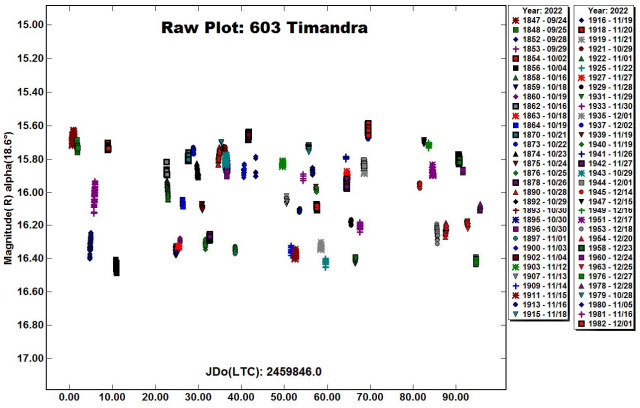

Fig. 4. The raw lightcurve of 603 Timandra for the interval 2022/09/24 to 2022/12/28.

It is instructive to explain how the 41.79-hour alias found in 2010 arose. The authors caution that similar mistakes may be present in other published data and warn all authors of lightcurves to look for evidence of the ambiguity explained in the next paragraph.

Let P1 = 41.79h, P2 = 330.1h, PE = Earth sidereal period 23.93h. Then (1/P1) - (1/P2) = 1/2PE within observational error. The calibrated data obtained in year 2022 immediately revealed the large amplitude and led to the correct period of 330.1 hours. If the data from the 2010 investigation had been calibrated instead of being arbitrarily adjusted, again the large amplitude would have been noted and the alias period rejected.

We consider this period to be highly reliable. The dense lightcurves from both the years 2010 and 2022 provide fits to a period very close to that obtained by LI modeling from sparse data in the years 2016-2018. The 330.5-hour lightcurve from year 2010 shows a maximum near JD2455513, shortly before zero epoch. Likewise, the 330.1-hour lightcurve from year 2022 shows a maximum near JD2459847, shortly after zero epoch. The DAMIT website has a provision that the LI model can be projected to any JD specified by the user. On both JD2455513 and JD2459847, the broad side of the model is toward the Earth and therefore the asteroid is at maximum light. The compatibility of rotation period, amplitude near 0.8 magnitudes predicted by the elongated shape model, and epoch of lightcurve maximum from three completely separate data sets improves the confidence in the shape and spin of the model, and in the validity of the 330.5-hour period obtained from the year 2010 dense but uncalibrated lightcurves.

Multiband photometry, acquired by P. Bacci and M. Maestriprieri (104) on 2022 October 15, allowed us to determine the color indices (B-V) = 0.80 ± 0.04 and (V-R) = 0.51 ± 0.02 (Fig. 5), consistent with a medium albedo asteroid (Shevchenko and Lupishko, 1998).

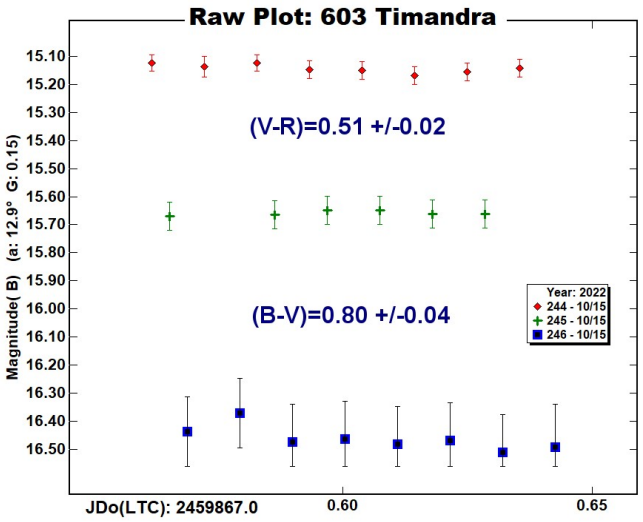

Fig. 5. Raw lightcurves of 603 Timandra in B, V, and R bands on 2022/10/15.

For H-G determination the R band magnitudes were converted to V band adding the color index (V-R). An H-G diagram was drawn for maximum, mean, and minimum light (Fig. 6). Considering the large amplitude of the lightcurve, for the H-G parameters were used separately the minimum and the maximum light magnitudes and evaluating the mean light solution (H = 12.18 ± 0.14 mag; G = 0.20 ± 0.17) which best represents the entire dataset.

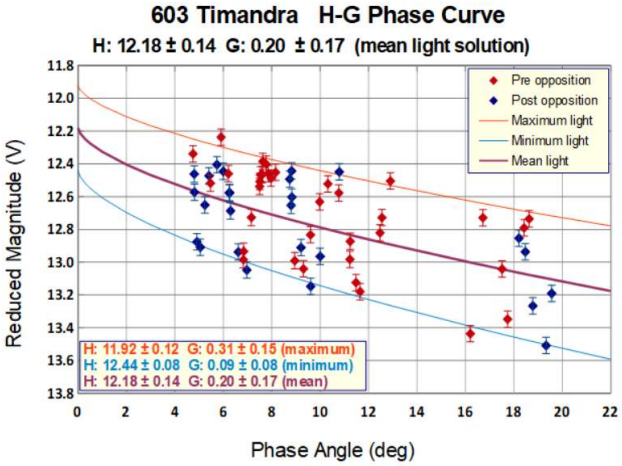

Fig. 6. V-band H-G diagram for 603 Timandra at maximum, mean, and minimum light.

The authors thank Petr Pravec for performing an independent analysis of our data, using software that includes the sum and difference of the primary and tumbling periods, and also the sum and difference of integer multiples of both periods. His analysis reads:

Number	Name	yyyy/mm/dd-yyyy/mm/dd	Phase	LPAB	BPAB	Period(h)	P.E	Amp	A.E.
603	Timandra	2010/11/13-2010/12/24	* 9.7, 13.4	67	11	330.5	0.5	0.80	0.10
603	Timandra	2022/09/24-2022/12/28	*18.6, 19.6	49	10	330.1	0.5	0.80	0.05

Table I. Observing circumstances and results. Pts is the number of data points. The phase angle is given for the first and last date, where the * indicates that a minimum was reached between these dates. LPAB and BPAB are the approximate phase angle bisector longitude and latitude at mid-date range (see Harris *et al.*, 1984).

Observatory (MPC code)	Telescope	CCD	Filter
Organ Mesa Observatory (G50)	0.35-m SCT f/10	SBIG STL-1001E	C
Astronomical Observatory of the University of Siena (K54)	0.30-m MCT f/5.6	SBIG STL-6303e(bin 2x2)	Rc
WBRO (K49)	0.235-m SCT f/10	SBIG ST8-XME	Rc
GAMP (104)	0.60-m NRT f/4	Apogee Alta	B,V,Rc
BSCR Observatory (K47)	0.41-m NRT f/3.2	DTA Discovery 1600	C
GiaGa Observatory (203)	0.36-m SCT f/5.8	MORAVIAN G2-3200	Rc
Tycho Observatory (M17)	0.20-m NRT f/4	SBIG ST10-XME	C
Beppe Forti Astronomical Observatory (K83)	0.40-m RCT f/8	SBIG STX 16803 (bin 3x3)	C
HOB Astronomical Observatory (L63)	0.20-m SCT f/6	ATIK 383L+	C
Iota Scorpii(K78)	0.40-m RCT f/8	SBIG STXL-6303e (bin 2x2)	Rc

Table II. Observing Instrumentations. MCT: Maksutov-Cassegrain, NRT: Newtonian Reflector, RCT: Ritchey-Chretien, SCT: Schmidt-Cassegrain.

While the main period of the tumbler is well established (330.5 h with a realistic error about 1h), its second period is not well determined. One of a few possible periods is 273.5 h, but it is possible that it is actually a linear combination of the real frequencies of the tumbler rather than the real second period. A part of the problem is that the data cannot be fitted to very high orders, so the fit is not perfect. I rate this one as PAR = -2. The primary period lightcurve is shown in Fig. 7.

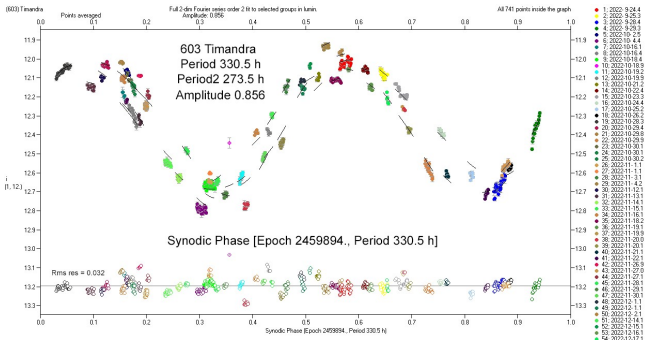

Fig. 7. Lightcurve of 603 Timandra for the year 2022 phased to 330.5 hours and drawn with multiple period software.

Acknowledgments

The authors thank Petr Pravec for his independent analysis of our data.

References

Durech, J. (2020) DAMIT website. *https://astro.troja.mff.cuni.cz/projects/damit/*

Harris, A.W.; Young, J.W.; Scaltriti, F.; Zappala, V. (1984). "Lightcurves and phase relations of the asteroids 82 Alkmene and 444 Gyptis." *Icarus* **57**, 251-258.

Pilcher, F. (2011). "Rotation period determinations for 25 Phocaea, 140 Siwa, 149 Medusa, 186 Celuta, 475 Ocllo, 574 Reginhild, and 603 Timandra." *Minor Planet Bull.* **38**, 76-78.

Shevchenko, V.G.; Lupishko, D.F. (1998). "Optical properties of Asteroids from Photometric Data." *Solar System Research* **32**, 220-232.

ROTATION PERIOD OF KORONIS FAMILY MEMBER (1497) TAMPERE

Stephen M. Slivan, Timothy C. Brothers, Abigail M. Colclasure, Skylar S. Larsen, Claire J. McLellan-Cassivi, Orisvaldo S. Neto, Maurielle I. Noto, Maya S. Redden
Massachusetts Institute of Technology
Dept. of Earth, Atmospheric, and Planetary Sciences
77 Mass. Ave. Rm. 54-424, Cambridge, MA 02139
slivan@mit.edu

Francis P. Wilkin, Niha Das
Union College, Dept. of Physics and Astronomy
Schenectady, NY

(Received: 2023 January 12)

Observations of (1497) Tampere during its 2022 apparition yield a determination of its synodic rotation period 3.30237 ± 0.00015 h assuming a doubly-periodic lightcurve.

Published rotation period determinations of Koronis family member (1497) Tampere fall within two significantly different ranges. The longer-period range near 3.6 h includes one result based on dense lightcurves (Brines et al., 2017) and a second result that is based on ATLAS survey data sparsely sampled in time (Erasmus et al., 2020), while both of the periods within the shorter-period range near 3.3 h are derived from survey "sparse data" (Chang et al., 2015; Waszczak et al., 2015). New observations reported here resolve that ambiguity in the rotation period, and also record complete coverage of the lightcurve at a previously unobserved viewing aspect. The published periods assume that the lightcurve is doubly-periodic in a single rotation; that same assumption is made here for the present work, subject to future verification by determining a corresponding sidereal period that can rule out a result twice as long.

Tampere was observed in 2022 from two sites. Lightcurves were recorded on seven nights prior to the asteroid reaching its eastern stationary point, using telescopes at the MIT Wallace Astrophysical Observatory (WAO) in Westford, MA; an additional longer lightcurve span deliberately covering more than two rotations was recorded about a month after opposition. Lightcurves also were recorded at the Union College Observatory (UCO) in Schenectady, NY on two nights near opposition and one more night about a month later, and likewise include a long span covering two rotations. Both sites imaged using Cousins *R* filters; nightly observing information is summarized in Table I and the instrumentation is detailed in Table II. Processing and measurement of the WAO images was as described by Slivan et al. (2008), except that for the observations made using the smaller 0.36-m telescopes the choices of synthetic aperture sizes for the on-chip relative photometry were guided by the experience of Howell (1989). The UCO images were measured using the *AstroImageJ* application.

The new data yield a self-consistent doubly-periodic folded composite lightcurve for a derived synodic period of 3.30237 ± 0.00015 h (Fig. 1), with the high precision resulting from the combination of Tampere's relatively short period with the 124-day interval spanned by the observations to count 952 rotations. The period result is consistent with both published periods comprising the shorter-period range (Chang et al., 2015; Waszczak et al., 2015).

In the longer-period range, the Erasmus et al. (2020) result corresponds to an alias period that undercounts rotations by 0.5 rotation per day, and composites of the new data folded at the Brines et al. (2017) result are not self-consistent.

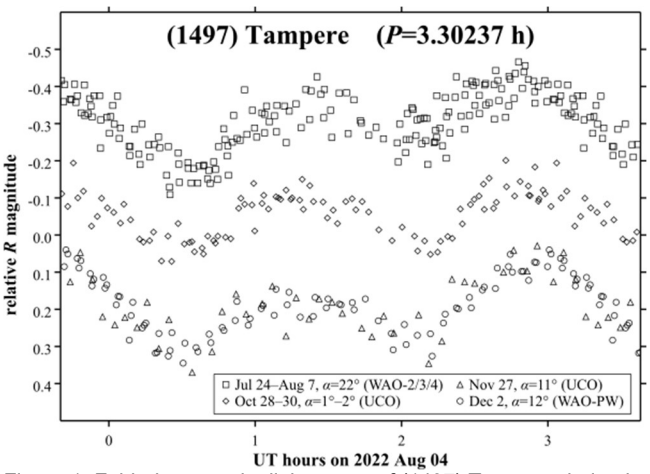

Figure 1. Folded composite lightcurves of (1497) Tampere during its 2022 apparition, light-time corrected, showing one rotation period plus the earliest and latest 10% repeated. The three lunations of composited data have been offset from each other in brightness for presentation. The legend gives UT dates, solar phase angles, and telescope ID (Table II).

UT date 2022	α (°)	Tel. ID	Data Span (h)	Integration time (s)
Jul 24.3	21.8	WAO-4	1.2	240
Jul 26.3	21.8	WAO-3	1.9	240
Jul 27.3	21.8	WAO-3	2.1	240
Jul 31.3	21.9	WAO-3	2.5	300
Aug 03.3	21.8	WAO-3	0.8	300
Aug 04.3	21.8	WAO-3	2.6	240
Aug 07.3	21.8	WAO-2	3.0	180
Oct 28.2	1.6	UCO	2.5	240
Oct 30.2	0.8	UCO	6.7	240
Nov 27.1	10.6	UCO	3.2	240
Dec 02.1	12.3	WAO-PW	7.6	300

Table I: Nightly observing information, with rows grouped by lunation. Columns are: UT date at lightcurve mid-time, solar phase angle *α*, telescope ID (Table II), lightcurve duration, and image integration time.

Number	Name	yyyy mm/dd	Phase	L_{PAB}	B_{PAB}	Period(h)	P.E.	Amp	A.E.
1497	Tampere	2022 07/24-12/02	*21.8,12.3	37	1	3.30237	0.00015	0.23	0.04

Table III. Observing circumstances and results. Solar phase angle is given for the first and last dates; the asterisk indicates that the phase angle reached a minimum during the period. L_{PAB} and B_{PAB} are the approximate phase angle bisector longitude/latitude at mid-date range.

Tel. ID	Dia. (m)	CCD camera	FOV (′)	Bin	Scale (″/pix)
UCO	0.51	SBIG SXTL-11002	30×20	2×2	0.93
WAO-2	0.36	FLI ML1001	22×22	1×1	1.26
WAO-3	0.36	FLI ML1001	20×20	1×1	1.18
WAO-4	0.36	SBIG STL-1001	21×21	1×1	1.25
WAO-PW	0.61	FLI PL16803	32×32	1×1	0.46

Table II: Telescopes and cameras information. Columns are: telescope ID (UCO, OGS RC20; WAO-2, shed pier #2 Celestron C14; WAO-3, shed pier #3 Celestron C14; WAO-4, shed pier #4 Celestron C14; WAO-PW, Elliot PlaneWave 24-in CDK), telescope diameter, CCD camera, detector field of view, image binning used, and binned image scale.

Acknowledgments

We thank Dr. Michael Person for allocation of telescope time at Wallace, and for observer instruction and support. The MIT student observers were supported by a grant from MIT's Undergraduate Research Opportunities Program.

References

Brines, P.; Lozano, J.; Rodrigo, O.; Fornas, A.; Herrero, D.; Mas, V.; Fornas, G.; Carreño, A.; Arce, E. (2017). "Sixteen Asteroids Lightcurves at Asteroids Observers (OBAS) - MPPD: 2016 June - November." *Minor Planet Bull.* **44**, 145-149.

Chang, C.; Ip, W.; Lin, H.; Cheng, Y.; Ngeow, C.; Yang, T.; Waszczak, A.; Kulkarni, S.; Levitan, D.; Sesar, B.; Laher, R.; Surace, J.; Prince, T.A. (2015). "Asteroid Spin-rate Study Using the Intermediate Palomar Transient Factory." *Astrophys. J. Suppl. Ser.* **219**, A27.

Erasmus, N.; Navarro-Meza, S.; McNeill, A.; Trilling, D.E.; Sickafoose, A.A.; Denneau, L.; Flewelling, H.; Heinze, A.; Tonry, J.L. (2020). "Investigating Taxonomic Diversity within Asteroid Families through ATLAS Dual-band Photometry." *Astrophys. J. Suppl. Ser.* **247**, A13.

Howell, S.B. (1989). "Two-dimensional Aperture Photometry: Signal-to-noise Ratio of Point-source Observations and Optimal Data-extraction Techniques." *PASP* **101**, 616-622.

Slivan, S.M.; Binzel, R.P.; Boroumand, S.C.; Pan, M.W.; Simpson, C.M.; Tanabe, J.T.; Villastrigo, R.M.; Yen, L.L.; Ditteon, R.P.; Pray, D.P.; Stephens, R.D. (2008). "Rotation Rates in the Koronis Family, Complete to $H \approx 11.2$." *Icarus* **195**, 226-276.

Waszczak, A.; Chang, C.; Ofek, E.O.; Laher, R.; Masci, F.; Levitan, D.; Surace, J.; Cheng, Y.; Ip, W.; Kinoshita, D.; Helou, G.; Prince, T.A.; Kulkarni, S. (2015). "Asteroid Light Curves from the Palomar Transient Factory Survey: Rotation Periods and Phase Functions from Sparse Photometry." *Astron. J.* **150**, A75.

LIGHTCURVE ANALYSIS OF TWO NEAR-EARTH ASTEROIDS

Paolo Bacci, Martina Maestripieri
GAMP - San Marcello Pistoiese (104), Pistoia, ITALY
b09.backman@gmail.com

Roberto Bacci
G. Pascoli Observatory (K63), Castelvecchio Pascoli, ITALY

(Received: 2023 January 10)

We report photometric analysis of two near-Earth asteroids observed during close approaches in 2022 October. For 2022 TG1 we found P = 0.1951 ± 0.0001 h, A = 0.46 mag; and for 2022 UR4 P = 0.0282 ± 0.0001 h, A = 1.08 mag.

CCD observations of two near-Earth asteroids were made in 2022 October using the instrumentation described in Table I. Lightcurve analysis was performed with *MPO Canopus* (Warner, 2022). All the images were calibrated with dark and flat frames and converted to R magnitudes using solar-colored field stars from CMC15 catalogue distributed with *MPO Canopus*. Table II shows the observing circumstances and results.

No previously reported results were found in the Asteroid Lightcurve Database (LCDB; Warner et al., 2009), The size estimates are calculated using *H* values from the Small-Body Database Lookup (JPL, 2022). Both asteroids are small in size and have a rotation period above the spin-barrier, they are probably monolithic objects.

2022 TG1 is an NEA Apollo; it was discovered by ATLAS-MLO, Mauna Loa, on 2022 October 4 (Bacci et al., 2022a). *H* =25.62 and the Minimum Orbit Intersection Distance (MOID) from Earth of 0.0011 au. Observations were made while the object was still on the NEOCP page of the Minor Planet Center, at V ~ 16.8. It was observed for 46 minutes starting at 2022 October 4, 19:10 UT, and for 55 minutes starting at 2022 October 5, 19:10 UT. We found a synodic period of $P = 0.1951 \pm 0.0001$ h with amplitude $A = 0.46 \pm 0.10$ mag. and ratio a/b = 1.5 ± 0.1 based on the amplitude and an assumed triaxial ellipsoid viewed equatorially (Zappala et al., 1990).

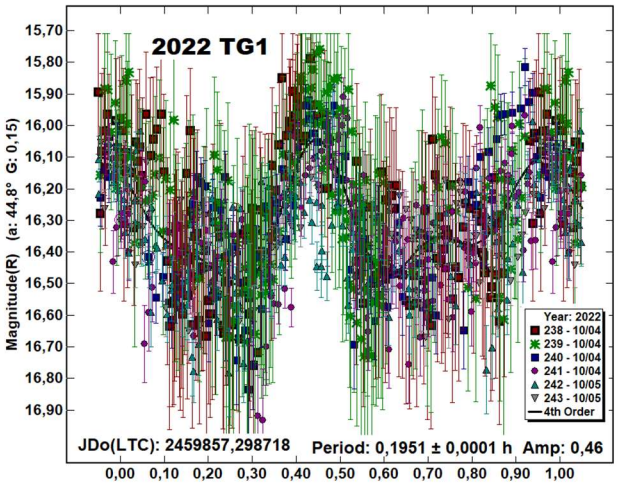

2022 UR4 is an NEA Apollo that was discovered on 2022 October 20 by ATLAS-MLO, Mauna Loa (Bacci et al., 2022b). H = 28.90 and the Minimum Orbit Intersection Distance (MOID) from Earth is 0.00053 au. Observations were made while the object was still on the NEOCP page of the Minor Planet Center, on 2022 October 10 at mag 13.9 V. It was observed for 13 minutes starting at 2022 October 20, 21:19 UT. We found a synodic period of P = 0.0282 ± 0.0001 h with amplitude A = 1.08 ± 0.10 mag and ratio a/b = 2.7 ± 0.1 based on the amplitude and an assumed triaxial ellipsoid viewed equatorially (Zappala et al., 1990).

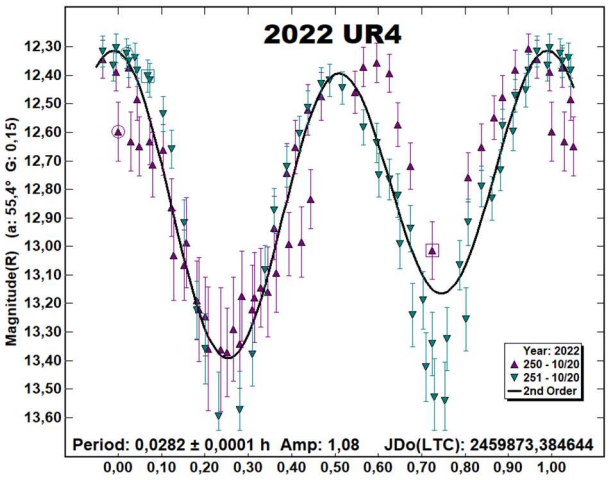

GAMP (104)			
2022 TG1			
2022 UR4	0.60-m NRT f/4.0	Apogee Alta	C
G. Pascoli (K63)			
2022 TG1	0.40-m NRT f/3.2	QHY22 C1318	C

Table I. Observing Instrumentations. The first column gives the asteroid while the second through fourth columns give, respectively, the telescope, CCD camera, and filter. NRT: Newtonian Reflector. C is Clear filter.

Acknowledgements

The author gratefully acknowledges a Gene Shoemaker NEO Grant from the Planetary Society (2019) and a Sirio System of Droise Paolo, both of which facilitated upgrades to observatory UAI 104 San Marcello equipment used in this study.

References

Bacci, P.; Maestripieri, M.; Tesi, L.; Fagioli; and 36 colleagues (2022a). "2022 TG1" *MPEC* **2022-T73**. *https://www.minorplanetcenter.net/mpec/K22/K22T73.html*

Bacci, P.; Maestripieri, M.; Tesi, L.; Fagioli, G.; and 34 colleagues (2022b). "2022 UR4" *MPEC* **2022-U145**. *https://www.minorplanetcenter.net/mpec/K22/K22UE5.html*

JPL (2022). Small-Body Database Lookup. *https://ssd.jpl.nasa.gov/tools/sbdb_lookup.html*

NEOCP The NEO Confirmation Page Minor Planet Center. *https://www.minorplanetcenter.net/iau/NEO/toconfirm_tabular.html*

Warner, B.D.; Harris, A.W.; Pravec, P. (2009). "The Asteroid Lightcurve Database." *Icarus* **202**, 134-146. Updated 2016 Sep. *http://www.minorplanet.info/lightcurvedatabase.html*

Warner, B.D. (2022). MPO Software, *MPO Canopus* v10.8.6.9. Bdw Publishing, Eaton, CO. *http://minorplanetobserver.com*

Zappala, V.; Cellini, A.; Barucci, A.M.; Fulchignoni, M.; Lupishko, D.E. (1990). "An analysis of the amplitude-phase relationship among asteroids." *Astron. Astrophys.* **231**, 548-560.

Number	Name	2022 mm/dd	Phase	L_{PAB}	B_{PAB}	Period(h)	P.E.	Amp	A.E.	H
	2022 TG1	10/04	44.8,44.3	356	17	0.1954	0.0002	0.46	0.1	25.62
		10/05	28.0,27.6	7	13					
	2022 UR4	10/10	55.4	26	11	0.0282	0.0001	1.04	0.1	28.90

Table II. Observing circumstances and results. The phase angle is given for the first and last date. If preceded by an asterisk, the phase angle reached an extrema during the period. L_{PAB} and B_{PAB} are the approximate phase angle bisector longitude/latitude at mid-date range (see Harris et al., 1984). Grp is the asteroid family/group (Warner et al., 2009). H is the absolute magnitude at 1 au from Sun and Earth taken from the Small-Body Database Lookup (JPL, 2022).

PHOTOMETRY AND LIGHTCURVE ANALYSIS FOR NEAR-EARTH ASTEROIDS 65803 DIDYMOS, (86829) 2000 GR146 AND 161989 CACUS

Aldo M. Panfichi
Pontificia Universidad Católica del Perú
Av. Universitaria 1801, San Miguel, 15088
Lima, Peru
panfichialdo@gmail.com

Myriam Pajuelo
Pontificia Universidad Católica del Perú
Lima, Peru

(Received: 2022 Dec 20)

We present lightcurves for 65803 Didymos, (86829) 2000 GR146, and 161989 Cacus. These observations were conducted in 2022 September, prior to the NASA DART impact. Lightcurve analysis for 65803 Didymos is in excellent agreement with prior results, while data for the other two asteroids comes close to matching prior published rotational periods, but does not strictly overlap. A larger number of data points on nights with good seeing would be required for better solutions.

CCD photometric observations of near-Earth asteroids 65803 Didymos, (86829) 2000 GR146 and 161989 Cacus were carried out over four nights between 2022 September 6 and 9 at the Cerro Tololo Inter-American Observatory in La Serena, Chile (IAU code 807). The data were taken with the SMARTS 0.9-m *f*/13.5 Cassegrain telescope on the mountain, which is equipped with a 2048×2046 Tek2K CCD detector; however, we used only a quarter of the chip for the observations because doing so reduced image readout times significantly. As such, our observations are 1074×1024-pixel arrays of 0.401 arcseconds per pixel.

Data processing and analysis were done using *MPO Canopus* software (Warner, 2019). Images were calibrated using bias and flat field frames with the same software. *MPO Canopus* implements the Fourier Analysis of Lightcurves (FALC) algorithm developed by Alan Harris (Harris et al., 1989); this was used to find best-fit periods for our observational data for each asteroid.

65803 Didymos is a potentially-hazardous binary Apollo asteroid discovered on 1996 April 11 by the Spacewatch survey at Kitt Peak National Observatory in Arizona. Didymos' published rotational period is 2.2600 ± 0.0001 h (Naidu, 2020). Recently, Didymos and its companion Dimorphos (Pravec, 2003) were the target of the Double Asteroid Redirection Test (DART), a mission led by NASA, which deliberately impacted Dimorphos with a spacecraft on 2022 September 26. The observations described in this report were taken a few weeks prior to the impact, with the intent to bolster pre-impact rotational period analysis and comparisons with post-impact observational results. We observed Didymos in both V and R filters throughout the nights of 2022 September 6-9.

Twentynine images of Didymos in the V filter were taken on 2022 September 6 with exposure times of 90 s. The seeing remained consistently low throughout the night and, despite the small number of images, we were able to observe a complete rotation of the asteroid. The data taken in V show a rotational period of 2.299 ± 0.128 h, which overlaps with previous results, albeit with a significant uncertainty due to the low number of data points.

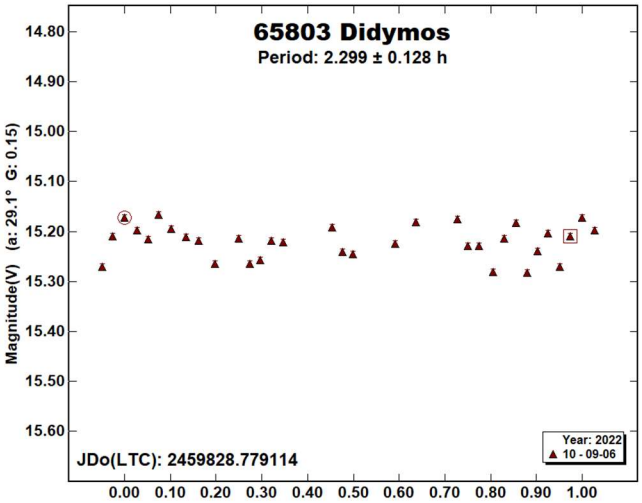

On the nights of 2022 September 7 and 9, we observed Didymos in the R filter, taking a total of 205 images at an exposure time of 60 s. Since the asteroid is brighter in the R filter than in V, we were able to use lower exposure times than the V filter images in order to take a larger number of observations. While the night of 2022 September 7 had pretty good seeing, the night of 2022 September 9 had higher humidity in the air than was desirable, as well as a bright, nearly-full moon, such that seeing fluctuated from 1.0 - 2.0 arcsec during the night - the fluctuations can be seen in the larger data spread for the 2022 September 9 data points in the lightcurve versus the 2022 September 7 data. Despite this, analysis of our observations in the R filter gives a rotational period of 2.261 ± 0.002 h, which is in excellent agreement with published results. Removing the 2022 September 9 data, on the other hand, gives a significantly worse solution.

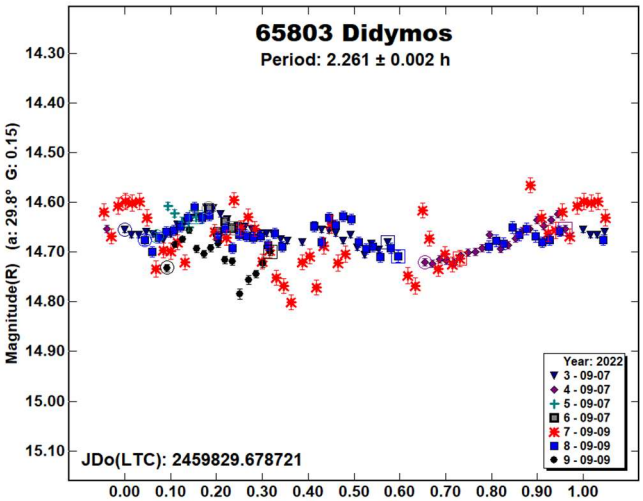

Number	Name	yyyy mm/dd	Phase	L_{PAB}	B_{PAB}	Period(h)	P.E.	Amp	A.E.	Grp
65803	Didymos	2022 09/06-09/09	29.1,31.7	349.1	-18.2	2.261	0.002	0.10	0.01	NEA
86829	2000 GR146	2022 09/06	22.7	322.4	-21.8	3.49	0.43	0.11	0.04	NEA
161989	Cacus	2022 09/08-09/09	55.4,54.8	4.1	-26.1	3.74	0.01	1.32	0.02	NEA

Table I. Observing circumstances and results. The phase angle is given for the first and last date. L_{PAB} and B_{PAB} are the approximate phase angle bisector longitude/latitude at mid-date range (Harris et al., 1984). Grp is the asteroid family/group (Warner et al., 2009).

(86829) 2000 GR146 is an Apollo asteroid discovered on 2000 April 12 by LINEAR at Socorro, New Mexico. We took 35 images of (86829) 2000 GR146 in the V filter at an exposure time of 180 s early in the night of 2022 September 6. This asteroid has a published period of 3.0996 ± 0.0001 h (Pravec, 2007web). Using our data, we calculated a period of 3.49 ± 0.43 h, which does not overlap the published period, but comes close. Due to the small number of images that we obtained for the asteroid, as well as the fact that we were not able to observe a full rotational period, our calculated period has a significant uncertainty; many more observations would have been required to obtain a good period solution. As such, we believe the actual significant error in our period to be larger than reported by *MPO Canopus*.

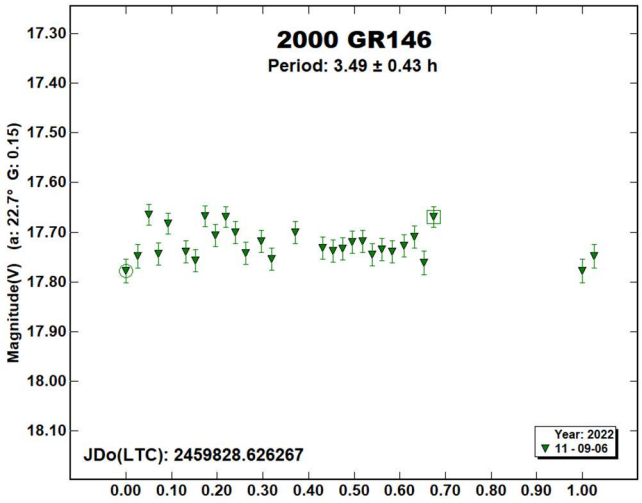

161989 Cacus is a potentially-hazardous Apollo asteroid initially discovered by German astronomer Hans-Emil Schuster at La Silla Observatory on 1978 February 8. We took 83 images of 161989 Cacus over the nights of 2022 September 8 and 9 in the R filter. Given its fast rate of in-sky motion and its comparative brightness in R, we took 15-s exposures, which we discovered was enough to get a significant signal while maintaining non-stretched, circular apertures. This asteroid has a published period of 3.7538 ± 0.0019 h (Pravec, 2003web).

The observing conditions on the nights we observed Cacus were far from ideal. On 2022 November 8, the humidity rose above 60% for almost the entire night; in fact, it went beyond the operational telescope limit of 80% for a couple of hours. This forced us to close the dome during that time, which prevented us from observing Cacus' full rotational period. As such, the seeing fluctuated at values consistently above 2.0 arcsec during that night. On 2022 November 9, the moon was nearly full, which also contributed to less-than-ideal conditions. Despite this, we were able to do good enough photometry that *MPO Canopus* reports confidently small error bars in its results.

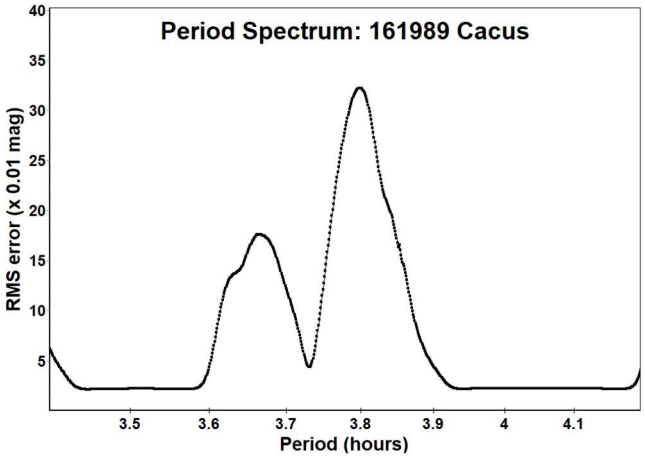

Analysis of the period spectrum given by *MPO Canopus* for our data shows wide minima that peak at 3.52 h and 4.00 h, with an additional minimum at an intermediate value of 3.74 h. The software calculates this minimum as a less likely fit than the other two, but comparing it with published periods from prior results (Degewij, 1978; Pravec, 2003web; Koehn, 2014), it would seem this minimum matches prior reported rotational periods for the asteroid. We present lightcurves for both the 3.52 ± 0.04 h solution and the 3.74 ± 0.01 h solution for the purposes of comparison. Looking at these lightcurves, if the 3.74 h solution is indeed the right one (it comes closest to matching previous results for the asteroid), then a significant portion of the asteroid's rotational period was missed. As such, we note that a larger number of observations on nights with better seeing would have given us a more complete solution, and once again state that we believe the actual error in period to be larger than that reported by *MPO Canopus*.

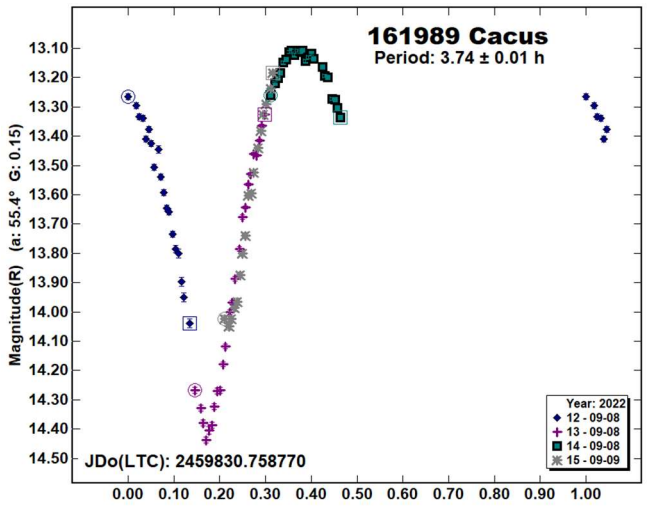

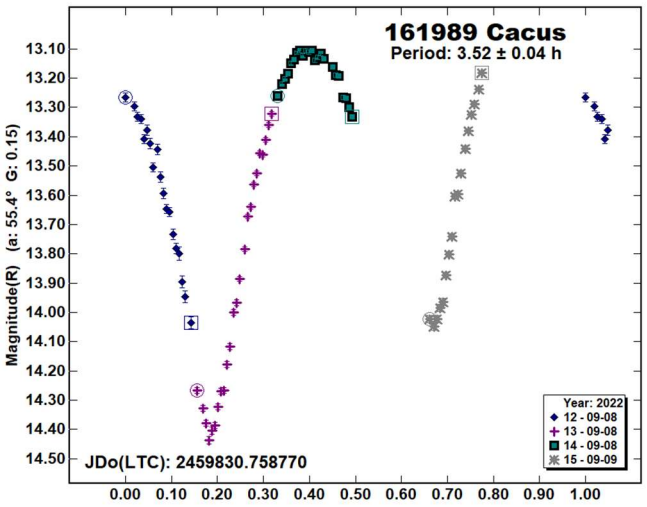

Acknowledgements

Funding for the observations and analysis was provided by the Pontificia Universidad Católica del Perú via a Fondo de Apoyo a la Investigación - FAI 2022 grant. We would like to thank Todd J. Henry and Elliot Vrijmoet for their mentorship in operating the telescope and obtaining data, Brian D. Warner for his assistance and patience in helping us work with *MPO Canopus*, and Petr Pravec for connecting us with the DART Observations Team. This research has made use of the Small Bodies Data *Ferret* tool (*http://sbn.psi.edu/ferret/*), supported by the NASA Planetary System, as well as the Asteroid Lightcurve Database (LCDB; *https://www.minorplanet.info/php/lcdb.php)*, and IMCCE's *Miriade VO* tool (*https://vo.imcce.fr/webservices/miriade/*).

References

Degewij, J. (1978). "1978 CA and 1978 DA." *IAUC* **3193**, #1.

Harris, A.W.; Young, J.W.; Scaltriti, F.; Zappala, V. (1984). "Lightcurves and phase relations of the asteroids 82 Alkmene and 444 Gyptis." *Icarus* **57**, 251-258.

Harris, A.W.; Young, J.W.; Bowell, E.; Martin, L.J.; Millis, R.L.; Poutanen, M.; Scaltriti, F.; Zappala, V.; Schober, H.J.; Debehogne, H.; Zeigler, K. (1989). "Photoelectric Observations of Asteroids 3, 24, 60, 261, and 863." *Icarus* **77**, 171-186.

Koehn, B.W.; Bowell, E.L.G; Skiff, B.A.; Sanborn, J.J.; McLelland, K.P.; Pravec, P.; Warner, B.D. (2014). "Lowell Observatory Near-Earth Asteroid Photometric Survey (NEAPS) - 2009 January through 2009 June." *Minor Planet Bulletin* **41**, 286-300.

Naidu, S.P.; Benner, L.A.M.; Brozovic, M.; Nolan, M.C.; Ostro, S.J.; Margot, J.L.; Giorgini, J.D.; Hirabayashi, T.; Scheeres, D.J.; Pravec, P.; Scheirich, P.; Magri, C.; Jao, J.S. (2000). "Radar observations and a physical model of binary near-Earth asteroid 65803 Didymos, target of the DART mission." *Icarus* **348**, 113777.

Pravec, P.; Benner, L.A.M.; Nolan, M.C.; Kusnirak, P.; Pray, D.; Giorgini, J.D.; Jurgens, R.F.; Ostro, S.J.; Margot, J.-L.; Magri, C.; Grauer, A.; Larson, S. (2003). "(65803) 1996 GT." *IAUC* **8244**, #2.

Pravec, P.; Wolf, M.; Sarounova, L. (2003web; 2007web). Ondrejov Asteroid Photometry Project website. *http://www.asu.cas.cz/~ppravec/neo.htm*

Warner, B.D.; Harris, A.W.; Pravec, P. (2009). "The Asteroid Lightcurve Database." *Icarus* **202**, 134-146. Updated 2021 Dec. *http://www.minorplanet.info/lightcurvedatabase.html*

Warner, B.D. (2019). MPO Software, *MPO Canopus* v10.8.6.3. Bdw Publishing. *http://minorplanetobserver.com*

CALL FOR OBSERVATIONS

Frederick Pilcher
4438 Organ Mesa Loop
Las Cruces, NM 88011 USA
fpilcher35@gmail.com

Observers who have made visual, photographic, or CCD measurements of positions of minor planets in calendar year 2022 are encouraged to report them to this author on or before 2023 April 15. This will be the deadline for receipt of reports, for which results can be included in the "General Report of Position Observations for 2022," to be published in *MPB* Vol. 50, No. 3.

LIGHTCURVE ANALYSIS FOR FOURTEEN NEAR-EARTH ASTEROIDS OBSERVED 2003 - 2022

Peter Birtwhistle
Great Shefford Observatory
Phlox Cottage, Wantage Road
Great Shefford, Berkshire, RG17 7DA
United Kingdom
peter@birtwhistle.org.uk

(Received: 2023 January 4)

Lightcurves and amplitudes for 14 small near-Earth asteroids observed from Great Shefford Observatory during close approaches between 2003 and 2022 are reported. All are superfast rotators with periods shorter than the 2.2 h spin barrier, 8 with periods shorter than 3 minutes and include 6 with reliably detected or suspected tumbling motion.

Photometric observations of near-Earth asteroids during close approaches to Earth between 2003 and November 2022 were made at Great Shefford Observatory using a 0.30-m Schmidt-Cassegrain and Apogee AP47p CCD camera (pre-2005 September) and a 0.40-m Schmidt-Cassegrain and Apogee Alta U47+ CCD camera from 2005 September onwards. All observations were made unfiltered and with the telescopes operating with a focal reducer at f/6. The 1K×1K, 13-micron CCDs were binned 2×2 resulting in an image scale of 3.0 arcsec/pixel (0.30-m telescope) and 2.16 arcsec/pixel (0.40-m telescope). All the images were calibrated with dark and flat frames and *Astrometrica* (Raab, 2018) was used to measure photometry using APASS Johnson V band data from the UCAC4 catalogue (Zacharias et al., 2013) unless otherwise stated. *MPO Canopus* (Warner, 2022), incorporating the Fourier algorithm developed by Harris (Harris et al., 1989) was used for lightcurve analysis.

No previously reported results for any of the objects reported here have been found in the Asteroid Lightcurve Database (LCDB) (Warner et al., 2009), from searches via the Astrophysics Data System (ADS, 2022) or from wider searches unless otherwise noted. All size estimates are calculated using H values from the Small-Body Database Lookup (JPL 2022a), using an assumed albedo for NEAs of 0.2 (LCDB readme.pdf file) and are therefore uncertain and offered for relative comparison only.

2003 EM1. This Aten was discovered at 16th mag from Črni Vrh on 2003 Mar 5.92 UTC and made an approach to 4 Lunar Distances (LD) 27 hours later (Tichy et al., 2003). It was observed for an hour starting at 2003 Mar 6.09 UTC when the apparent speed was 54 arcsec/min and 95 exposures of 4 s duration and 2 of 10 s were obtained. The resulting analysis indicates a 1.0 magnitude amplitude lightcurve with a rotation period of 0.03097 ± 0.00002 h at phase angle 29.1°. A previously reported result with P = 0.030968 ± 0.000003 h and amplitude 0.6 (Behrend, 2003web) obtained from measurements made over the period 2003 Mar 7.8 - 2003 Mar 8.8 UTC, when the phase angle ranged from 18 - 23° is in good agreement with this result.

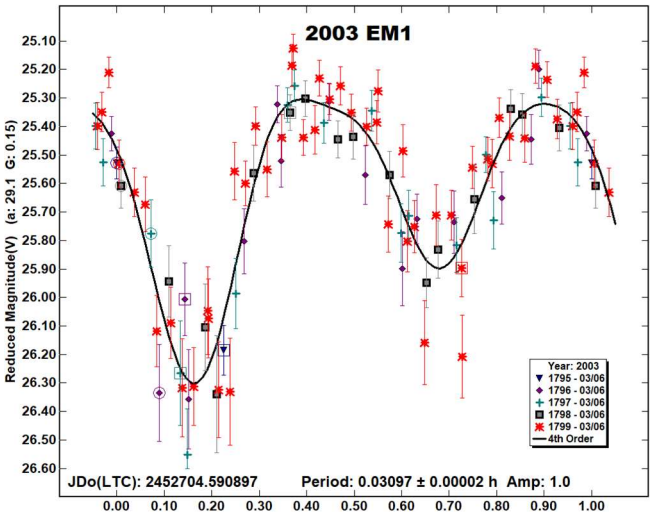

2008 EZ7. A ~12 m diameter Apollo discovered by the Siding Spring Survey using the 0.5-m Uppsala Schmidt on 2008 Mar 7.49 UTC (Gilmore et al., 2008), it passed Earth at a geocentric distance of 0.42 LD on 2008 Mar 9.06 UTC. It was observed over a period of 2.4 h starting less than an hour after closest approach when its topocentric distance increased from 0.41 to 0.48 LD and apparent speed reduced from 620 to 470 arcsec/min. A range of exposures of 0.2, 0.4, 0.6 and 1 second were taken, but the photometric reduction uses 189 measurements from just the 0.6 and 1 s exposures, the shorter exposures being unsuitable for measurement due to both low SNr and, especially for the 0.2 s images, uneven illumination of the field as the CCD shutter opened and closed. The period spectrum shows a number of short period solutions, with the best fit producing a bimodal lightcurve of period 0.016514 h = 59 s.

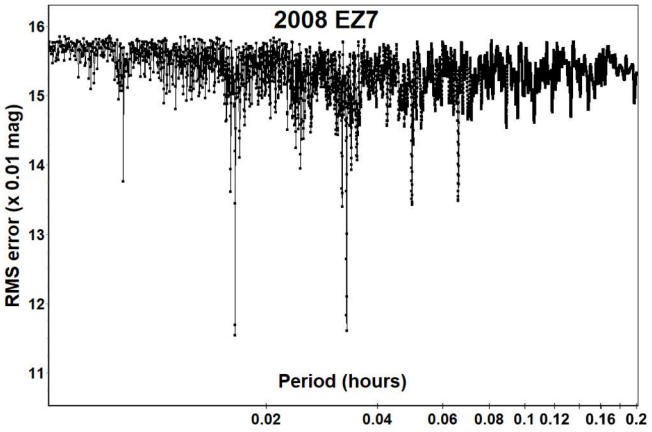

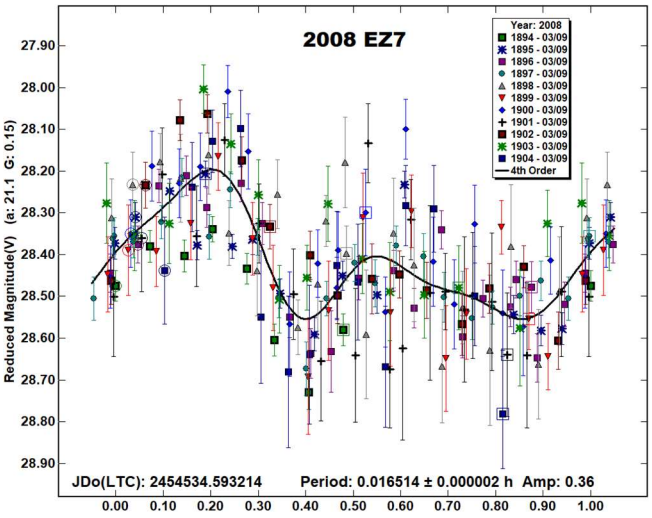

2011 EY11. This small Apollo (H=28.5, dia. ~6 m) was discovered by the Catalina Sky Survey on 2011 Mar 3.56 UTC (Hill et al., 2011), already less than 5 LD from Earth and 43 hours ahead of a close approach to 0.34 LD. It was observed extensively on its approach from Great Shefford over the 4-hour period 2011 Mar 6.91 -7.08 UTC when its distance decreased from 0.7 - 0.4 LD. Apparent sky motion increased from 280 to 924 arcsec/min and exposures of 1 s, decreasing to 0.5 s were used throughout to reduce image trailing. Phase angle reached a minimum for the apparition at 15.5°, 10 minutes before observations began and only reached 39.2° by the end of the session. Large amplitude variations were visible in consecutive images and an initial reduction of the lightcurve (labelled as PAR) indicated a very fast rotation period of 65 s and amplitude of 0.74.

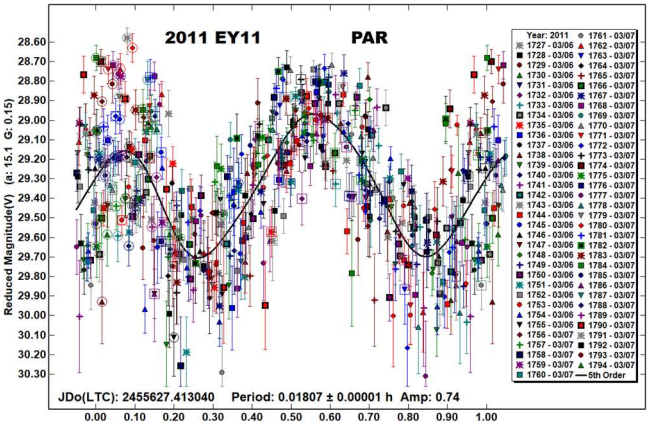

However, more scatter is apparent in the first maxima than the two minima in the bimodal curve, indicating the possibility of tumbling or non-principal axis (NPA) rotation being present. A linearly scaled period spectrum covering periods from 24 - 240 s shows multiple potential solutions and on inspection these appear to consist of two sets of equally spaced values, here labelled P1 (spaced by 32.5 s) and P2 (spaced by 45.2 s).The Dual Period Analysis function in *MPO Canopus* was then used to attempt a NPA solution and even though not designed for this type of analysis it did manage to locate a period of 65 s and, after iterative subtractions, also a secondary period of 90 s, the lightcurves here are labelled P1 and P2 respectively. As the two periods are well resolved it is expected that the rotation may be characterised using the coding described in Pravec et al. (2005) with a PAR code of -3, i.e., *NPA rotation reliably detected with the two periods resolved*. (Petr Pravec, personal communication).

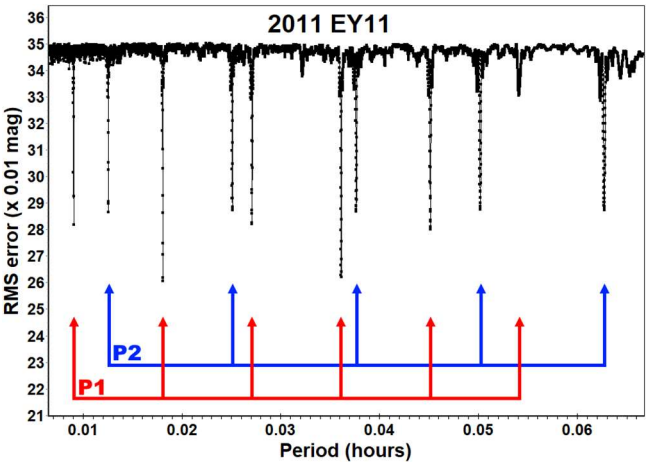

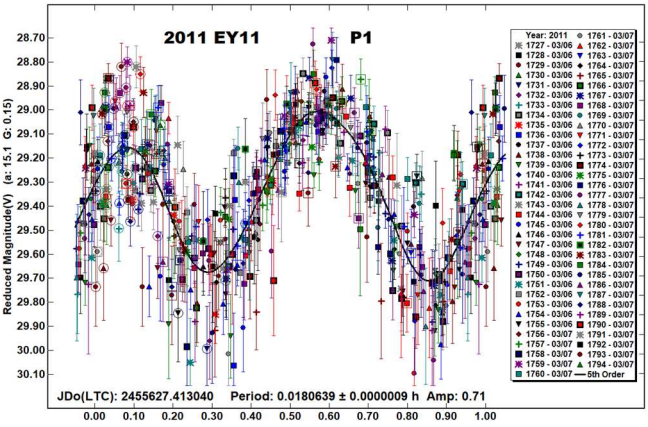

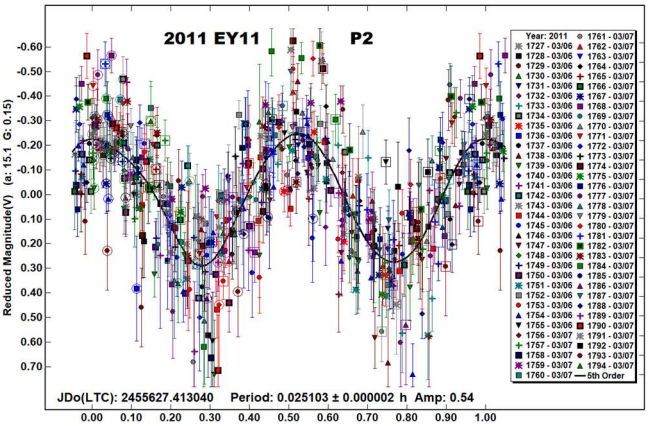

2011 MD. Following discovery by LINEAR on 2011 June 22.26 UTC this asteroid made a very close approach to Earth on 2011 June 27.71 UTC, to 12,300 km of the Earth's surface (Blythe et al., 2011). It has been relatively well studied for such a small body due in part to its potential as a candidate for a spacecraft mission (JPL, 2022b), its diameter being estimated to be in the range 4 - 10 m (Mommert et al., 2014). It was observed for 1.6 h starting on 2011 June 27.01 UTC and photometry was measured using *Astrometrica* in the Gaia G band against reference stars from the Gaia DR2 catalogue. Analysis in *MPO Canopus* resulted in the best fit lightcurve having a period of 0.196361 ± 0.000012 h and amplitude 0.74 ± 0.11 with the RMS of scatter around the Fourier curve being 0.078 magnitudes. There are a number of previously published results listed in the LCDB, all obtained between 2011 June 25 - 28, with Ryan and Ryan (2012) and Skiff et al. (2022) reporting results in close agreement with this determination and Apitzsch (2011web), Franco (2011web) and Vaduvescu et al. (2017)

reporting double that period, near 0.39 h. Trying to fit the longer period to the data points in this paper results in the RMS increasing by 29% to 0.101 magnitudes and a Split Halves plot in *MPO Canopus* shows the two halves matching to within 0.04 magnitudes, supporting the adoption of the shorter period in this determination.

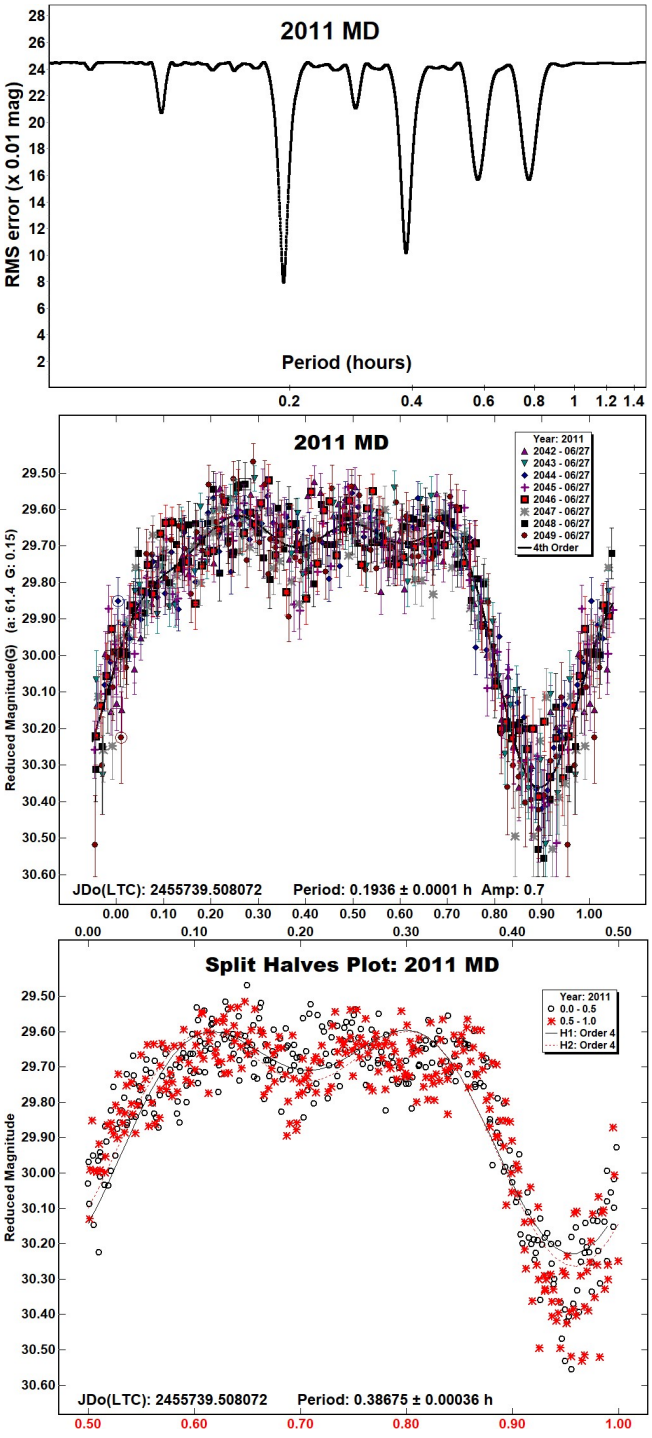

2012 FP35. This small Apollo asteroid was discovered by the Catalina Sky Survey 48 hours before it passed Earth at 0.4 LD (Buzzi et al., 2012). During its final approach it was followed from 2012 Mar 25.841 - 25.948 UTC when the phase angle reduced from 9.6° to a minimum of 9.5°, then increased to 10.6°. After a gap of 2.76 h, it was then followed again from 2012 Mar. 26.063 - 26.088 UTC during which time the phase angle increased from 19.2° to 22.8°. Over the two sets of observations the telescope had to be repositioned a total of 33 times. Apparent speed increased from 100 to 450 arcsec/minute as the distance to the NEO decreased from 1.3 to 0.6 LD, with exposures being reduced from 2 to 1 and finally to 0.5 seconds due to the increasing speed.

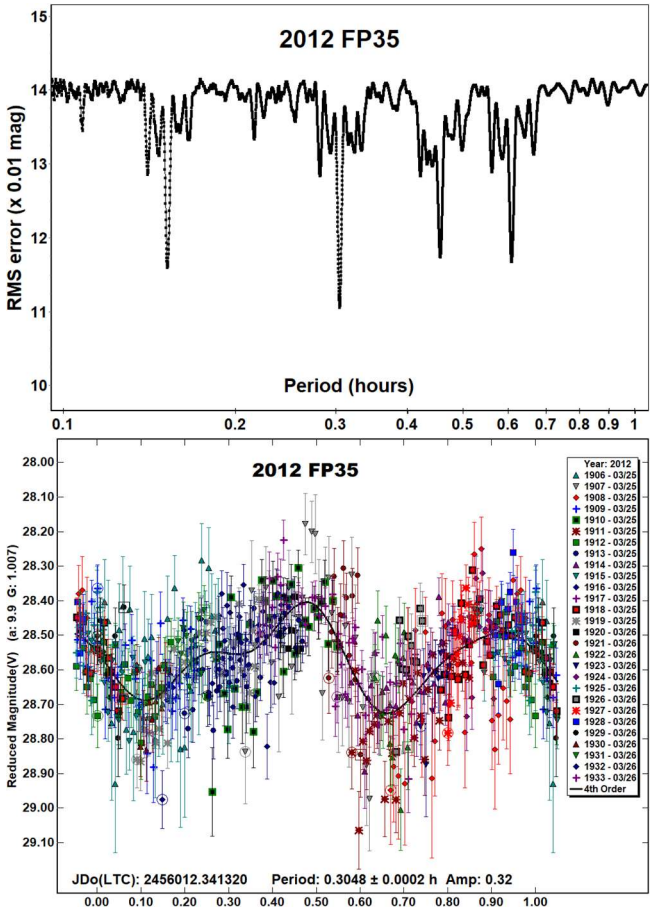

The lightcurve analysis indicated that a phase slope parameter (G) of 0.15 was inadequate to model the observed changes as the phase increased from 9.6° to 22.8°, with less fading observed than was predicted. Therefore, to independently determine the absolute magnitude Hv and the phase slope parameter G, the apparent magnitudes for each of the 33 individual sessions were averaged, corrected for unit distance and entered into the *MPO Canopus* H/G Calculator.

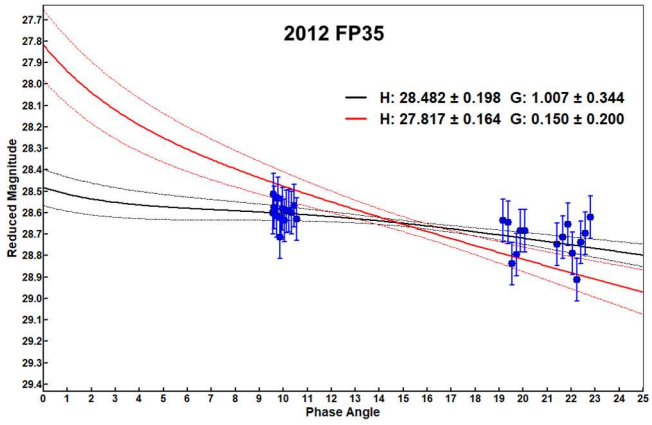

A plot of the resulting best fit solution gives Hv = 28.482 ± 0.198 and G = 1.007 ± 0.344 and is used to produce the phased lightcurve plot. The Minor Planet Center uses a value of Hv = 27.9 using an assumed value of G = 0.15 (MPC, 2022). Forcing the H/G Calculator to use a value of G = 0.15 results in a value of Hv = 27.82 ± 0.16 and G = 0.15 ± 0.20, in good agreement with the MPC, but providing a poorer lightcurve fit.

2016 GP221. Another Catalina Sky Survey discovery, found on 2016 Apr 14.34 UTC (Knoefel et al., 2016) and with H = 25.9 its estimated diameter is ~20 m. It passed Earth at 1.5 LD four days later and was observed for a total of 28 minutes over a period of 1.3 h starting at 2016 Apr 18.03 UTC. Apparent speed rose from 280 to 320 arcsec/minute and exposures were limited to 1 second throughout. The best fit to the 124 measurements gave a rather noisy bimodal lightcurve with a 54 second period and 1 magnitude amplitude.

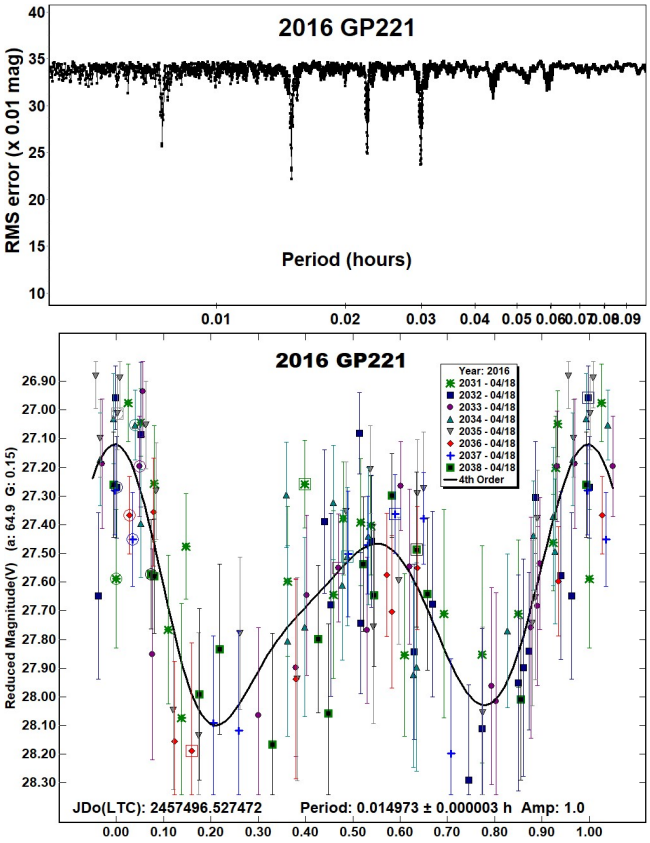

2017 TE5. This was discovered by the Catalina Sky Survey 3 days before an approach to 1.3 LD and with H = 26.0 has an estimated diameter of ~19 m (Janda et al., 2017). It was observed for 4 minutes starting at 2017 Oct 16.900 UTC and then again 4.65 h later for 16 minutes, the telescope needed to be repositioned 3 times for the later imaging due to the high apparent speed of 180 arcsec/min. and exposures were limited to 2 seconds throughout. Analysis of the first set of observations with *MPO Canopus* produced a lightcurve with an amplitude of 0.52 mags and period of 0.02250 ± 0.00015 h, indicating that 2.8 revolutions had been covered in the 4 minutes of observations. The second set of observations also produced a similar lightcurve of amplitude 0.65 mags and a period of 0.022102 ± 0.000013 h, with 12 rotations being covered. Using the latter as the better-defined period, the likely error in number of rotations ΔN between the two sets of observations was estimated using eq. (3) in Kwiatkowski et al. (2010):

$$\Delta N \approx \Delta t \, \Delta P / P^2$$

where Δt is the time interval separating the two lightcurves, P is the period from one of the individual solutions and ΔP is the maximum period uncertainty, with Δt, ΔP and P expressed in the same units. This gives ΔN ≈ 0.1, indicating that the two sets of observations can be matched to a tenth of a rotation and so the two data sets can be unambiguously combined, this producing the phased lightcurve with period of 0.0221192 ± 0.0000006 h. It is noted that there is a zero-point issue between the first and second set of measurements, with the first session requiring an adjustment of -0.18 mags to minimize scatter in the overall lightcurve and this has been applied in the phased curve given here. An equivalent fit can also be obtained using the unusually large value of G = 1.286 which then implies H_v = 27.34, but with observations taken at just two short ranges of phase angles (at 9.3° and 15.4-16.1°) there is not enough data to verify whether that relationship is valid.

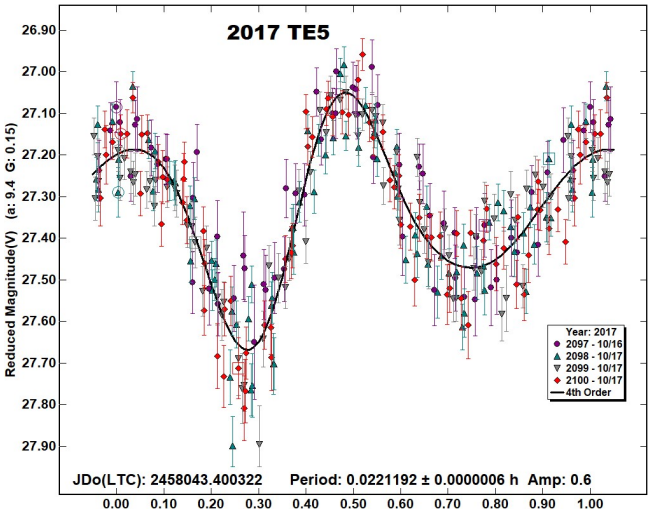

2018 SM1. The Minor Planet Center classifies this object as an Amor because its perihelion distance, q = 1.004 AU is > 1, but using a slightly different definition, the JPL SBDB lists 2018 SM1 as an Apollo, q being less than the Earth's aphelion distance of 1.017 AU and therefore the orbit is considered to be Earth-crossing. With H = 22.9 it has an estimated diameter of ~78m and following discovery by ATLAS on 2018 Sep 18 (Lehmann et al., 2018) it spent the next 9 days between apparent mag +16 and +17. It was followed over three consecutive nights, 2018 Sep 26.9, 27.9 and 29.0 UTC when the ephemeris magnitude was forecast to drop from mag +16.4 to +16.7. Observations were collected on the three nights for 2.7, 2.1 and 1.3 h respectively and raw diagrams of the three nights show variability, with maxima and minima on the last two nights occurring approximately every 25 minutes. However, the first night shows less regular variation and, with the amplitude also decreasing throughout the second night, it is possible that the object may be tumbling. However, the *MPO Canopus* Dual Period Search function could not resolve a consistent solution across all three nights. A phased solution from the second and third nights only is given, indicating an apparent bimodal lightcurve of period 1.598 h. It is suspected that 2018 SM1 is tumbling but not conclusively, so would be rated as PAR = -1 (*NPA rotation possible, some deviations from the single periodicity are seen but not at a conclusive level*) on the scale of Pravec et al. (2005).

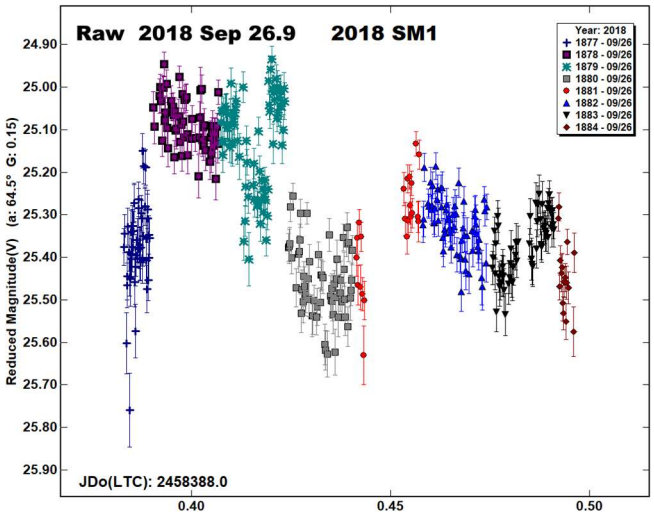

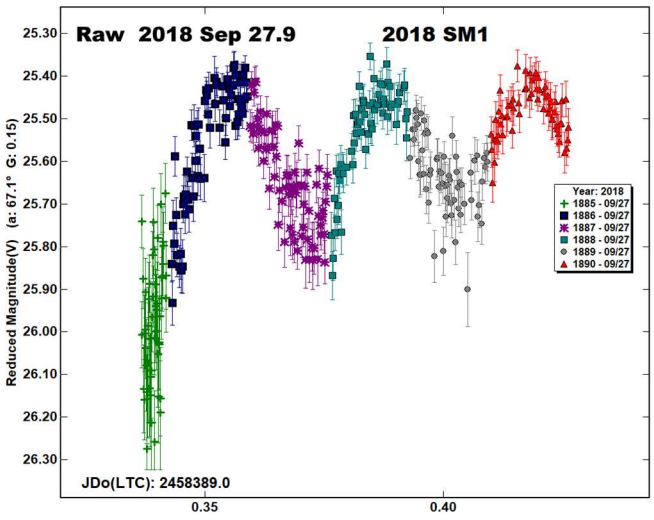

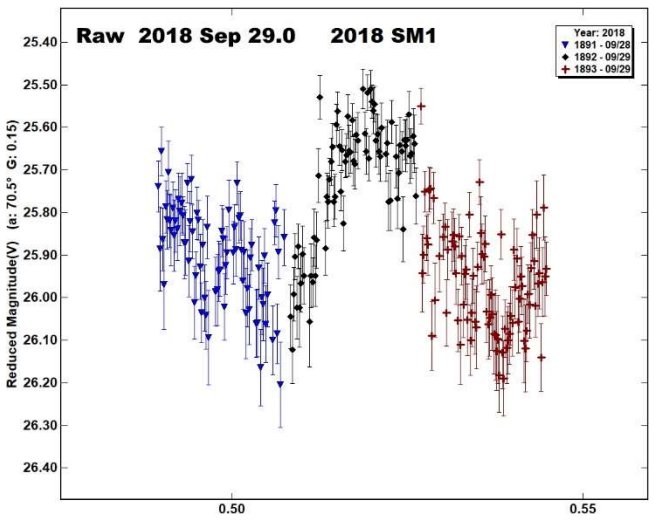

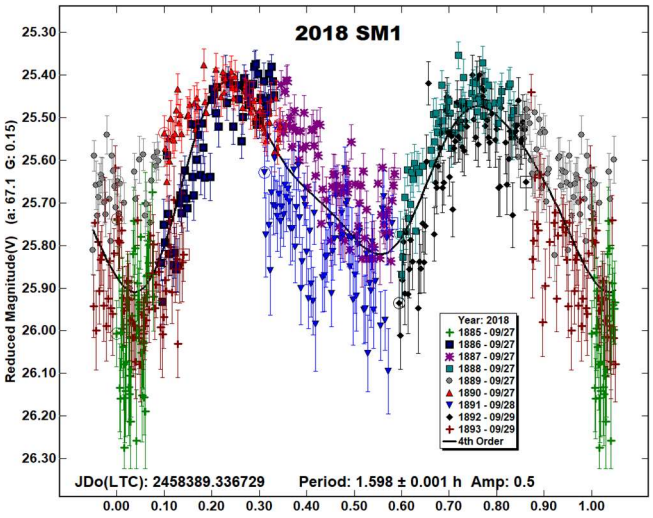

2018 ST1. This Apollo was discovered by the ZTF team at Palomar on 2018 Sept 22.24 UTC and only observed for 65 hours which covered either side of a close approach to 4.3 LD from Earth on 2018 Sept 24.28 UTC (Bacci et al., 2018). It was followed for 4.4 h at Great Shefford starting at 2018 Sept 23.87 UTC. Apparent motion was 85 arcsec/min and 2081 images were obtained, exposures being limited to 2 and 5 s throughout. Visual inspection of the raw images showed large brightness variations with maxima occurring approximately every 15 minutes. However, it was too faint to see on individual images during some minima and therefore, for further analysis the images were stacked using *Astrometrica*. Assuming a bimodal lightcurve, the rotation period was expected to be ~30 minutes, this was used to estimate the optimum effective exposure length Δt for a rotation period P to maximize SNR with minimal lightcurve smoothing, from $\Delta t = 0.185$ P (Pravec et al., 2000). In this case $\Delta t = 0.185 \times 30$ min = 5.6 min was taken as an upper limit on effective exposure length. In case the real period was actually somewhat shorter, the images were then arranged in groups for stacking so that the maximum time from start of first image to end of last image in any one stack was at most 2.5 minutes but generally shorter. Five measurements with a SNR of 3 or less were excluded from the analysis, leaving a total of 155 points from the stacked images for the final analysis. A period spectrum indicates the best fit period to be 0.645 h, or 38.7 min.

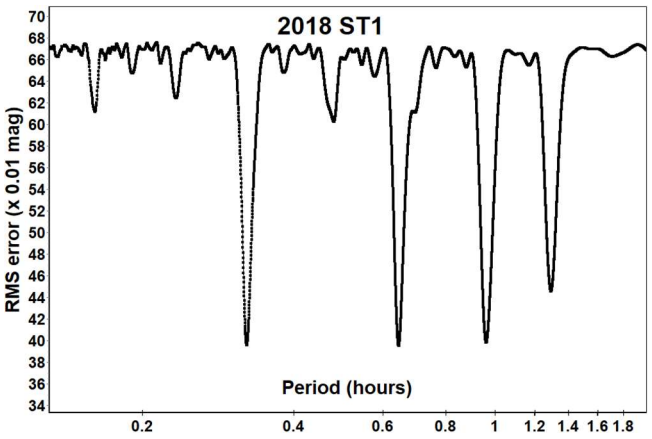

However, the lightcurve, labeled PAR shows significant scatter in places and suggests systematic trends in some of the sets of points.

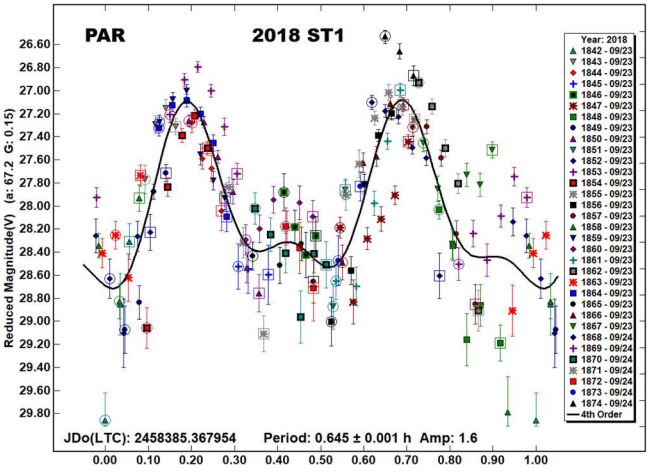

An attempt was therefore made to try and resolve a second period in case non-principal axis (NPA) rotation, or tumbling is present. A number of other less significant minima in the period spectrum hint at solutions and the best fit to a dual-period solution using *MPO Canopus* gives periods of 0.645 and 0.472 h, these two lightcurves are given here, labeled P1 and P2.

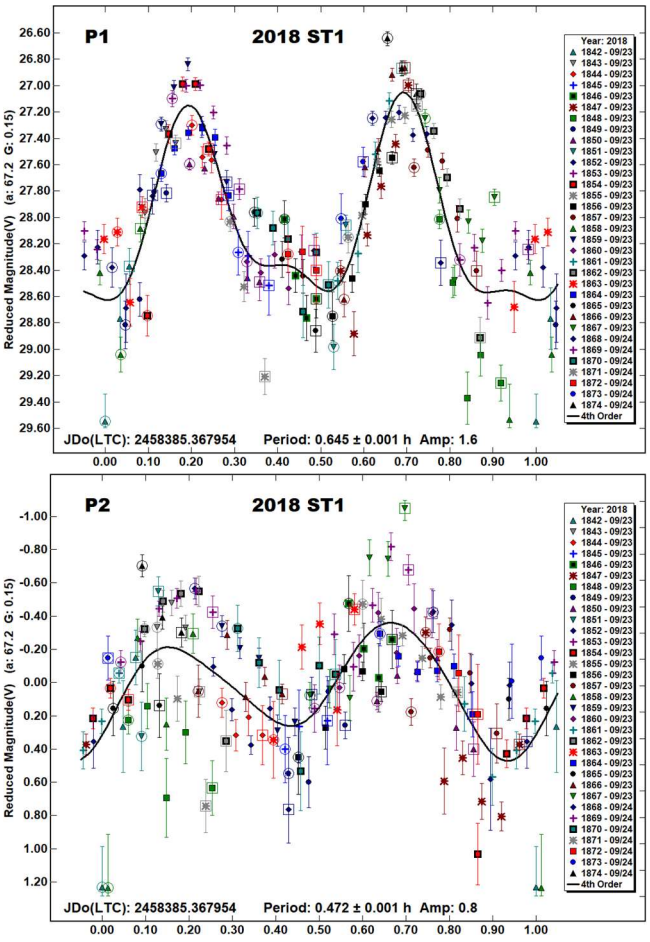

The scatter shown in the dominant and well-defined 0.645 h period P1 lightcurve is reduced but still significant, especially between phase 0.85 and 1.00 and there are obvious problems in the P2 lightcurve throughout. Further attempts at dual-period solutions were less successful and so it is expected that 2018 ST1 may be rated with a PAR code of -2, i.e., *NPA rotation detected based on deviations from the single periodicity but the second period not resolved* (Petr Pravec, personal communication).

The value of H given in the SBDB quotes the MPC derived value of H = 25.1 from MPCORB, based on 43 of the 45 available observations and assuming G = 0.15 (MPC, 2022). The 1-sigma value for the error on H in the SBDB is given as 0.68, presumably a value calculated by JPL, also from the available astrometry, as this is not part of the MPCORB data set. These 43 observations cover a constantly increasing range of phase angles from 38.9 - 98.5°. The lightcurve fitting in this paper results in a value of H_V = 25.6 ± 0.3, also assuming G = 0.15, over phase angles 67.2 - 72.4°. The half magnitude difference in H may be due at least in part to the large observed amplitude, when observed at Great Shefford 2018 ST1 was within 0.1 mag of its predicted peak ephemeris brightness of mag +17.9 and the observed maxima ranged between +17.7 and +16.9 but minima were often +19.5 or fainter. It is possible that the available astrometry may have a bias towards the brighter part of the lightcurve, causing the MPC value of H to be overstated and equivalently, the inferred diameter to be overestimated by ~26%.

2021 LO2. Another small Apollo (H = 28.0, dia. ~7 m) discovered by the Mt. Lemmon Survey on 2021 June 8.33 UTC, it passed Earth at 0.6 LD 5 days later (Bulger et al., 2021). It was observed at a range of 1.4 LD for 70 minutes starting at 2021 June 13.00 UTC. Although relatively bright at 16th magnitude it was at low altitude (17 - 14°), moving rapidly south in a rich star field in southern Ophiuchus and with its apparent speed increasing from 77 to 87 arcsec/min exposures were limited to 5.1 seconds or shorter. Initial analysis with *MPO Canopus* produced the lightcurve labelled PAR, indicating a short rotation period of 41 s. However, multiple minima in the period spectrum suggest there may be tumbling motion present. The period spectrum diagram shows three sets of 4 equally spaced minima, (4 each due to the 4th order Fourier fit utilised) and have been labelled P1, P2 and P3. The 4 minima in each set correspond to monomodal solutions on the left, to quadrimodal on the right and it can be seen that P1, P2 and P3 are commensurate, where approximately (not exactly) 3 P1 = 2 P2 = 1 P3. Using the *MPO Canopus* Dual Period Search function, lightcurves for the dominant P1 period and the next strongest solution, P2 are given here, labelled appropriately. Due to the ambiguity in the secondary solutions, it is expected that 2021 LO2 may be rated with a PAR code of -2, i.e., *NPA rotation detected based on deviations from the single periodicity but the second period not resolved* (Petr Pravec, personal communication).

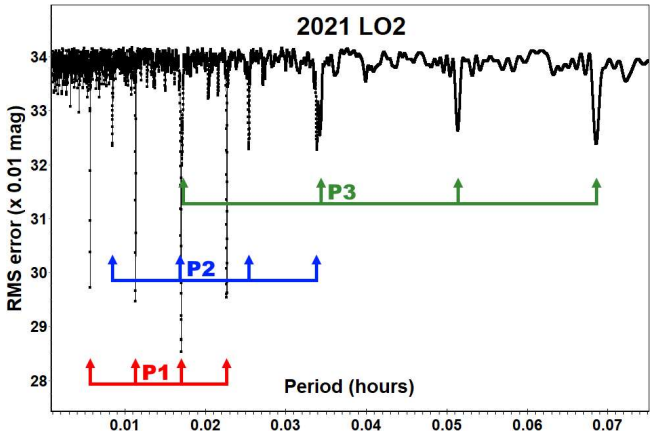

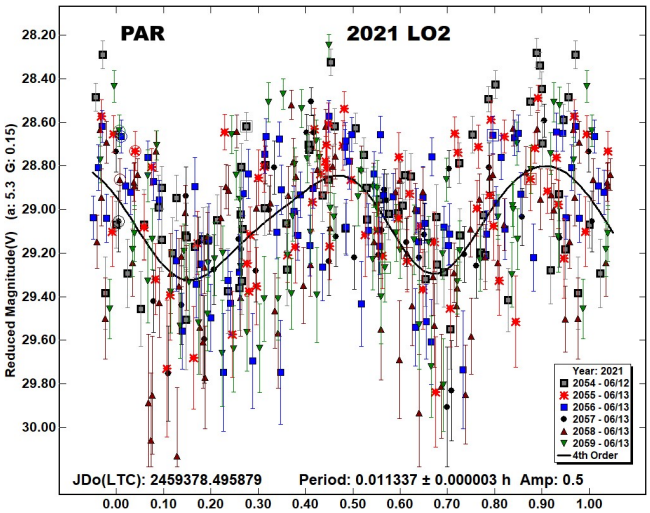

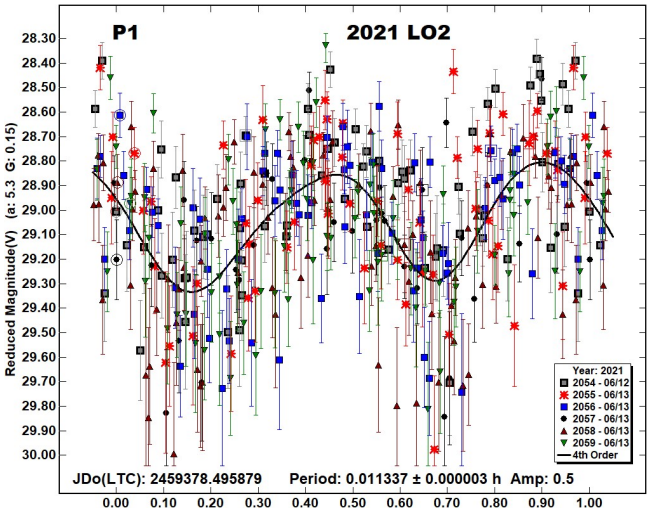

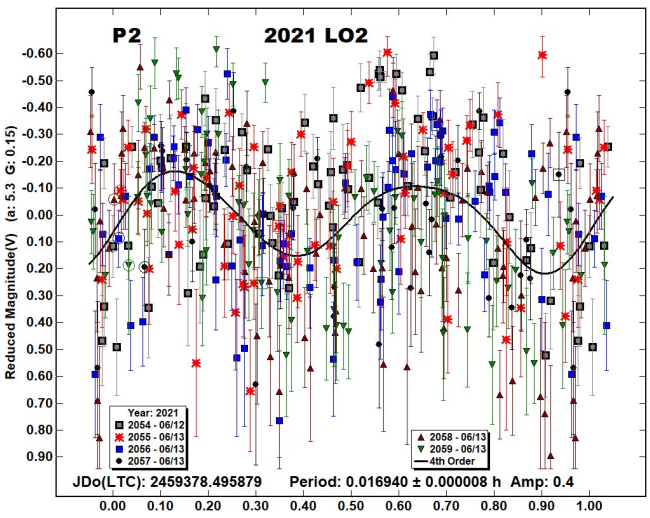

2022 TG. An Apollo with H = 25.1 (estimated dia. ~29 m) which made an approach to within 5 LD of Earth at high southerly declinations 3 days before being discovered by Pan-STARRS 1 on 2022 Oct 2.45 UTC (Coffano et al., 2022). It was observed for 2.8 h starting on 2022 Oct 2.93 UTC when apparent sky motion was 20 arcsec/min. Exposures were 14 s throughout and the telescope was repositioned 6 times. Analysis with *MPO Canopus* indicates a slightly asymmetric bimodal lightcurve and that 14 complete revolutions were covered during the period of observation.

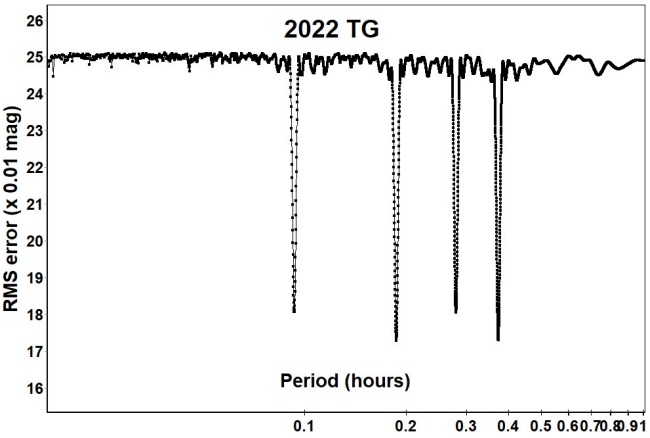

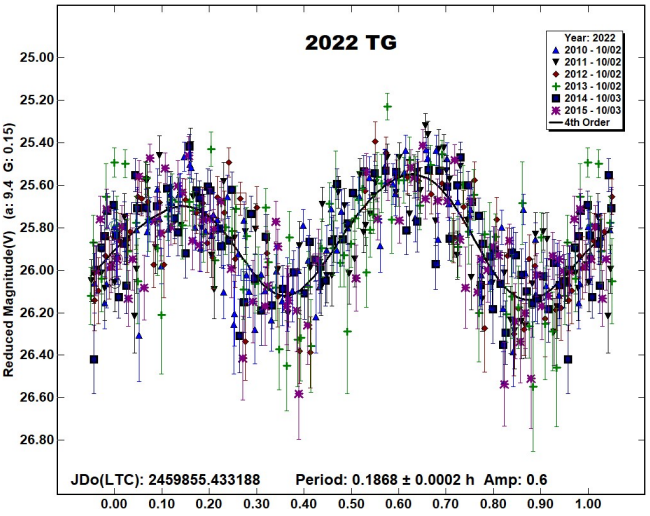

2022 TG1. This was an ATLAS-MLO discovery on 2022 Oct 4.32 UTC made 5 hours after 2022 TG1 passed Earth at 2.8 LD (Bacci et al., 2022). It was observed for a total of 5 h over the nights of 2022 Oct 5 and 6. Initial analysis of the two nights indicated a bimodal lightcurve with a 0.19513 h period, labelled here as PAR. However, both the large amount of scatter in the curve, especially at maxima and also some secondary minima in the period spectrum near 0.13 and 0.26 h suggest there may be tumbling rotation present.

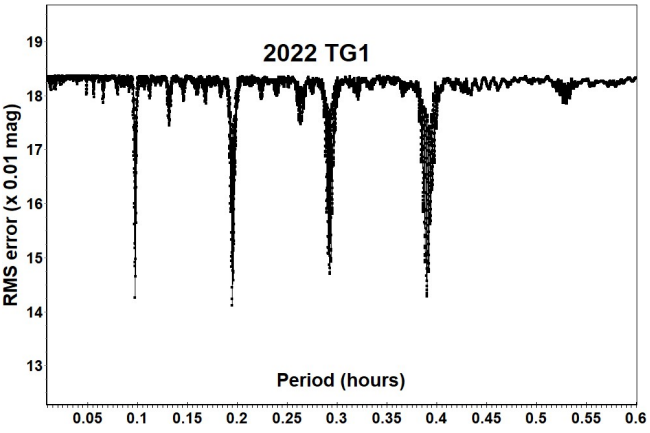

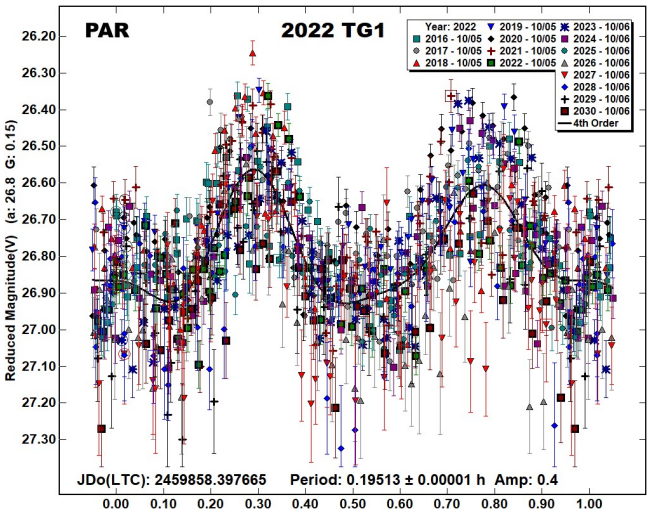

The *MPO Canopus* Dual Period Search was again used and, as well as the dominant 0.19514 h period it also isolated a lower amplitude 0.13176 h secondary period.

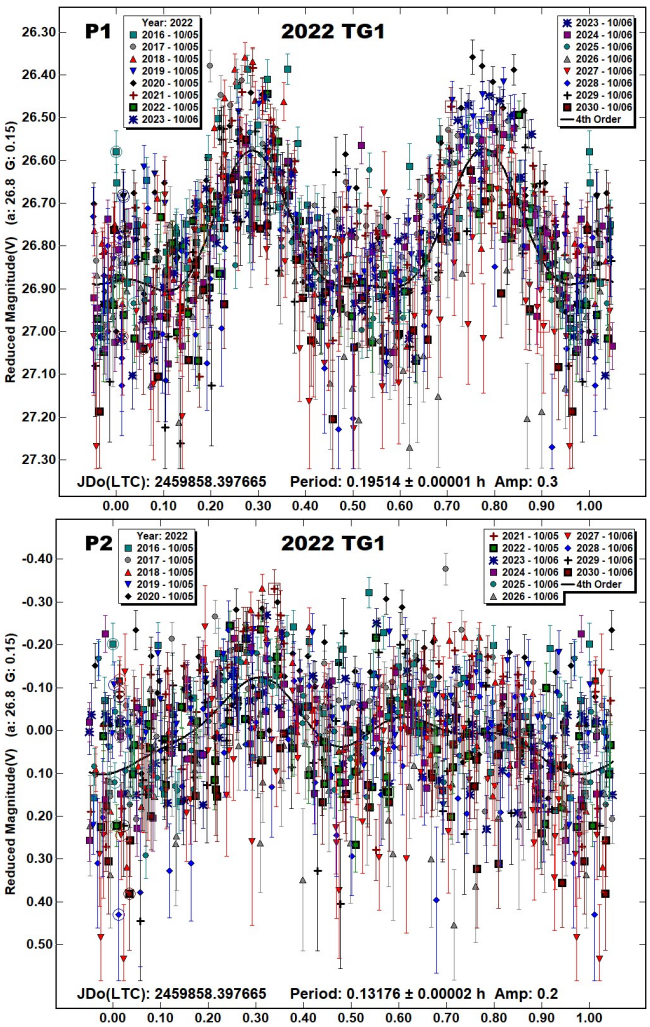

These two curves are given, labelled P1 and P2. It is noted that the two periods are near but not exactly in the ratio 2 P1 = 3 P2. Period P1 is reasonably well defined but the P2 period is not so certain, not helped by the commensurability in the periods, but nevertheless it is clear that 2022 TG1 is tumbling. It is expected that 2022 TG1 may also be rated with a PAR code of -2, i.e., *NPA rotation detected based on deviations from the single periodicity but the second period not resolved* (Petr Pravec, personal communication).

2022 VL1. With H = 26.8 this is a small (~13 m dia.) Apollo, discovered by ATLAS-MLO on 2022 Nov 11.3 UTC (Melnikov et al., 2022) and it passed Earth at 1.2 LD 2 days later on 2022 Nov 13.7 UTC. It was observed for a total of 1.7 h starting on 2022 Nov 12.81 UTC and its apparent speed increased from 75 to 90 arcsec/min. Exposures were reduced from 6.9 to 5.8 seconds to keep the image trails within the measurement annulus in *Astrometrica*. The strongest signals in the period spectrum produced in *MPO Canopus* using a 4th order Fourier fit are multiples of 0.015 h with the best fit being a period of 0.030811 h and the resulting lightcurve is labelled as PAR.

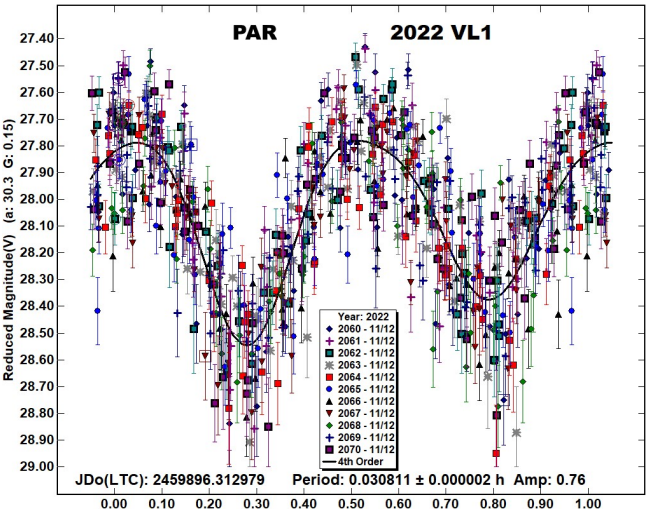

However, the linearly scaled period spectrum also shows a set of weaker solutions at multiples of 0.012 h and using the *MPO Canopus* Dual Period Search two well defined periods of P1 = 0.030811 h and P2 = 0.023860 h are evident and given here labelled P1 and P2.

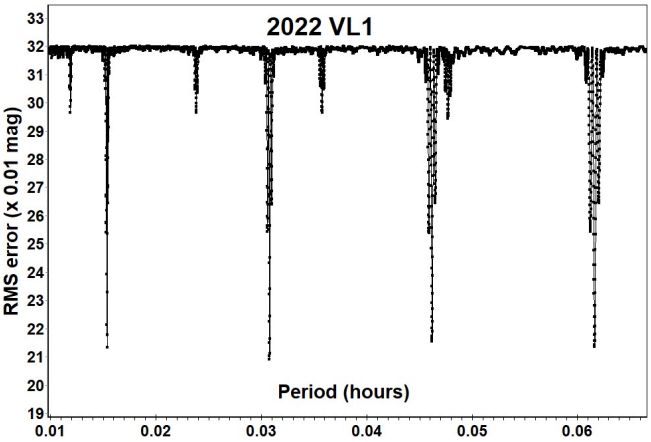

It is therefore expected that it may be rated with a PAR code of -3, i.e., *NPA rotation reliably detected with the two periods resolved*. (Petr Pravec, personal communication).

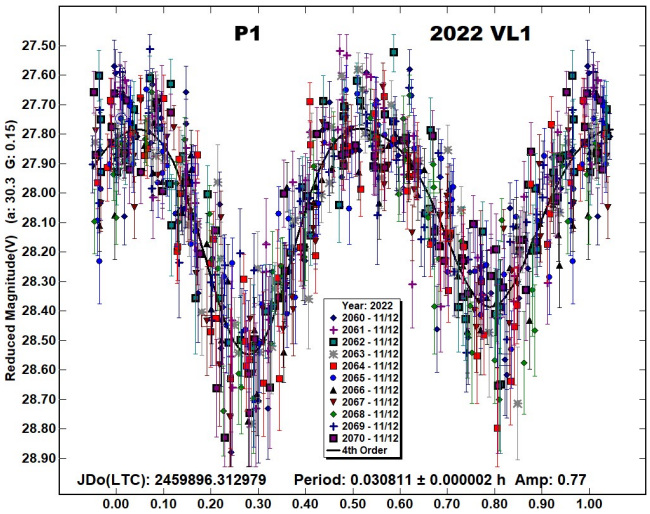

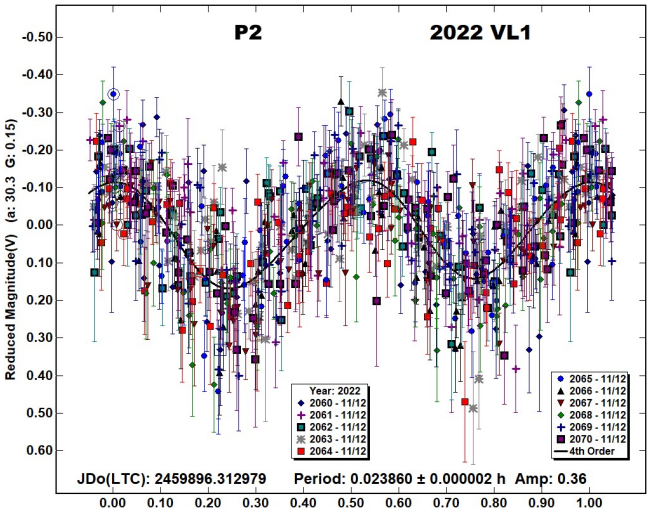

2022 WG5. This Apollo (H = 22.4, est. dia. ~97 m) had been at low solar elongations before being discovered by the Catalina Sky Survey on 2022 Nov 24.51 UTC at a large phase angle of 111°, less than a day after passing Earth at a distance of 4 LD (Serrano et al., 2022). It was observed for 1.0 h starting at 2022 Nov 25.1 UTC when the phase angle had reduced to 96° and for 2.2 h starting 2022 Nov 28.0 UTC at phase angle 65°. Independent period spectrum and phased lightcurve diagrams for the two nights give very similar best fit periods of 0.04413 ± 0.00004 h and 0.04407 ± 0.00001 h, though the shape of the curve has obviously evolved between the two dates. Unusually, the amplitude increased significantly as the phase angle reduced, possibly due to the changing aspect between the two dates if a more equatorial view was presented on the second date compared to the first.

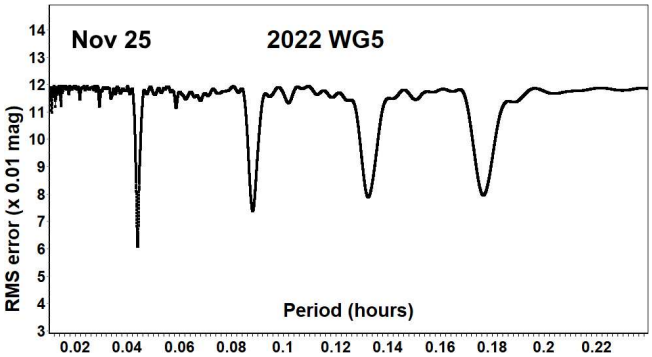

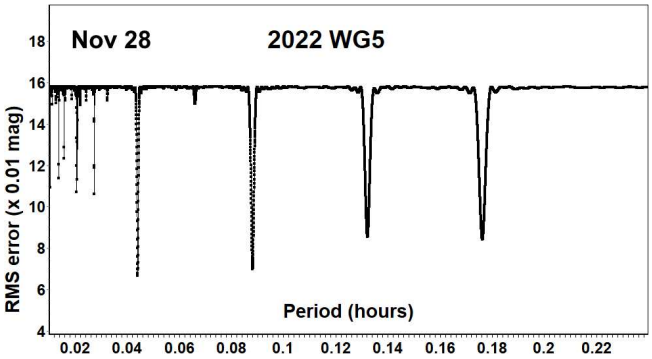

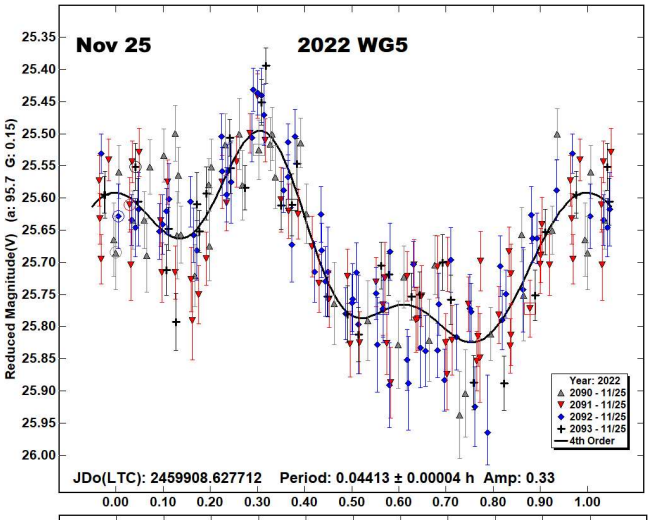

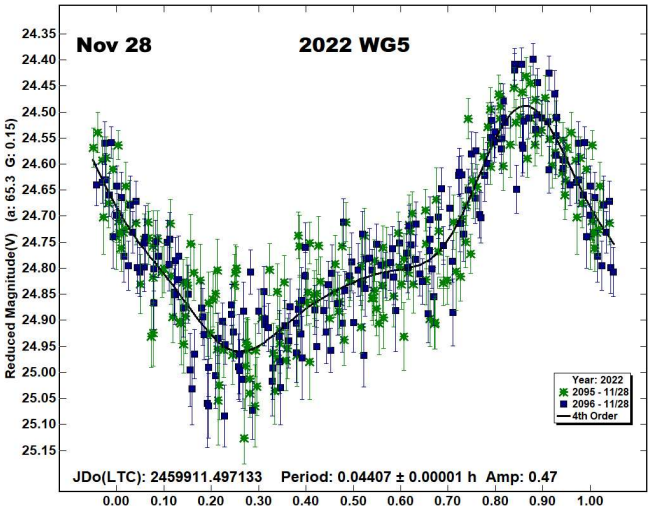

To see whether the results from the two dates could be safely combined to provide a more precise estimate of P, the likely error in number of rotations ΔN between the two dates was again estimated, by propagating the better-defined period from the second date back to the first, using eq. (3) in Kwiatkowski et al. (2010) with the same definitions as given for 2017 TE5:

$$\Delta N \approx \Delta t \, \Delta P / P^2$$

This gives ΔN ≈ 0.34, nominally indicating that, with an error less than half a rotation it should be possible to combine the two data sets unambiguously. However, with the changing shape of the lightcurve and the probable underestimation of the error in P, the actual uncertainty in ΔN is expected to be somewhat larger, therefore, the data from the two dates have not been combined and

the value of P from the second date is selected as the most likely result from this analysis.

Acknowledgements

The author wishes to thank Petr Pravec for his generous help and great patience reviewing analyses of tumbling asteroids. The author also gratefully acknowledges a Gene Shoemaker NEO Grant from the Planetary Society (2005) and a Ridley Grant from the British Astronomical Association (2005), both of which facilitated upgrades to observatory equipment used in this study.

Number	Name	Integration times	Max intg/Pd	Min a/b	Pts	Flds
	2003 EM1	4,10	0.090	1.6	97	5
	2008 EZ7	0.6,1	0.017	1.2	189	11
	2011 EY11	0.5,1	0.015	1.4	524	68
	2011 MD	2	0.003	1.3*	585	8
	2012 FP35	0.5,1,2	0.002	1.2	627	28
	2016 GP221	1	0.019	1.3*	124	8
	2017 TE5	2	0.025	1.5	292	4
	2018 SM1	6-16	0.003	1.2*	1017	17
	2018 ST1	260Σ	0.124	1.9*	155	33
	2021 LO2	4.6-5.1	0.125	1.5	396	6
	2022 TG	14	0.021	1.5	468	6
	2022 TG1	14,20	0.028	1.3	594	15
	2022 VL1	5.8-6.9	0.080	1.7	847	11
	2022 WG5	9.2-20	0.126	1.2*	548	7

Table I. Ancillary information, listing the integration times used (seconds), the fraction of the period represented by the longest integration time (Pravec et al., 2000), the calculated minimum elongation of the asteroid (Kwiatkowski et al., 2010), the number of data points used in the analysis and the number of times the telescope was repositioned to different fields. Note: Σ = Longest elapsed integration time for stacked images (start of first to end of last exposure used), * = Value uncertain, based on phase angle > 40°.

References

ADS (2022). Astrophysics Data System.
https://ui.adsabs.harvard.edu/

Apitzsch, R. (2011web).
http://www.dangl.at/2011/2011_md/2011_md_e.htm

Bacci, P.; Maestripieri, M.; Grazia, M.D.; Tesi, L.; Fagioli, G.; Ye, Q.-Z.; Briggs, D.; Birtwhistle, P.; Rankin, D.; Wells, G.; Bamberger, D. (2018). "2018 ST1." MPEC 2018-S60.
https://minorplanetcenter.net/mpec/K18/K18S60.html

Bacci, P.; Maestripieri, M.; Pettarin, E.; Dupouy, P.; de Vanssay, J.B.; Ivanov, A.; Barcov, A.; Ivanov, V.; Lysenko, V.; Yakovenko, N.; Ivanova, N.; Gorbunov, N.; Kurbatov, G.; Shchukin, P.; Ruocco, N. and 24 colleagues (2022). "2022 TG1." MPEC 2022-T73. *https://minorplanetcenter.net/mpec/K22/K22T73.html*

Behrend, R. (2003web). Observatoire de Geneve web site.
http://obswww.unige.ch/~behrend/page5cou.html

Blythe, M.; Spitz, G.; Brungard, R.; Paige, J.; Festler, P.; McVey, T.; Valdivia, A.; McGaha, J.E.; Sato, H.; Hug, G.; Birtwhistle, P. (2011). "2011 MD." MPEC 2011-M23.
https://minorplanetcenter.net/mpec/K11/K11M23.html

Bulger, J.; Chambers, K.; Lowe, T.; Schultz, A.; Smith, I.; Chastel, S.; Huber, M.; Ramanjooloo, Y.; Wainscoat, R.; Weryk, R.; Leonard, G.J.; Christensen, E.J.; Farneth, G.A.; Fuls, D.C.; Gibbs, A.R. and 11 colleagues (2021). "2021 LO2." MPEC 2021-L88.
https://minorplanetcenter.net/mpec/K21/K21L88.html

Buzzi, L.; Tichy, M.; Ticha, J.; Kocer, M.; Honkova, M.; Sakamoto, T.; Hashimoto, N.; Boattini, A.; Ahern, J.D.; Beshore, E.C.; Garradd, G.J.; Gibbs, A.R.; Tricarico, P.; Grauer, A.D.; Hill, R.E. and 8 colleagues (2012). "2012 FP35." MPEC 2012-F78.
https://minorplanetcenter.net/mpec/K12/K12F78.html

Coffano, A.; Marinello, W.; Micheli, M.; Pizzetti, G.; Soffiantini, A.; Foglia, S.; Galli, G.; Buzzi, L.; Pettarin, E.; Leonard, G.J.; Christensen, E.J.; Fay, D.; Fazekas, J.B.; Fuls, D.C.; Gibbs, A.R. and 54 colleagues (2022). "2022 TG." MPEC 2022-T38.
https://minorplanetcenter.net/mpec/K22/K22T38.html

Franco, L. (2011web).
https://digilander.libero.it/A81_Observatory/7270/index.html

Gilmore, A.C.; Kilmartin, P.M.; McGaha, J.E.; Hill, R.E.; Beshore, E.C.; Boattini, A.; Garradd, G.J.; Gibbs, A.R.; Grauer, A.D.; Kowalski, R.A.; Larson, S.M.; McNaught, R.H.; Ries, J.G.; Birtwhistle, P. (2008). "2008 EZ7." MPEC 2008-E67.
https://minorplanetcenter.net/mpec/K08/K08E67.html

Harris, A.W.; Young, J.W.; Scaltriti, F.; Zappala, V. (1984). "Lightcurves and phase relations of the asteroids 82 Alkmene and 444 Gyptis." *Icarus* **57**, 251-258.

Harris, A.W.; Young, J.W.; Bowell, E.; Martin, L.J.; Millis, R.L.; Poutanen, M.; Scaltriti, F.; Zappala, V.; Schober, H.J.; Debehogne, H.; Zeigler, K. (1989). "Photoelectric Observations of Asteroids 3, 24, 60, 261, and 863." *Icarus* **77**, 171-186.

Hill, R.E.; Ahern, J.D.; Beshore, E.C.; Boattini, A.; Garradd, G.J.; Gibbs, A.R.; Grauer, A.D.; Kowalski, R.A.; Larson, S.M.; McNaught, R.H.; Ryan, W.H.; Ryan, E.V. (2011). "2011 EY11." MPEC 2011-E29.
https://www.minorplanetcenter.net/mpec/K11/K11E29.html

Janda, M.; Tichy, M.; Bacci, P.; Maestripieri, M.; Grazia, M.D.; Fie, N.; Tesi, L.; Fagioli, G.; Jaeger, M.; Prosperi, E.; Prosperi, S.; Vollmann, W.; Ticha, J.; Matheny, R.G.; Christensen, E.J. and 19 colleagues (2017). "2017 TE5." MPEC 2017-U12.
https://minorplanetcenter.net/mpec/K17/K17U12.html

JPL (2022a). Small-Body Database Lookup.
https://ssd.jpl.nasa.gov/tools/sbdb_lookup.html

JPL (2022b). CNEOS NHATS: Accessible NEAs.
https://cneos.jpl.nasa.gov/nhats/details.html#?des=2011%20MD

Knoefel, A.; Okumura, S.; Nimura, T.; Fuls, D.C.; Christensen, E.J.; Gibbs, A.R.; Grauer, A.D.; Johnson, J.A.; Kowalski, R.A.; Larson, S.M.; Leonard, G.J.; Matheny, R.G.; Seaman, R.L.; Shelly, F.C.; Hug, G. (2016). "2016 GP221." MPEC 2016-G176.
https://minorplanetcenter.net/mpec/K16/K16GH6.html

Kwiatkowski, T.; Buckley, D.A.H.; O'Donoghue, D.; Crause, L.; Crawford, S.; Hashimoto, Y.; Kniazev, A.; Loaring, N.; Romero Colmenero, E.; Sefako, R.; Still, M.; Vaisanen, P. (2010). "Photometric survey of the very small near-Earth asteroids with the SALT telescope - I. Lightcurves and periods for 14 objects." *Astronomy & Astrophysics* **509**, A94.

Number	Name	yyyy mm/ dd	Phase	L_{PAB}	B_{PAB}	Period(h)	P.E.	Amp	A.E	PAR	H
	2003 EM1	2003 03/06	29.1-28.4	161	14	0.03097	0.00002	1.0	0.2		24.5
	2008 EZ7	2008 03/09	21.5-40.5	183	5	0.016514	0.000002	0.36	0.15		27.0
	2011 EY11	2011 03/06	*15.5-39.2	177	-3	0.0180639	0.0000009	0.7	0.3	-3	28.5
						0.025103	0.000002	0.5	0.3		
	2011 MD	2011 06/27	61.1-60.8	258	26	0.1936	0.0001	0.7	0.1		28.0
	2012 FP35	2012 03/25-03/26	*9.6-22.9	179	3	0.3047	0.0002	0.33	0.15		27.9
	2016 GP221	2016 04/18	65.0-71.6	238	18	0.014973	0.000003	1.0	0.3		25.9
	2017 TE5	2017 10/16-10/17	9.3-16.1	21	5	0.0221191	0.0000006	0.6	0.1		26.0
	2018 SM1	2018 09/26-09/29	64.5-70.7	24	29	1.598	0.001	0.5	0.3	-1	22.9
	2018 ST1	2018 09/23-09/24	67.2-72.4	21	30	0.645	0.001	2.2	0.4	-2	25.1
	2021 LO2	2021 06/12-06/13	5.1-3.9	260	1	0.011337	0.000003	0.5	0.4	-2	28.0
						0.016940	0.000008	0.4	0.4		
	2022 TG	2022 10/02-10/03	9.3-10.0	14	3	0.1868	0.0002	0.6	0.2		25.1
	2022 TG1	2022 10/05-10/06	26.8-26.7	8	13	0.19514	0.00001	0.3	0.2	-2	25.6
						0.13176	0.00002	0.2	0.2		
	2022 VL1	2022 11/12	30.4-30.3	35	-4	0.030811	0.000002	0.8	0.2	-3	26.8
						0.023860	0.000002	0.4	0.2		
	2022 WG5	2022 11/25-11/28	95.9-65.0	96	27	0.04407	0.00001	0.5	0.1		22.4

Table II. Observing circumstances and results. The phase angle is given for the first and last date. If preceded by an asterisk, the phase angle reached an extrema during the period. LPAB and BPAB are the approximate phase angle bisector longitude/latitude at mid-date range (see Harris et al., 1984). Amplitude error (A.E.) is calculated as √2 × (lightcurve RMS residual). PAR is the expected Principal Axis Rotation quality detection code (Pravec et al., 2005) and H is the absolute magnitude at 1 au from Sun and Earth taken from the Small-Body Database Lookup (JPL, 2022a).

Lehmann, G.; Lehmann, K.; Gajdos, S.; Jaeger, M.; Prosperi, E.; Prosperi, S.; Vollmann, W.; Buzzi, L.; Pittichova, J.; Wiggins, P.; Durig, D.T.; Robson, M.; Marmaropoulou, D.; Emmerich, M.; Melchert, S. and 32 colleagues (2018). "2018 SM1." MPEC 2018-S47. *https://minorplanetcenter.net/mpec/K18/K18S47.html*

Melnikov, S.; Hoegner, C.; Ludwig, F.; Stecklum, B.; Tichy, M.; Ticha, J.; Honkova, M.; Janda, M.; Hug, G.; Zoltowski, F.B.; Ikari, Y.; Dupouy, P.; Felber, T.; Birtwhistle, P.; Korlevic, K. and 17 colleagues (2022). "2022 VL1." MPEC 2022-V132. *https://minorplanetcenter.net/mpec/K22/K22VD2.html*

Mommert, M.; Farnocchia, D.; Hora, J.L.; Chesley, S.R.; Trilling, D.E.; Chodas, P.W.; Mueller, M.; Harris, A.W.; Smith, H.A.; Fazio, G.G. (2014). "Physical Properties of Near-Earth Asteroid 2011 MD." *ApJL* **789,** L22.

MPC (2022). Minor Planet Center. MPCORB data file. *https://www.minorplanetcenter.net/iau/MPCORB.html*

Pravec, P.; Hergenrother, C.; Whiteley, R.; Sarounova, L.; Kusnirak, P.; Wolf, M. (2000). "Fast Rotating Asteroids 1999 TY2, 1999 SF10, and 1998 WB2." *Icarus* **147**, 477-486.

Pravec, P.; Harris, A.W.; Scheirich, P.; Kušnirák, P.; Šarounová, L.; Hergenrother, C.W.; Mottola, S.; Hicks, M.D.; Masi, G.; Krugly, Yu.N.; Shevchenko, V.G.; Nolan, M.C.; Howell, E.S.; Kaasalainen, M.; Galád, A. and 5 colleagues. (2005). "Tumbling Asteroids." *Icarus* **173**, 108-131.

Raab, H. (2018). Astrometrica software, version 4.12.0.448. *http://www.astrometrica.at/*

Ryan, E.V.; Ryan, W.H. (2012). Advanced Maui Optical and Space Surveillance Technologies Conference. *http://www.amostech.com/TechnicalPapers/2012/Astronomy/RYAN.pdf*

Serrano, A.; Christensen, E.J.; Fay, D.; Fazekas, J.B.; Fuls, D.C.; Gibbs, A.R.; Grauer, A.D.; Groeller, H.; Hogan, J.K.; Kowalski, R.A.; Larson, S.M.; Leonard, G.J.; Rankin, D.; Seaman, R.L.; Shelly, F.C. and 9 colleagues (2022). "2022 WG5." MPEC 2022-W178. *https://minorplanetcenter.net/mpec/K22/K22WH8.html*

Skiff, B.A.; McLelland, K.P.; Sanborn, J.J.; Koehn, B.W.; Bowell, E. (2022). "Lowell Observatory Near-Earth Asteroid Photometric Survey (NEAPS): Paper 5." *Minor Planet Bulletin* **50**, 74-101.

Tichy, M.; Dintinjana, B.; Skvarc, J.; Gajdos, S.; Toth, J.; Yeung, B.; McClusky, J.; Stevens, B.; Gilmore, A.C.; Kilmartin, P.M.; Sanchez, S.; Stoss, R.; Trentman, R.; Glaze, M.; McGaha, J.E. and 7 colleagues (2003) "2003 EM1" MPEC 2003-E28. *https://minorplanetcenter.net/mpec/K03/K03E28.html*

Vaduvescu, O.; Aznar Macias, A.; Tudor, V.; Predatu, M.; Galád, A.; Gajdoš, Š.; Világi, J.; Stevance, H.F.; Errmann, R.; Unda-Sanzana, E.; Char, F.; Peixinho, N.; Popescu, M.; Sonka, A.; Cornea, R. and 12 colleagues (2017). "The EURONEAR Lightcurve Survey of Near Earth Asteroids." *Earth, Moon, and Planets* **120**, 41-100.

Warner, B.D.; Harris, A.W.; Pravec, P. (2009). "The Asteroid Lightcurve Database." *Icarus* **202**, 134-146. Updated 2021 Dec. *https://minplanobs.org/mpinfo/php/lcdb.php*

Warner, B.D. (2022). MPO Software, Canopus version 10.8.6.12. Bdw Publishing, Colorado Springs, CO.

Zacharias, N.; Finch, C.T.; Girard, T.M.; Henden, A.; Bartlett, J.L.; Monet, D.G.; Zacharias, M.I. (2013). "The Fourth US Naval Observatory CCD Astrograph Catalog (UCAC4)." *The Astronomical Journal* **145**, 44-57.

LIGHTCURVES AND SYNODIC ROTATION PERIODS FOR 17 ASTEROIDS FROM SOPOT ASTRONOMICAL OBSERVATORY: 2022 JUNE – 2023 JANUARY

Vladimir Benishek
Belgrade Astronomical Observatory
Volgina 7, 11060 Belgrade 38, SERBIA
vlaben@yahoo.com

(Received: 2023 January 15)

This summary report presents the lightcurve and synodic rotation period results derived using photometric data for 17 asteroids obtained at the Sopot Astronomical Observatory in the time span 2022 June - 2023 January.

Photometric observations of 17 asteroids were conducted at Sopot Astronomical Observatory (SAO) from 2022 June through 2023 January in order to determine the asteroids' synodic rotation periods. For this purpose, two 0.35-m *f*/6.3 Meade LX200GPS Schmidt-Cassegrain telescopes were employed. The telescopes are equipped with a SBIG ST-8 XME and a SBIG ST-10 XME CCD cameras. The exposures were unfiltered and unguided for all targets. Both cameras were operated in 2×2 binning mode, which produces image scales of 1.66 arcsec/pixel and 1.25 arcsec/pixel for ST-8 XME and ST-10 XME cameras, respectively. Prior to measurements, all images were corrected using dark and flat field frames.

Photometric reduction was conducted using *MPO Canopus* (Warner, 2018). Differential photometry with up to five comparison stars of near solar color ($0.5 \leq$ B-V ≤ 0.9) was performed using the Comparison Star Selector (CSS) utility. This helped ensure a satisfactory quality level of night-to-night zero-point calibrations and correlation of the measurements within the standard magnitude framework. Field comparison stars were calibrated using standard Cousins R magnitudes derived from the Carlsberg Meridian Catalog 15 (VizieR, 2022) Sloan r' magnitudes using the formula: R = r' - 0.22 in all cases presented in this paper. In some instances, small zero-point adjustments were necessary in order to achieve the best match between individual data sets in terms of achieving the most favorable statistical indicators of Fourier fit goodness.

Lightcurve construction and period analysis was performed using *Perfindia* custom-made software developed in the R statistical programming language (R Core Team, 2020) by the author of this paper. The essence of its algorithm is reflected in finding the most favorable solution for rotational period by minimizing the *residual standard error* of the lightcurve Fourier fit.

The lightcurve plots presented in this paper show so-called 2% error for rotational periods, i.e., an error that would cause the last data point in a combined data set by date order to be shifted by 2% (Warner, 2012) and represented by the following formula:

$$\Delta P = (0.02 \cdot P^2) / T$$

where P and T are the rotational period and the total time span of observations, respectively. Both of these quantities must be expressed in the same units.

Some of the targets presented in this paper were observed within the Photometric Survey for Asynchronous Binary Asteroids (*BinAstPhot Survey*) under the leadership of Dr Petr Pravec from Ondřejov Observatory, Czech Republic.

Table I gives the observing circumstances and results.

Observations and results

1589 Fanatica. Photometric observations were carried out over two nights in 2022 December - 2023 January at SAO, indicating a bimodal result for the synodic rotational period of P = 2.5808 ± 0.0008 h as the statistically most favorable solution. This result is consistent with most previous rotation period determinations: 2.58 h (Warner, 2004), 2.582 h (Stephens, 2015), 2.578 h (Stephens and Warner, 2019), 2.58144 h (Pál et al., 2020), and 2.5832 h (Stephens and Warner, 2020).

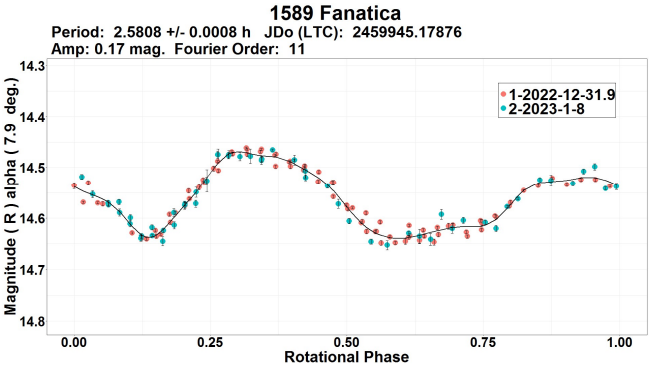

1636 Porter. A bimodal lightcurve phased to a period of P = 2.9660 ± 0.0004 h emerges as the most favorable solution in period analysis conducted over 6 datasets obtained in 2022 December - 2023 January. Previously found rotation period results by Albers et al. (2010, 2.9653 h), Behrend (2014web, 2.9658 h), and a sidereal one by Durech et al. (2020, 2.965591 h) are very close to the newly established value.

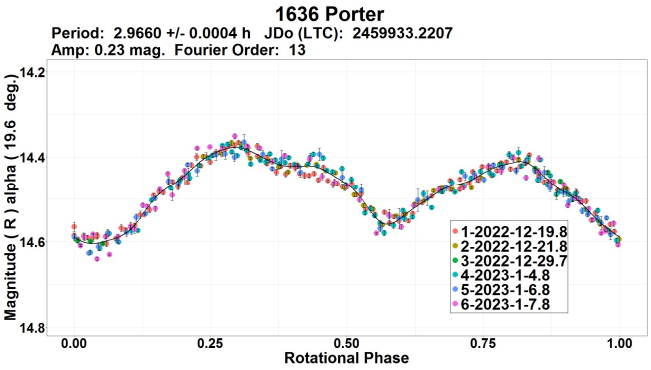

1756 Giacobini. There is no substantial difference between a bimodal period solution (P = 3.854 ± 0.003 h) found from the SAO data taken over four nights in 2023 January and previous period determinations by Warner (2007, 3.8527 h), Behrend (2018web, 3.85311 h), and Stephens and Warner (2019, 3.854 h).

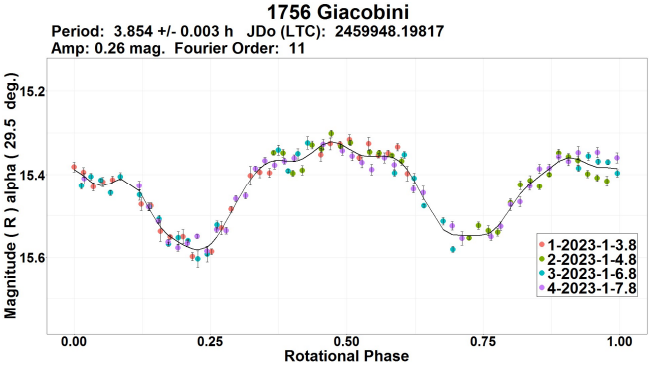

1857 Parchomenko. The four-night 2022 November SAO photometric data yielded a large-amplitude (> 0.3 mag.) bimodal lightcurve phased to a period of P = 3.1174 ± 0.0007 h. Period determinations consistent with the nelwly determined result found in the Asteroid Lightcurve Database (LCDB; Warner et al., 2009) are by Stephens et al. (2006, 3.1177 h), Behrend (2008web, 3.08 h), and a sidereal period value by Durech et al. (2020, 3.117177 h).

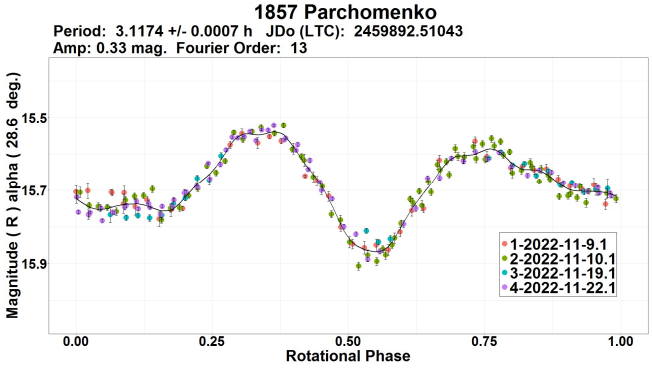

2151 Hadwiger. Photometric datasets obtained over two consecutive nights in 2022 November show a unique bimodal rotation period of P = 5.87 ± 0.03 h. This result is in full accordance with a number of previously obtained rotation periods found in the LCDB: 5.872 h (Sada et al., 2005), 5.87 h (Kim et al., 2014), 5.870 h and 5.871 h (Waszczak et al., 2015), and 5.870 h (Benishek, 2021).

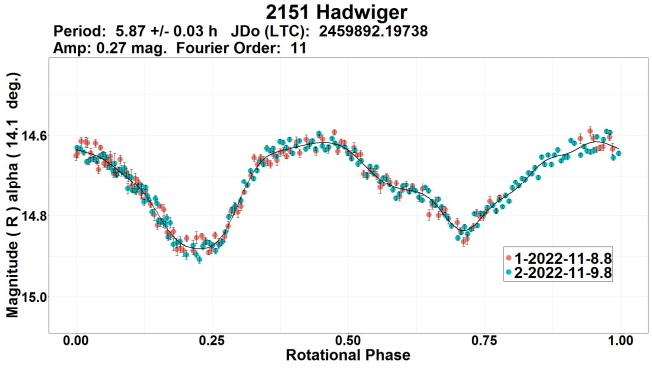

2243 Lonnrot. The only prior rotation period determination is by Marchini et al. (2021, 3.813 h). The relevant bimodal lightcurve associated with this only previous period result is quite noisy and consists of small number of data points obtained over two observing nights. An uncertainty flag of U = 2 has been assigned to this result in the LCDB. A somewhat different value for rotation period of P = 3.680 ± 0.005 h was obtained at SAO using the considerably less scattered photometric data collected on three consecutive nights in 2022 November showing a bimodal lightcurve with an amplitude of 0.11 mag.

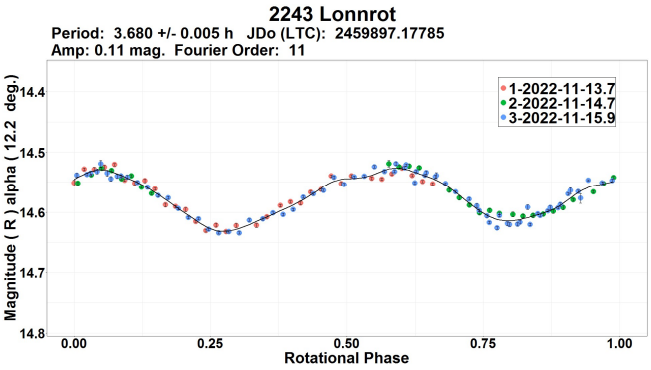

2820 Iisalmi. Behrend (2020web) found a value of 2.7580 h for rotation period, which is the only previously known rotation period determination according to the LCDB. An almost exactly identical result for period (P = 2.7579 ± 0.0004 h) was obtained using the SAO data from five datasets acquired in 2022 October - November.

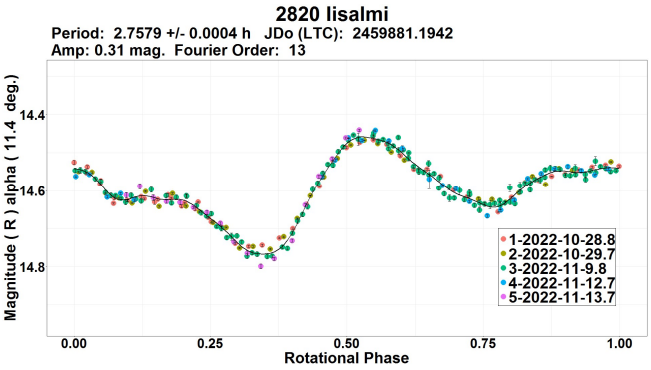

3180 Morgan. According to the LCDB records this is the first rotation period determination for this asteroid. Period analysis conducted upon a dense photometric composite dataset obtained on six nights in 2022 October indicates an unambiguous bimodal solution for a synodic rotation period of P = 2.4477 ± 0.0003 h.

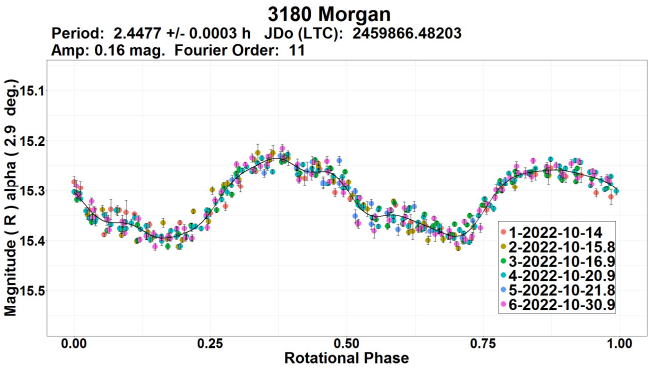

3382 Cassidy. An unequivocal bimodal period solution of $P = 4.2530 \pm 0.0009$ h derived from the dense six-night combined SAO dataset obtained in 2022 October is fully consistent with all previously determined rotation periods found in the LCDB: 4.258 h (Pravec, 2012web), 4.254 h (Risley, 2013), 4.253 h (Waszczak et al., 2015) and a sidereal period of 4.25310 h by Durech et al. (2020).

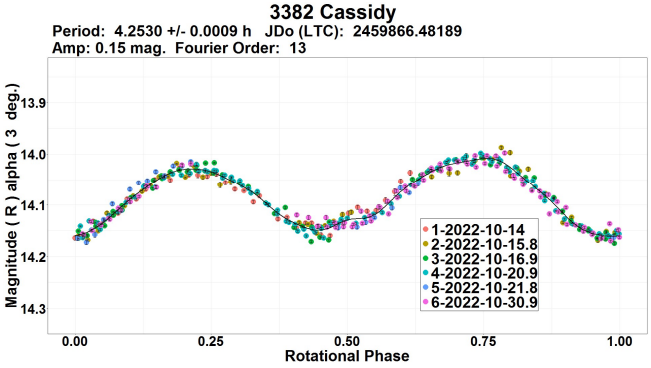

3385 Bronnina. Period analysis of observations obtained over three nights in 2022 October - November led to a unique bimodal period solution of $P = 2.959 \pm 0.003$ h. In this case the obtained result is highly consistent with most of the previous deteminations, as well. Some of these are as follows: 2.95893 h, 2.95897 h, and 2.95877 by Dykhuis et al. (2016), 2.95911 h (Benishek, 2020), 2.959 h (Franco et al., 2021), and a sidereal period by Durech et al. (2020, 2.958806 h).

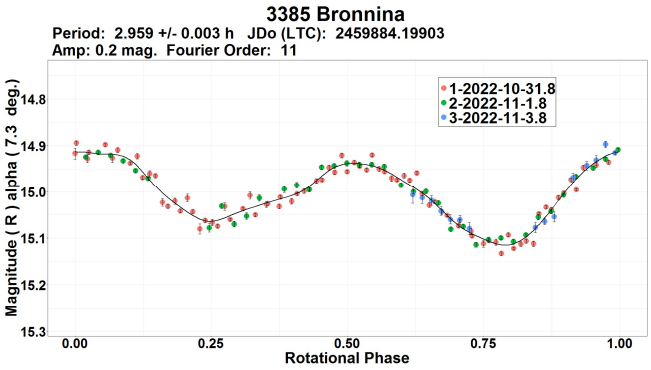

4338 Velez. A search of LCDB records show the only previous period reference by Waszczak et al. (2015, 3.166 h and 3.162 h). These results are in full agreement with the bimodal period solution of $P = 3.1692 \pm 0.0006$ h shown here.

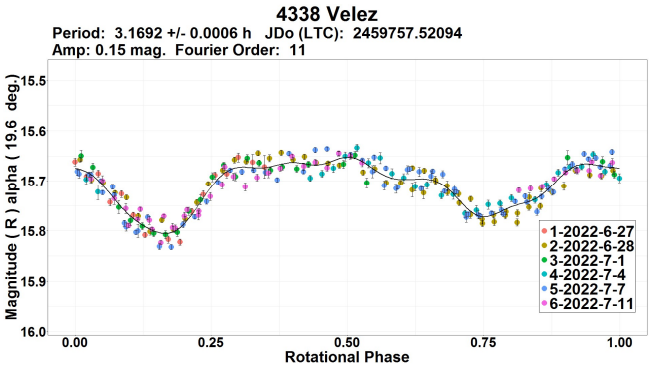

4497 Taguchi. Data obtained on two consecutive nights in 2022 November at SAO indicate a unique bimodal period result of $P = 3.58 \pm 0.01$ h. A comparison with previous period determinations indicates clear agreement with a range of the following results: 3.563 h (Almeida et al., 2004), 3.57 h (Behrend, 2008web), 3.567 h (Behrend, 2012web), 3.563 h (Warner, 2013), and Pál et al. (3.5639 h, 2020).

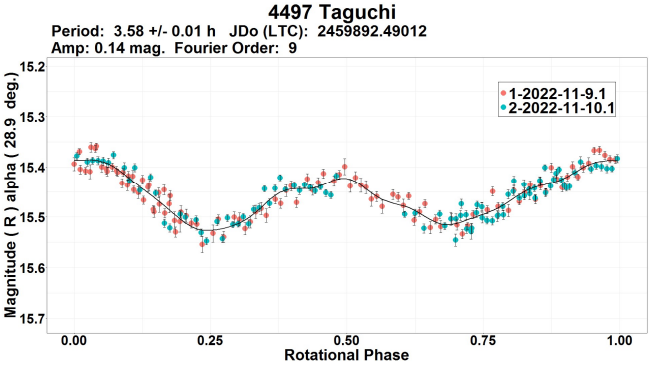

6363 Doggett. No prior rotation period determination records were present in the LCDB. Data taken over four nights in 2022 December - 2023 January yielded a unique period solution of $P = 4.299 \pm 0.004$ h associated with a bimodal lightcurve with a considerable amplitude of 0.26 mag.

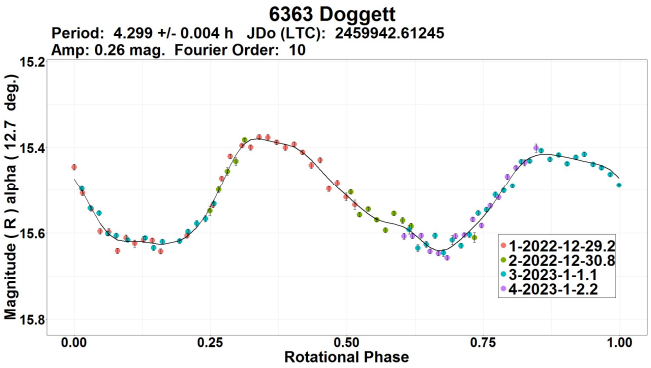

(7357) 1995 UJ7. No records on previous rotation period determinations for this *BinAstPhot Survey* target were found in the LCDB. Photometric observations carried out at SAO on seven nights in 2022 August reveal a bimodal lightcurve phased to a period of $P = 2.8511 \pm 0.0004$ h as a statistically most favorable solution.

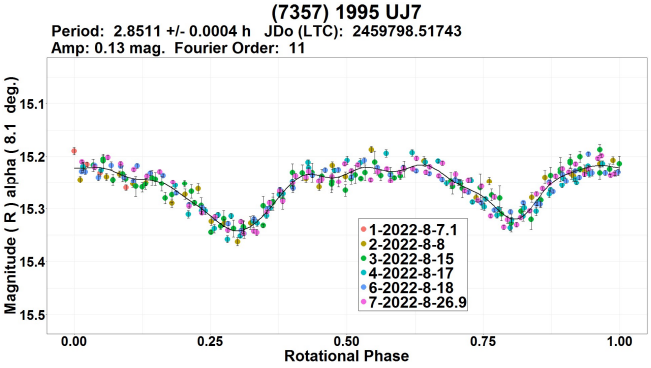

8548 Sumizihara. Waszczak et al. (2015) found a synodic rotation period of 3.192 h, which is fairly close to the bimodal period of P = 3.187 ± 0.008 h obtained from the SAO data obtained on two consecutive nights in early 2023 January.

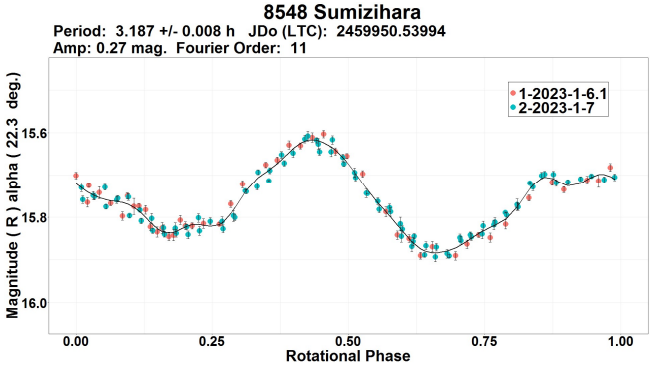

(50379) 2000 CB89. Pál et al. (2020) reported the only prior result for rotation period of 2.99993 h. A bimodal period solution of P = 2.9982 h obtained from the 2022 September - October SAO data firmly corroborates the previously found result.

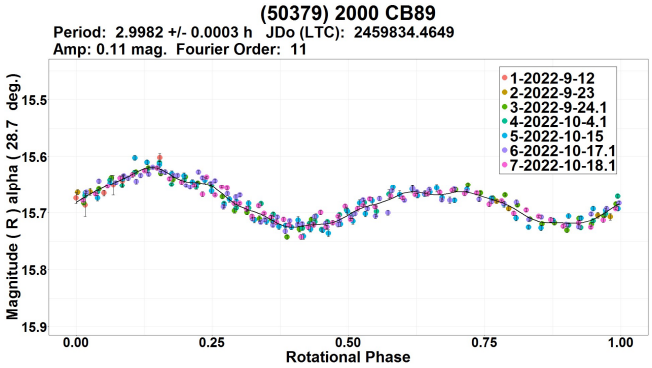

(70411) 1999 SF3. A *BinAstPhot Survey* target observed within this survey back in 2014 by Donald Pray, when from the obtained data Pravec (2014web) found a rotation period of 2.8420 h. An exactly identical value for period (P = 2.842 ± 0.002 h) was found from the 2023 January SAO data acquired on four nights.

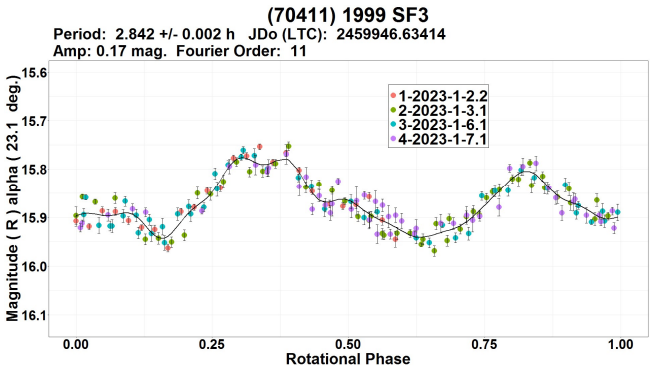

Acknowledgements

Observational work at Sopot Astronomical Observatory is generously supported by Gene Shoemaker NEO Grants awarded by the Planetary Society in 2018 and 2022.

References

Albers, K.; Kragh, K.; Monnier, A.; Pligge, Z.; Stolze, K.; West, J.; Yim, A.; Ditteon, R. (2010). "Asteroid Lightcurve Analysis at the Oakley Southern Sky Observatory: 2009 October thru 2010 April." *Minor Planet Bull.* **37**, 152-158.

Almeida, R.; Angeli, C.A.; Duffard, R.; Lazzaro, D. (2004). "Rotation periods for small main-belt asteroids." *Astronomy and Astrophysics* **415**, 403-406.

Behrend, R. (2008web, 2012web, 2014web, 2018web, 2020web). Observatoire de Geneve web site. *http://obswww.unige.ch/~behrend/page_cou.html*

Benishek, V. (2020). "Photometry of 39 Asteroids at Sopot Astronomical Observatory: 2019 September - 2020 March." *Minor Planet Bull.* **47**, 231-241.

Benishek, V. (2021). "Photometry of 30 Asteroids at Sopot Astronomical Observatory: 2020 February - October." *Minor Planet Bull.* **48**, 77-83.

Durech, J.; Tonry, J.; Erasmus, N.; Denneau, L.; Heinze, A.N.; Flewelling, H.; Vančo, R. (2020). "Asteroid models reconstructed from ATLAS photometry." *Astron. Astrophys*. **643**, A59-A63.

Dykhuis, M.J.; Molnar, L.A.; Gates, C.J.; Gonzales, J.A.; Huffman, J.J.; Maat, A.R.; Maat, S.L.; Marks, M.I.; Massey-Plantinga, A.R.; McReynolds, M.D.; Schut, J.A.; Stoep, J.P.; Stutzman, A.J.; Thomas, B.C.; Vander Tuig, G.W. and 2 colleagues (2016). "Efficient spin sense determination of Flora-region asteroids via the epoch method." *Icarus* **267**, 174-203.

Franco, L.; Marchini, A.; Iozzi, M.; Scarfi, G.; Montigiani, N.; Mannucci, M.; Aceti, P.; Banfi, M.; Mortari, F.; Galli, G.; Bacci, P.; Maestripieri, M.; Valvasori, A.; Guido, E. (2021). "Collaborative Asteroid Photometry from UAI: 2021 April - June." *Minor Planet Bull.* **48**, 372-374.

Kim, M.-J.; Choi, Y.-J.; Moon, H.-K.; Byun, Y.-I. and 12 colleagues (2014). "Rotational Properties of the Maria Asteroid Family." *Astron. J.* **147**, A56.

Marchini, A.; Cavaglioni, L.; Privitera, C.A.; Papini, R.; Salvaggio, F. (2021). "Rotation Period Determination for Asteroids 2243 Lonnrot, (10859) 1995 GJ7, (18640) 1998 EF9, and (49483) 1999 BP13." *Minor Planet Bull.* **48**, 206-208.

Pál, A.; Szakáts, R.; Kiss, C.; Bódi, A.; Bognár, Z.; Kalup, C.; Kiss, L.L.; Marton, G.; Molnár, L.; Plachy, E.; Sárneczky, K.; Szabó, G.M.; Szabó, R. (2020). "Solar System Objects Observed with TESS - First Data Release: Bright Main-belt and Trojan Asteroids from the Southern Survey." *Ap. J. Supl. Ser.* **247**, 26-34.

Number	Name	20yy/mm/dd	Phase	L_{PAB}	B_{PAB}	Period (h)	P.E.	Amp	A.E.	Grp
1589	Fanatica	22/12/31-23/01/08	7.9,11.4	85	0	2.5808	0.0008	0.17	0.02	MB-I
1636	Porter	22/12/19-23/01/07	19.6,25.6	58	-6	2.9660	0.0004	0.23	0.02	FLOR
1756	Giacobini	23/01/03-23/01/07	29.5,29.6	36	5	3.854	0.003	0.26	0.03	MB-I
1857	Parchomenko	22/11/09-22/11/22	28.6,26.4	110	-3	3.1174	0.0007	0.33	0.02	MB-I
2151	Hadwiger	22/11/08-22/11/09	14.1,14.6	14	-2	5.87	0.03	0.27	0.03	MAR
2243	Lonnrot	22/11/13-22/11/15	12.2,13.3	32	3	3.680	0.005	0.11	0.01	FLOR
2820	Iisalmi	22/10/28-22/11/13	11.4,19.6	20	-1	2.7579	0.0004	0.31	0.02	FLOR
3180	Morgan	22/10/13-22/10/31	2.9,12.5	19	4	2.4477	0.0003	0.16	0.02	MB-I
3382	Cassidy	22/10/13-22/10/31	12.4,3.0	19	4	4.2530	0.0009	0.15	0.02	FLOR
3385	Bronnina	22/10/31-22/11/03	7.3,8.8	25	-2	2.959	0.003	0.20	0.02	MB-I
4338	Velez	22/06/27-22/07/11	19.6,13.0	303	9	3.1692	0.0006	0.15	0.02	FLOR
4497	Taguchi	22/08/11-22/11/10	28.9,28.6	101	-1	3.58	0.01	0.14	0.03	MB-I
6363	Doggett	22/12/29-23/01/02	12.7,10.7	116	8	4.299	0.004	0.26	0.02	MB-I
7357	1995 UJ7	22/08/07-22/08/27	*8.1,4.6	326	0	2.8511	0.0004	0.13	0.02	MB-I
8548	Sumizihara	23/01/06-23/01/07	22.3,21.9	142	-2	3.187	0.008	0.27	0.02	MB-I
50379	2000 CB89	22/09/11-22/10/18	28.7,15.3	39	-14	2.9982	0.0003	0.11	0.01	MB-I
70411	1999 SF3	23/01/02-23/01/07	23.1,21.1	140	-11	2.842	0.002	0.17	0.03	PHO

Table I. Observing circumstances and results. Phase is the solar phase angle given at the start and end of the date range. If preceded by an asterisk, the phase angle reached an extrema during the period. L_{PAB} and B_{PAB} are the average phase angle bisector longitude and latitude. Grp is the asteroid family/group (Warner *et al.*, 2009): FLOR = Flora, MAR = Maria, MB-I = main-belt inner, PHO = Phocaea, EUN = Eunomia.

Pravec, P. (2012web, 2014web). Photometric Survey for Asynchronous Binary Asteroids web site. *http://www.asu.cas.cz/~ppravec/newres.txt*

R Core Team (2020). R: A language and environment for statistical computing. R Foundation for Statistical Computing. Vienna, Austria. *https://www.R-project.org/*

Risley, E. (2013). "3382 Cassidy: A Short Period Asteroid." *Minor Planet Bull.* **40**, 80-81.

Sada, P.V.; Canizales, E.D.; Armada, E.M. (2005). "CCD photometry of asteroids 651 Antikleia, 738 Alagasta, and 2151 Hadwiger using a remote commercial telescope." *Minor Planet Bull.* **32**, 73-75.

Stephens, R.D.; Warner, B.D.; Pravec, P. (2006). "1857 Parchomenko: a possible main-belt binary asteroids. " *Minor Planet Bull.* **33**, 52.

Stephens, R.D. (2015). "Asteroids Observed from CS3: 2014 July - September." *Minor Planet Bull.* **42**, 70-74.

Stephens, R.D.; Warner, B.D. (2019). "Main-belt Asteroids Observed from CS3: 2018 October - December." *Minor Planet Bull.* **46**, 180-187.

Stephens, R.D.; Warner, B.D. (2020). "Main-belt Asteroids Observed from CS3: 2020 January to March." *Minor Planet Bull.* **47**, 224-230.

VizieR (2022). *http://vizier.u-strasbg.fr/viz-bin/VizieR*

Warner, B.D. (2004). "Lightcurve analysis for numbered asteroids 1351, 1589, 2778, 5076, 5892, and 6386." *Minor Planet Bull.* **31**, 36-39.

Warner, B.D. (2007). "Asteroid Lightcurve Analysis at the Palmer Divide Observatory – September - December 2006." *Minor Planet Bull.* **34**, 32-37.

Warner, B.D.; Harris, A.W.; Pravec, P. (2009). "The Asteroid Lightcurve Database." *Icarus* **202**, 134-146. Updated 2021 Dec 14. *http://www.minorplanet.info/lightcurvedatabase.html*

Warner, B.D. (2012). *The MPO Users Guide: A Companion Guide to the MPO Canopus/PhotoRed Reference Manuals*. BDW Publishing, Eaton, CO.

Warner, B.D. (2013). "Asteroid Lightcurve Analysis at CS3-Palmer Divide Station: 2013 May-June." *Minor Planet Bull.* **40**, 208-212.

Warner, B.D. (2018). MPO Canopus software, version 10.7.11.3. *http://www.bdwpublishing.com*

Waszczak, A.; Chang, C.-K.; Ofek, E.O.; Laher, R.; Masci, F.; Levitan, D.; Surace, J.; Cheng, Y.-C.; Ip, W.-H.; Kinoshita, D.; Helou, G.; Prince, T.A.; Kulkarni, S. (2015). "Asteroid Light Curves from the Palomar Transient Factory Survey: Rotation Periods and Phase Functions from Sparse Photometry." *Astron. J.* **150**, A75.

ASTEROID PHOTOMETRY AND LIGHTCURVES OF TWELVE ASTEROIDS – JANUARY 2023

Milagros Colazo
Instituto de Astronomía Teórica y Experimental (IATE-CONICET), ARGENTINA
Facultad de Matemática, Astronomía y Física, Universidad Nacional de Córdoba, ARGENTINA
Grupo de Observadores de Rotaciones de Asteroides (GORA), ARGENTINA
https://aoacm.com.ar/gora/index.php
milirita.colazovinovo@gmail.com

Bruno Monteleone, Alberto García, Mario Morales, Francisco Santos, Néstor Suárez, Damián Scotta, César Fornari, Aldo Wilberger, Raúl Melia, Ricardo Nolte, Ariel Stechina, Giuseppe Ciancia, Marcos Anzola, Ezequiel Bellocchio, Andrés Chapman, Aldo Mottino, Carlos Colazo.

Grupo de Observadores de Rotaciones de Asteroides (GORA), ARGENTINA

Estación Astrofísica Bosque Alegre (MPC 821) - Bosque Alegre (Córdoba-ARGENTINA)

Complejo Astronómico El Leoncito (829) - Calingasta (San Juan-ARGENTINA)

Observatorio Astronómico Giordano Bruno (MPC G05) - Piconcillo (Córdoba-ESPAÑA)

Observatorio Astronómico El Gato Gris (MPC I19) - Tanti (Córdoba- ARGENTINA)

Observatorio Cruz del Sur (MPC I39) - San Justo (Buenos Aires- ARGENTINA)

Observatorio de Sencelles (MPC K14) - Sencelles (Mallorca-Islas Baleares- ESPAÑA)

Osservatorio Astronomico "La Macchina del Tempo" (MPC M24) Ardore Marina (Reggio Calabria-ITALY)

Observatorio Los Cabezones (MPC X12) - Santa Rosa (La Pampa- ARGENTINA)

Observatorio Galileo Galilei (MPC X31) - Oro Verde (Entre Ríos- ARGENTINA)

Observatorio Antares (MPC X39) - Pilar (Buenos Aires- ARGENTINA)

Observatorio Río Cofio (MPC Z03) - Robledo de Chavela (Madrid-ESPANA)

Observatorio AstroPilar (GORA APB) - Pilar (Buenos Aires- ARGENTINA)

Specola "Giuseppe Pustorino 3" (GORA GC3) - Palizzi Marina (Reggio Calabria-ITALY)

Observatorio de Ariel Stechina 1 (GORA OAS) - Reconquista (Santa Fe- ARGENTINA)

Observatorio de Damián Scotta 1 (GORA ODS) - San Carlos Centro (Santa Fe- ARGENTINA)

Observatorio de Damián Scotta 2 (GORA OD2) - San Carlos Centro (Santa Fe- ARGENTINA)

Observatorio Astronómico Vuelta por el Universo (GORA OMA) - Córdoba (Córdoba- ARGENTINA)

Observatorio Ricardo Nolte (GORA ORN) - Córdoba (Córdoba- ARGENTINA)

Observatorio de Raúl Melia Carlos Paz (GORA RMG) - Carlos Paz (Córdoba- ARGENTINA)

(Received: 2023 January 18)

Synodic rotation periods and amplitudes are reported for 622 Esther, 783 Nora, 879 Ricarda, 960 Birgit, 1048 Feodosia, 1543 Bourgeois, 2035 Stearns, 2052 Tamriko, 2243 Lonnrot, 4376 Shigemori, 4429 Chinmoy, and 4538 Vishyanand.

The periods and amplitudes of asteroid lightcurves presented here are the product of collaborative work by GORA (Grupo de Observadores de Rotaciones de Asteroides). In all the studies, we have applied relative photometry assigning V magnitudes to the calibration stars.

Image acquisition was performed without filters and with exposure times of a few minutes. All images used were corrected using dark frames and, in some cases, bias and flat-fields were also used. Photometry measurements were performed using *FotoDif* software and for the analysis, we employed *Periodos* software (Mazzone, 2012).

Below, we present the results for each asteroid under study. The lightcurve figures contain the following information: the estimated period and period error and the estimated amplitude and amplitude error. In the reference boxes, the columns represent, respectively, the marker, observatory MPC code, or - failing that - the GORA internal code, session date, session offset, and several data points.

Targets were selected based on the following criteria: 1) those asteroids with magnitudes accessible to the equipment of all participants, 2) those with favorable observation conditions from Argentina, Spain, or Italy, i.e., with negative or positive declinations δ, respectively, and 3) objects with few periods reported in the literature and/or with Asteroid Lightcurve Database (LCDB; Warner et al., 2009) quality codes (U) of less than 3.

622 Esther is an S-type asteroid discovered in 1906 by J. F. Metcalf. The two more recent periods published in the literature correspond to $P = 47.5042 \pm 0.0005$ h (Hanuš et al., 2011) and $P = 47.5039 \pm 0.0005$ h (Hanuš et al., 2016). We have determined a period of 47.413 ± 0.014 h, which is consistent with those previous results.

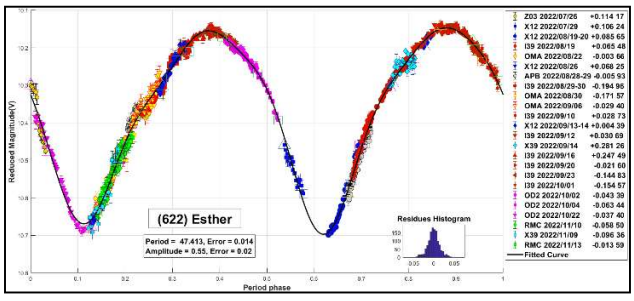

783 Nora was discovered in 1914 by J. Palisa. Several periods were measured for this asteroid with the following results: P = 24 h (Lagerkevist et al., 1992), P = 34.4 ± 0.5 h (Florczak et al., 1997), P = 9.6 h (Behrend, 2007web), and P = 55.53 ± 0.08 h (Polakis, 2018). The results we obtained, P = 56.153 ± 0.011 h with Δm = 0.12 ± 0.02 mag, are consistent with the longer period proposed by Polakis.

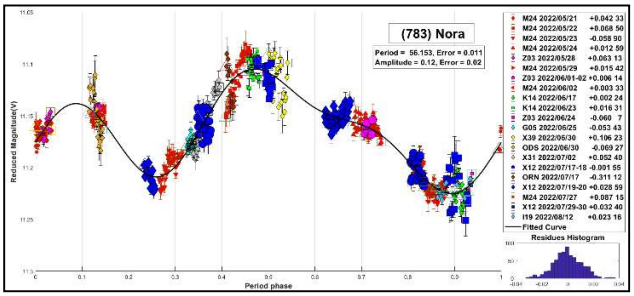

879 Ricarda was discovered in 1917 by M. Wolf. The most recent period published in the literature corresponds to P = 82.9 ± 0.5 h (Kim et al., 2014). In this work, we provide rather different results and propose a longer period of P = 134.748 ± 0.020 h and Δm = 0.9 ± 0.03 mag.

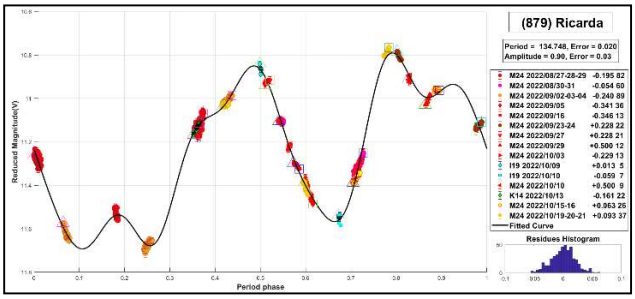

960 Birgit was discovered in 1921 by K. Reinmuth. We found in the literature two rather different periods calculated for this object: P = 17.3558 ± 0.0005 h with Δm = 0.25 ± 0.01 mag (Behrend, 2005web) and P = 8.85 ± 0.05 h with Δm = 0.28 ± 0.02 mag (Kryszczyńska et al., 2012). The results we obtained are P = 9.572 ± 0.024 h and Δm = 0.15 ± 0.03 mag. Our period agrees well with the one measured by Kryszczyńska.

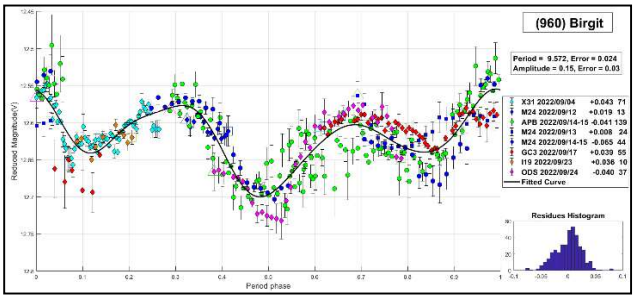

1048 Feodosia is an XC-type asteroid discovered in 1924 by K. Reinmuth. We found two different periods reported in the literature: P = 23 ± 1 h with Δm = 0.04 ± 0.01 mag (Behrend, 2007web) and P = 10.417 ± 0.001 h with Δm = 0.09 ± 0.05 mag (Franco, 2021). In contrast to these reports, our analysis yields a period of P = 15.635 ± 0.006 h with Δm = 0.03 ± 0.01 mag.

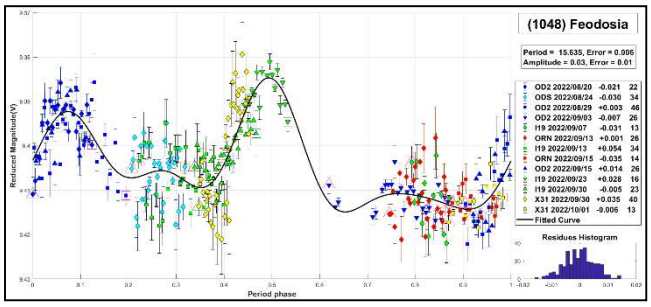

1543 Bourgeois was discovered in 1941 by E. Delporte. In the literature, we found only one reported period for this asteroid: P = 2.48 ± 0.01 h with Δm = 0.03 ± 0.01 mag (Behrend, 2005web). In this work, we propose a much longer period of P = 29.587 ± 0.006 h with Δm = 0.09 ± 0.01 mag.

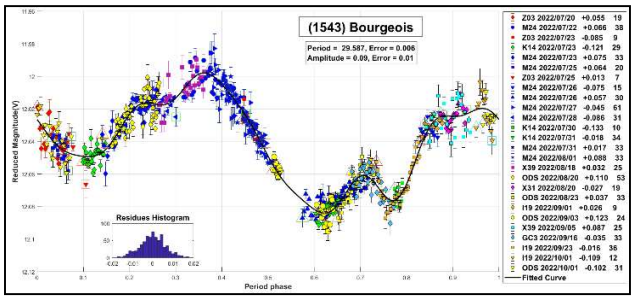

2035 Stearns is an E-type asteroid discovered in 1973 by J. Gibson. Several periods were measured for this asteroid with the following results: P = 85.0 ± 0.1 h (Schevchenko et al., 2003), P = 51.89 ± 0.20 h (Warner, 2011), and P = 93 ± 1 h (Stephens, 2014). We have determined a period of 48.863 ± 0.015 h, which is consistent with the one proposed by Warner.

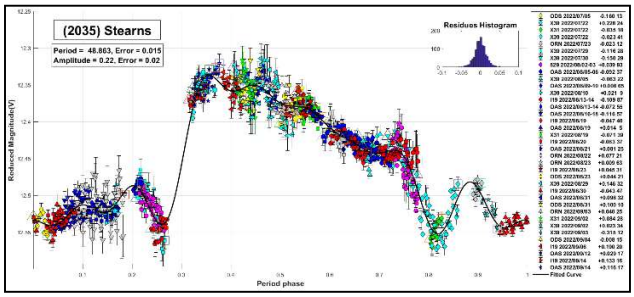

2052 Tamriko is an S-type asteroid, discovered in 1976 by R.M. West. Recent periods found in the literature coincide with the period formerly measured by Foylan (2018): P = 7.470 ± 0.002 h with Δm = 0.15 ± 0.05 mag. In this work, we present a lightcurve with full coverage that also agrees with previous assessments, P = 7.469 ± 0.008 h with Δm = 0.14 ± 0.01 mag. The shape of our lightcurve shows three maxima and three minima, in full agreement with the results obtained by other authors.

Number	Name	2022/ mm/dd	Phase	L_{PAB}	B_{PAB}	Period(h)	P.E.	Amp	A.E.	Grp
622	Esther	07/26-11/14	*14.5,30.9	331	-4	47.413	0.014	0.55	0.02	MB-I
783	Nora	05/21-08/13	*19.7,26.8	272	11	56.153	0.011	0.12	0.02	MB-I
879	Ricarda	08/27-10/21	*18.2,16.1	3	19	134.748	0.020	0.90	0.03	Maria
960	Birgit	09/04-09/24	*5.1,09.4	347	5	9.572	0.024	0.15	0.03	MB-I
1048	Feodosia	08/20-10/02	*9.3,16.3	329	-20	15.635	0.006	0.03	0.01	MB-O
1543	Bourgeois	07/20-10/02	*15.2,25.6	322	11	29.587	0.006	0.09	0.01	MB-M
2035	Stearns	07/05-09/15	23.2,34.0	297	-34	48.863	0.015	0.22	0.02	HUN
2052	Tamriko	10/02-10/14	8.5,3.7	28	2	7.469	0.008	0.14	0.01	
2243	Lonnrot	10/04-10/29	*12.4,3.3	30	1	3.989	0.014	0.10	0.02	Flora
4376	Shigemori	09/19-11/01	*19.8,4.8	30	1	35.992	0.020	0.21	0.03	MB-I
4429	Chinmoy	08/24-09/23	*9.0,8.9	345	1	4.940	0.035	0.07	0.05	HER
4538	Vishyanand	09/29-11/16	*17.2,9.4	36	1	115.748	0.017	0.57	0.02	MB-I

Table I. Observing circumstances and results. The phase angle is given for the first and last date. If preceded by an asterisk, the phase angle reached an extremum during the period. L_{PAB} and B_{PAB} are the approximate phase angle bisector longitude/latitude at mid-date range (see Harris et al., 1984). Grp is the asteroid family/group (Warner et al., 2009). MB-I: main-belt inner; Maria: 170 Maria; MB-O: main-belt outer; MB-M: main-belt middle; HUN: Hungaria; HER: Hertha.

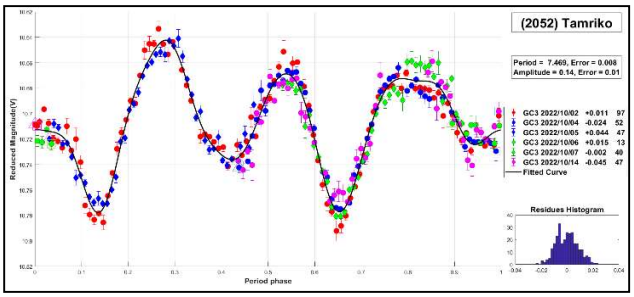

2243 Lonnrot was discovered in 1941 by Y. Vaisala. In the literature, we found only one reported period for this asteroid: P = 3.813 ± 0.004 h with Δm = 0.14 ± 0.05 mag (Marchini et al., 2021). Our study supports the aforementioned period and yielded the following results: P = 3.989 ± 0.014 h with Δm = 0.10 ± 0.02 mag.

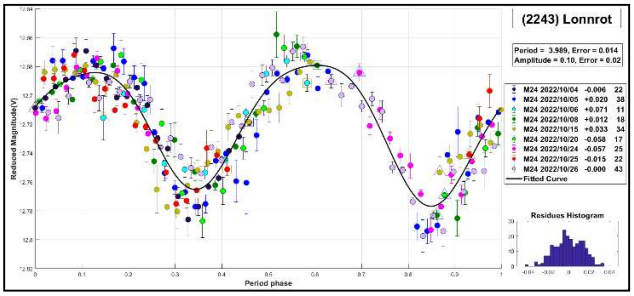

4376 Shigemori was discovered in 1987 by Nijima and Urata. Interestingly, we couldn't find a reported period for this object in the literature. According to our observations and after a thorough analysis, we propose a period of P = 35.992 ± 0.020 h and Δm = 0.21 ± 0.03 mag. We performed several observations on this object leading to a very good coverage of the lightcurve.

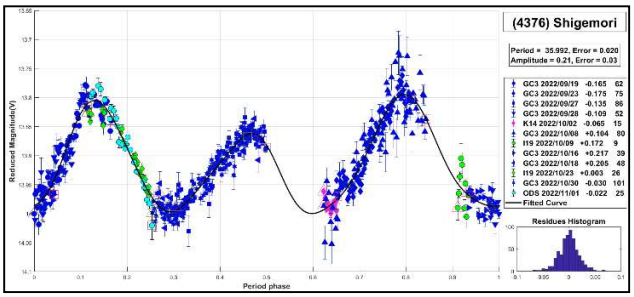

4429 Chinmoy was named in honor of Sri Chinmoy, a Bengali poet, artist and philosopher, preacher of peace, who travels the world, inspiring peace-loving peoples with his music, poetry and works of art. It was discovered in 1978 by N.S. Chernyj.

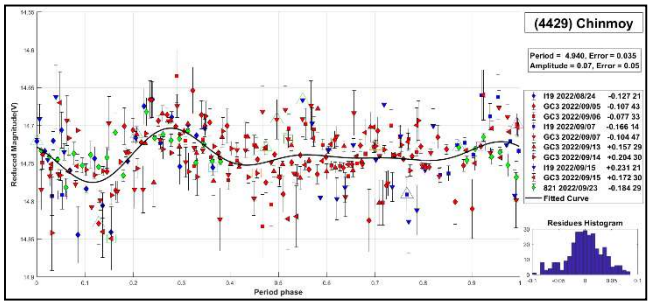

We couldn't find previously published periods in the literature. We propose a candidate period of P = 4.940 ± 0.035 h with Δm = 0.07 ± 0.05 mag. Given its estimated diameter of 3.5 kilometers and our proposed period, this object likely corresponds to a rubble-pile type asteroid.

4538 Vishyanand was discovered in 1988 byK. Suzuki. For this asteroid, we couldn't find published periods in the literature. In this work, we propose a long-term period of P = 115.748 ± 0.017 h with Δm = 0.57 ± 0.02 mag.

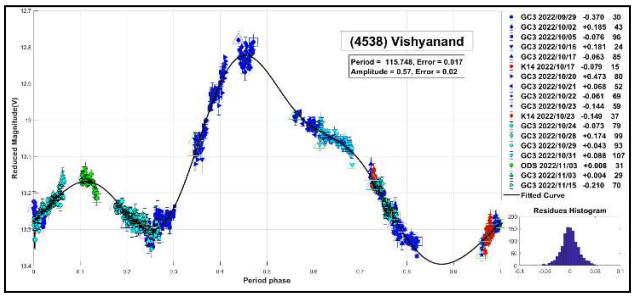

Acknowledgements

We want to thank Julio Castellano as we use his *FotoDif* program for preliminary analyses, Fernando Mazzone for his *Periods* program, used in final analyses, and Matías Martini for his *CalculadorMDE* v0.2 used for generating ephemerides used in the planning stage of the observations. This research has made use of the Small Bodies Data Ferret (*http://sbn.psi.edu/ferret/*), supported by the NASA Planetary System. This research has made use of data

Observatory	Telescope	Camera
821 Est.Astrof.Bosque Alegre	Newtonian (D=1540mm; f=4.9)	CCD APOGEE Alta U9
829 Complejo Astronómico El Leoncito	RCT (D=2150mm; f=8.48)	CCD Roper 2048
G05 Obs.Astr.Giordano Bruno	SCT (D=203mm; f=6.3)	CCD Atik 420 m
I19 Obs.Astr.El Gato Gris	SCT (D=355mm; f=10.6)	CCD SBIG STF-8300M
I39 Obs.Astr.Cruz del Sur	Newtonian (D=254mm; f=4.7)	CMOS QHY 174M
K14 Obs.Astr.de Sencelles	Newtonian (D=250mm; f=4.0)	CCD SBIG ST-7XME
M24 Oss.Astr.La Macchina del Tempo	RCT (D250mm; f=8.0)	CMOS ZWO ASI 1600MM
X12 Obs.Astr.Los Cabezones	Newtonian (D=200mm; f=5.0)	CMOS QHY 174M
X31 Obs.Astr.Galileo Galilei	RCT ap (D=405mm; f=8.0)	CCD SBIG STF-8300M
X39 Obs.Astr.Antares	Newtonian (D=250mm; f=4.72)	CCD QHY9 Mono
Z03 Obs.Astr.Río Cofio	SCT (D=254mm; f=6.3)	CCD SBIG ST-8XME
APB Obs.Astr.AstroPilar	Refractor (D=150mm; f=7.0)	CCD ZWO ASI 183
GC3 Specola Giuseppe Pustorino 3	RCT (D=400mm; f=5.7)	CCD Atik 383L+Mono
OAS Obs.Astr.de Ariel Stechina 1	Newtonian (D=254mm; f=4.7)	CCD SBIG STF-402
ODS Obs.Astr.de Damián Scotta 1	Newtonian (D=300mm; f=4.0)	CMOS QHY 174M
OD2 Obs.Astr.de Damián Scotta 2	Newtonian (D=250mm; f=4.0)	CCD SBIG STF-8300M
OMA Obs.Astr.Vuelta por el Universo	Newtonian (D=150mm; f=5.0)	CMOS POA Neptune-M
ORN Obs.Astr.de Ricardo Nolte	Newtonian (D=200mm; f=5.0)	CMOS POA Neptune-M
RMC Obs.Astr.de Raúl Melia Carlos Paz	Newtonian (D=254mm; f=4.7)	CMOS QHY 174M

Table II. List of observatories and equipment.

and/or services provided by the International Astronomical Union's Minor Planet Center.

References

Behrend, R. (2005web, 2007web). Observatoire de Geneve website. *http://obswww.unige.ch/~behrend/page_cou.html*

Florczak, M.; Dotto, E.; Barucci, M.A.; Birlan, M.; Erikson, A.; Fulchignoni, M.; Nathues, A.; Perret, L.; Thebault, P. (1997). "Rotational properties of main belt asteroids: photoelectric and CCD observations of 15 objects." *Planetary and Space Science* **45**, 1423-1435.

Foylan, M. (2018). "Lightcurve and Rotation Period for Minor Planet Tamriko." *Minor Planet Bulletin* **45**, 119-120.

Franco, L.; Marchini, A.; Iozzi, M.; Scarfi, G.; Montigiani, N.; Mannucci, M.; Aceti, P.; Banfi, M.; Mortari, F.; Galli, G.; Bacci, P.; Maestripieri, M.; Valvasori, A.; Guido, E. (2021). "Collaborative Asteroid Photometry from UAI: 2021 April-June." *Minor Planet Bulletin* **48**, 372-374.

Hanuš, J.; Ďurech, J.; Brož, M.; Warner, B.D.; Pilcher, F.; Stephens, R.; Oey, J.; Bernasconi, L.; Casulli, S.; Behrend, R.; Polishook, D.; Henych, T.; Lehký, M.; Yoshida, F., Ito, T. (2011). "A study of asteroid pole-latitude distribution based on an extended set of shape models derived by the lightcurve inversion method." *Astronomy & Astrophysics* **530**, A134.

Hanuš, J.; Ďurech, J.; Oszkiewicz, D.A.; Behrend, R.; Carry, B.; and 1643 colleagues (2016). "New and updated convex shape models of asteroids based on optical data from a large collaboration network." *Astronomy & Astrophysics* **586**, A108.

Harris, A.W.; Young, J.W.; Scaltriti, F.; Zappala, V. (1984). "Lightcurves and phase relations of the asteroids 82 Alkmene and 444 Gyptis." *Icarus* **57**, 251-258.

Kim, M.-J.; Choi, Y.-J.; Moon, H.-K.; Byun, Y.-I.; Brosch, N.; Kaplan, M.; Kaynar, S.; Uysal, Ö.; Güzel, E.; Behrend, R.; Yoon, J.-N.; Mottola, S.; Hellmich, S.; Hinse, T.C.; Eker, Z.; Park, J.-H. (2014). "Rotational properties of the Maria asteroid family." *Astronomical Journal* **147**, 56.

Kryszczyńska, A.; Colas, F.; Polińska, M.; Hirsch, R.; Ivanova, V.; and 25 colleagues (2012). "Do Slivan states exist in the Flora family? - I. Photometric survey of the Flora region." *Astronomy & Astrophysics* **546**, A72.

Lagerkvist, C.-I.; Magnusson, P.; Debehogne, H.; Hoffmann, M.; Erikson, A.; De Campos, A.; Cutispoto, G. (1992). "Physical studies of asteroids. XXV - Photoelectric photometry of asteroids obtained at ESO and Hoher List Observatory." *Astronomy and Astrophysics Supplement Series* **95**, 461-470.

Marchini, A.; Cavaglioni, L.; Privitera, C.A.; Papini, R.; Salvaggio, F. (2021). "Rotation Period Determination for Asteroids 2243 Lonnrot, (10859) 1995 GJ7, (18640) 1998 EF9 and (49483) 1999 BP13." *Minor Planet Bulletin* **48**, 206-208.

Mazzone, F.D. (2012). Periodos software, version 1.0. *http://www.astrosurf.com/salvador/Programas.html*

Polakis, T. (2018). "Lightcurve Analysis for Eleven Main-belt Asteroids." *Minor Planet Bulletin* **45**, 199-203.

Shevchenko, V.G.; Krugly, Y.N.; Chiorny, V.G.; Belskaya, I.N.; Gaftonyuk, N.M. (2003). "Rotation and photometric properties of E-type asteroids." *Planetary and Space Science* **51**, 525-532.

Stephens, R.D. (2014). "Asteroids Observed from CS3: 2014 April - June." *Minor Planet Bulletin* **41**, 226-230.

Warner, B.D.; Harris, A.W.; Pravec, P. (2009). "The asteroid lightcurve database." *Icarus* **202**, 134-146.

Warner, B.D. (2011). "Asteroid Lightcurve Analysis at the Palmer Divide Observatory: 2010 December - 2011 March." *Minor Planet Bulletin* **38**, 142-149.

LIGHTCURVES OF TWELVE ASTEROIDS

Eric V. Dose
3167 San Mateo Blvd NE #329
Albuquerque, NM 87110
mp@ericdose.com

(Received: 2023 January 14)

We present lightcurves, synodic rotation periods, and G value (H-G) estimates for twelve asteroids.

We present asteroid lightcurves obtained via the workflow process described by Dose (2020) and as later improved (Dose, 2021). This workflow applies to each image an ensemble of typically 15-60 nearby comparison ("comp") stars selected from the ATLAS refcat2 catalog (Tonry et al., 2018). Custom diagnostic plots and the abundance of comp stars allow for rapid identification and removal of outlier, variable, and poorly measured comp stars.

The product of this custom workflow is one night's time series of absolute magnitudes for the target asteroid, all on Sloan r' (SR) catalog basis. These magnitudes are corrected for instrument transforms, sky extinction, and image-to-image ("cirrus") fluctuations and thus represent magnitudes at the top of earth's atmosphere. These magnitudes are imported directly into *MPO Canopus* software (Warner, 2021) where they are adjusted for distances and phase-angle dependence, fit by Fourier analysis including identifying and ruling out of aliases, and plotted.

Phase-angle dependence is corrected with a H-G model, using the G value minimizing best-fit RMS error across all nights' data; in rare cases for which we cannot estimate an asteroid's G value, we apply the Minor Planet Center's nominal value of 0.15. No nightly zero-point adjustments (Delta Comps in *MPO Canopus* terminology) were made to any session herein, other than by estimating G, which practice we note introduces only one new fitting term vs many more terms (number of nights - 1) when applying non-zero Delta Comps.

Lightcurve Results

Twelve asteroids were observed from New Mexico Skies observatory at 2310 meters elevation in southern New Mexico. Images were acquired with a 0.35-meter SCT reduced to f/7.7; a SBIG STXL-6303E camera cooled to -35 C and fitted with an Exoplanet/Blue Blocker (BB) filter (Astrodon); and a PlaneWave L-500 mount. The equipment was operated remotely via ACP software (DC-3 Dreams, version 8.3), running plan files generated for each night by the author's python scripts (Dose, 2020). Exposures were autoguided, and exposure times targeted 3-5 millimagnitudes uncertainty in asteroid instrumental magnitude, subject to a minimum exposure of 150 seconds to ensure suitable comp-star photometry, and to a maximum of 900 seconds.

The BB filter, a yellow filter with relatively sharp wavelength cut-off, requires only a modest first-order transform to the standard Sloan r' passband. In our hands, using this filter rather than a clear filter or no filter improves night-to-night reproducibility to a degree outweighing loss of signal-to-noise ratio from loss of flux.

FITS images were plate-solved by *PinPoint* (DC-3 Dreams) or *TheSkyX* (Software Bisque) and were calibrated using temperature-matched, median-averaged dark images and recent flat images of a flux-adjustable flat panel. Every photometric image was visually inspected; the author excluded images with poor tracking, obvious interference by cloud or moon, or having stars, satellite tracks, cosmic ray artifacts, or other apparent light sources within 10 arcseconds of the target asteroid. Images passing these screens were submitted to the workflow.

Comparison stars from the ATLAS refcat2 catalog were selected if they had: distance from image boundaries and other catalogued flux sources of at least 15 arcseconds, no catalog VARIABLE flag, Sloan r' magnitude within [-1, +2] of the target asteroid's r' magnitude on that night (except that very faint asteroids used comp stars with magnitudes in the range 14 to 16), Sloan r'-i' color value in the range 0.10 to 0.34, and absence of variability as seen in session plots of each comp star's instrumental magnitude vs time.

In this work, "period" refers to an asteroid's synodic rotation period, "SR" denotes the Sloan r' passband, and "mmag" denotes millimagnitudes (0.001 magnitude).

478 Tergeste. We confirm most known reports of synodic rotational period (15 h, Harris and Young, 1989; 16.104 h, Behrend, 2005web; 16.105 h, Marciniak et al., 2015; 16.107 h, Aznar Macías, 2017; 16.101 h, Brines et al., 2017; several reports near 16.104 h, Marciniak et al., 2018; 16.1011 h, Pál et al., 2020; 16.1 h, Behrend, 2021web) with our estimate of 16.114 ± 0.003 h for this bright outer main-belt asteroid. The lightcurve shape is clearly bimodal, so that our period estimate very probably represents this asteroid's true rotation period. Our Fourier fit RMS error is 4 mmag; best G (H-G model) estimate is 0.15, equal to the MPC nominal G value.

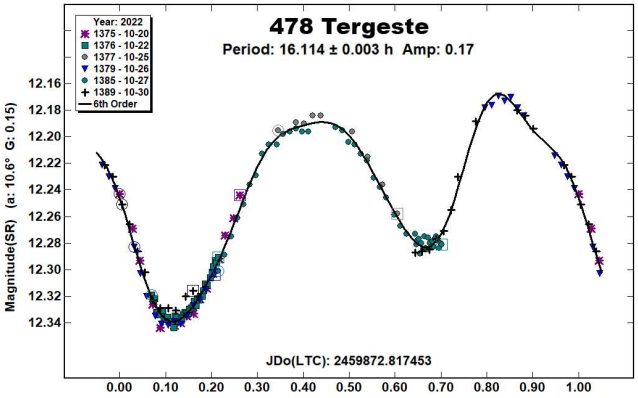

960 Birgit. For this inner main-belt asteroid, we find a rotational period of 8.681 ± 0.002 h, confirming two previous reports (8.85 h, Kryszczyńska et al., 2012; 8.67648 h, Ďurech et al., 2020) but differing from a third (17.3558 h, Behrend, 2005web). The lightcurve shape is unusual enough that this asteroid may represent a shape-modeling opportunity. Our Fourier fit RMS error is 12 mmag.

Number	Name	yyyy mm/dd	Phase	L_{PAB}	B_{PAB}	Period(h)	P.E.	Amp	A.E.	Grp
478	Tergeste	2022 10/20-10/30	10.8,7.2	53	1	16.114	0.003	0.17	0.02	MB-O
960	Birgit	2022 11/07-11/22	26.7,29.0	2	3	8.681	0.002	0.24	0.03	MB-I
1543	Bourgeois	2022 07/09-10/13	*20.1,27.9	324	10	90.768	0.018	0.23	0.04	MB-M
1690	Mayrhofer	2022 10/20-11/24	*8.9,6.0	47	1	19.026	0.002	0.28	0.03	MB-O
1780	Kippes	2022 10/25-12/22	*10.9,10.2	61	8	13.684	0.001	0.09	0.04	EOS
1946	Walraven	2022 12/01-12/27	16.3,6.3	97	10	10.210	0.001	0.88	0.04	MB-I
2085	Henan	2022 09/17-10/22	*11.5,5.4	18	-5	216.890	0.360	0.43	0.08	HEN
3166	Klondike	2022-2023 11/05-01/14	*12.5,20.0	68	0	226.140	0.110	0.77	0.07	MB-I
3229	Solnhofen	2022 10/30-12/01	8.0,17.5	38	12	15.332	0.001	0.43	0.04	MB-I
3560	Chenqian	2022 09/05-10/21	*5.8,13.7	355	6	18.859	0.007	0.05	0.03	EOS
10044	Squyres	2022 10/04-10/26	16.8,20.2	15	20	1.668	0.001	0.10	0.05	MB-I
12746	Yumeginga	2022-2023 11/02-01/05	7.1,27.8	38	4	1239.130	2.240	1.33	0.12	FLO

Table I. Observing circumstances and results. The phase angle is given for the first and last date. If preceded by an asterisk, the phase angle reached an extrema during the period. L_{PAB} and B_{PAB} are the approximate phase angle bisector longitude/latitude at mid-date range (see Harris et al., 1984a). Grp is the asteroid family/group (Warner et al., 2009).

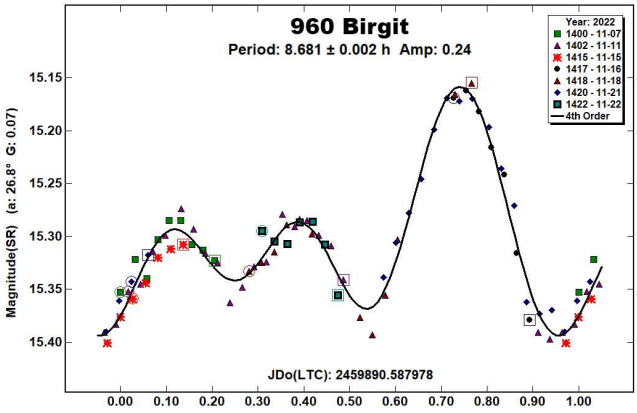

Despite our lightcurve's having only one dominant brightness maximum as well as an amplitude suitable to either a monomodal or bimodal lightcurve interpretation, the period spectrum strongly supports a monomodal (or trimodel if counting all maxima) interpretation with our period estimate as given.

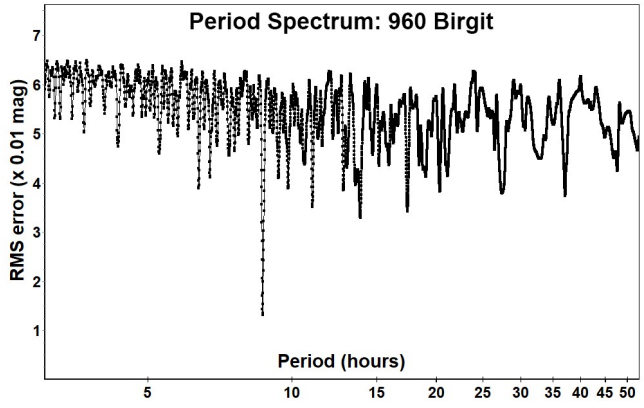

1543 Bourgeois. Our rotational period estimate for this middle main-belt asteroid is 90.768 ± 0.018 h, at wide variance from the sole known report of 2.48 h (Behrend, 2005web), for which the amplitude was reported to be at most 0.03 magnitudes. Several nights of our observations show some evidence of systematic deviation from the best single-period Fourier curve to perhaps 0.02-0.03 magnitudes, which suggests a moderate effect of precession ("tumbling"). Our RMS error is 13 mmag; the best G value is 0.22.

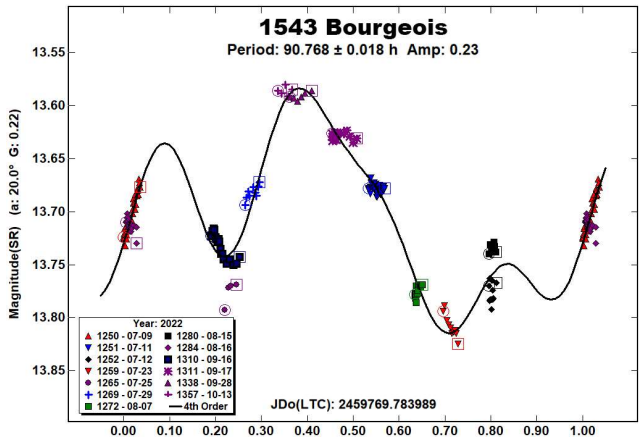

The period spectrum supports our proposed rotational period, though with a noisy character that often accompanies period spectra of processing asteroids. The period spectrum disfavors the previously reported period of 2.48 hours.

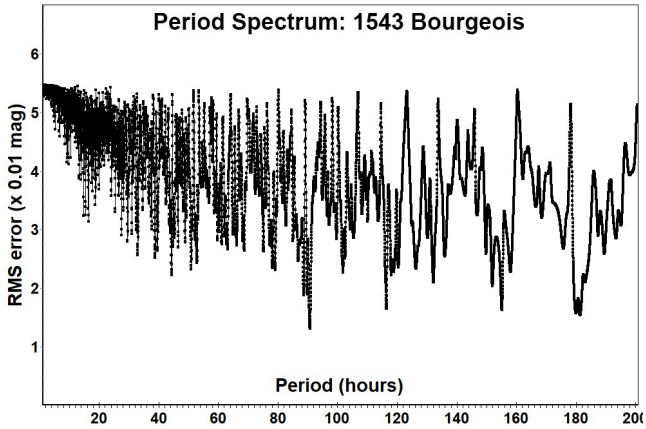

1690 Mayrhofer. For this outer main-belt asteroid during its very favorable 2022 apparition, we find a rotational period of 19.026 ± 0.002 h, agreeing closely with one previous report (19.081 h, Waszczak et al., 2015) and less closely with another (19.5375 h, Pál et al., 2020) but differing from a third (22.194 h, Behrend, 2006web). The lightcurve appears bimodal. Our Fourier fit RMS error is 11 mmag and the best G value was indistinguishable from the MPC nominal value of 0.15.

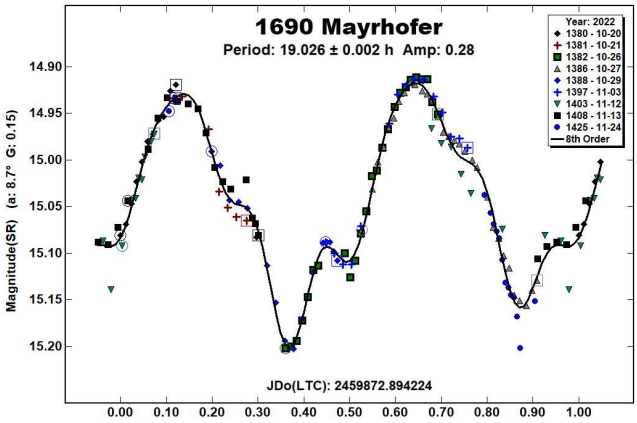

The period spectrum supports our proposed period but offers no support for possible periods near 22-23 h. We can also find no credible alias to associate our proposed period with a period of 22.194 h.

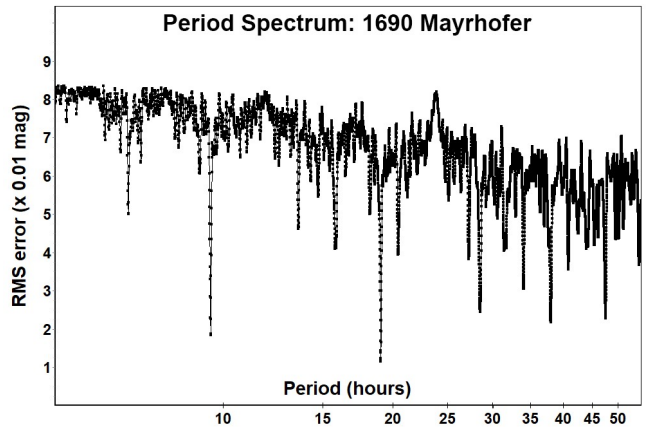

1780 Kippes. Our bimodal period estimate of 13.684 ± 0.01 h differs from both previous reports (18.0 h, Binzel, 1987; 6.83899 h, Pál et al., 2020) for this Eos-family asteroid. The 6.83899 h period candidate is close to one-half of our proposed bimodal period, and is plausible as a monomodal interpretation given the modest amplitude (Harris et al., 2014). We cannot reconcile an 18-hour period with our data, either by fractional multiples or by aliasing. Our RMS error is 15 mmag, and our best G value is very close to MPC's nominal value of 0.15.

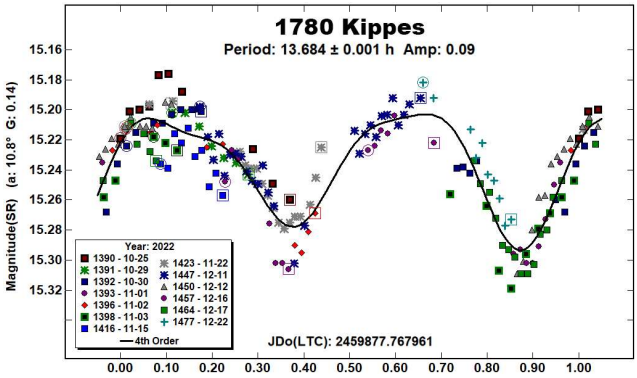

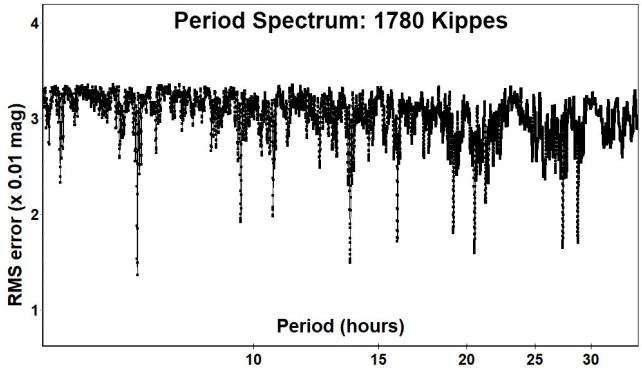

A split-halves phased plot of our data suggests but does not compel a bimodal interpretation in preference to monomodality.

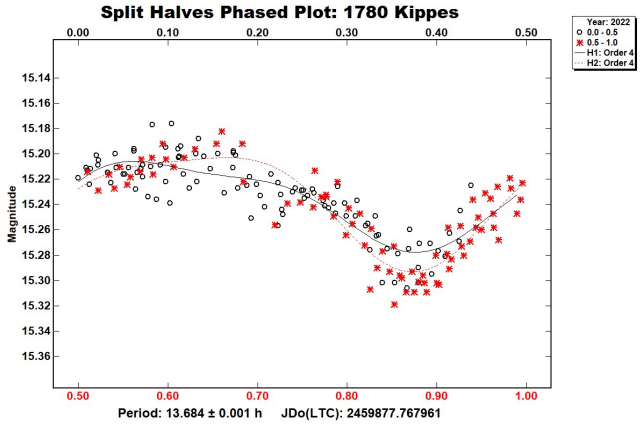

1946 Walraven. Our lightcurve for this high-amplitude inner main-belt asteroid matches all known reports (10.233 h, van Gent, 1933; 10.22 h, Folberth et al., 2012; 10.21 h, Aznar Macías et al., 2016; 10.2101 h, Hanuš et al., 2016; 10.1881 h, Pál et al., 2020). For our proposed period of 10.2095 ± 0.0005 h, our RMS error is 21 mmag, and our best G value estimate is 0.45.

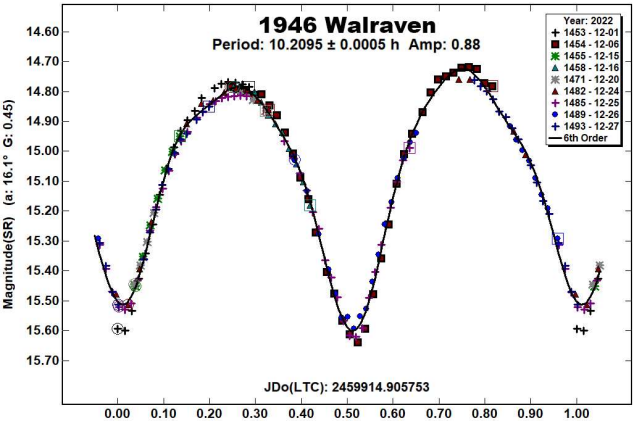

The period spectrum shows major signals only at multiples of ½ our proposed period. Of these, the deepest signal and high amplitude strongly recommend a bimodal interpretation.

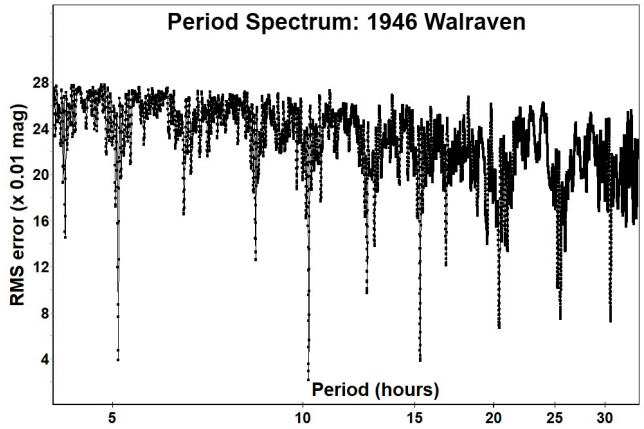

2085 Henan. This asteroid, the parent body of the Henan family, has three period reports (110 h, Devogèle et al., 2017; 221.71 h, Ďurech et al., 2020; 221.709550 h, Martikainen et al., 2021), as well as one reported constraint (> 24 h, Behrend, 2004web) which the LCDB currently gives as the best current period estimate. We find a period of 216.89 ± 0.36 h from 14 nights of data over 5 weeks (3.9 period cycles). Systematic deviations from a smooth lightcurve suggest precession ("tumbling") for this long-period asteroid. Our Fourier fit RMS error is 34 mmag; our best G estimate is 0.19, but that estimate does not give a clearly superior fit relative to the MPC nominal value of 0.15.

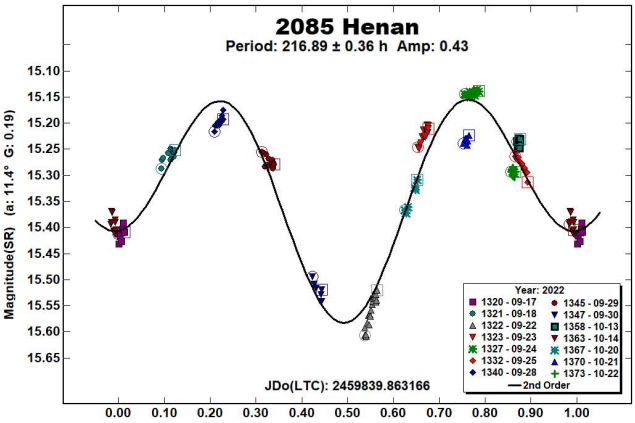

The relatively high amplitude of 0.43 magnitudes, the lightcurve shape, and the period spectrum's single major feature all suggest a bimodal interpretation with period near 220 h, disfavoring a monomodal interpretation that would yield a period near 110 h.

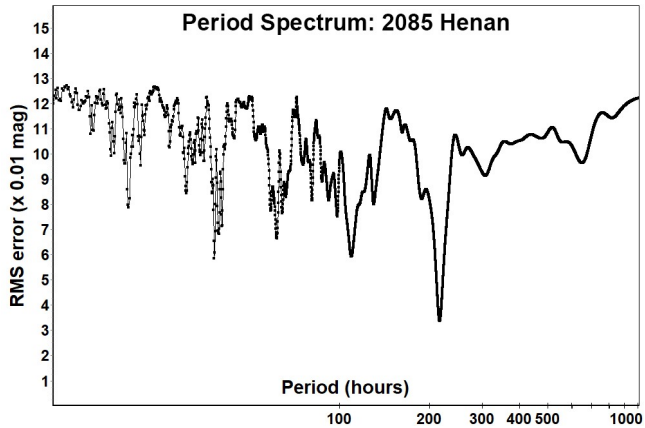

3166 Klondike. For this inner main-belt asteroid, we find a rotational period of 226.14 h, consistent with two reported lower limits (>20 h, Behrend, 2007web; >20h, Pravec et al., 2007web) but differing from all known period estimate reports (11.72 h, Sauppe et al., 2007; 150.707 h, Ďurech et al., 2020; 75.288 h, Pál et al., 2020; 150.19 h, Ferrero, 2020; 157.7 h, Polakis, 2020). Our Fourier fit RMS error is 30 mmag; fits with our G estimate of 0.27 were much better than those with MPC's nominal value of 0.15.

The lightcurve has a remarkable shape, being essentially trimodal, and it shows little or no effect of any precession ("tumbling"). Lightcurve and period determination were aided not only by the large amplitude, but by the short feature durations, which resulted in sizeable brightness changes, even within several of the shorter observing sessions.

The trimodal shape persisted through our observing campaign of almost 8 rotations, and it is likely the cause of our estimate's being 1.5 times the estimate of several recent reports.

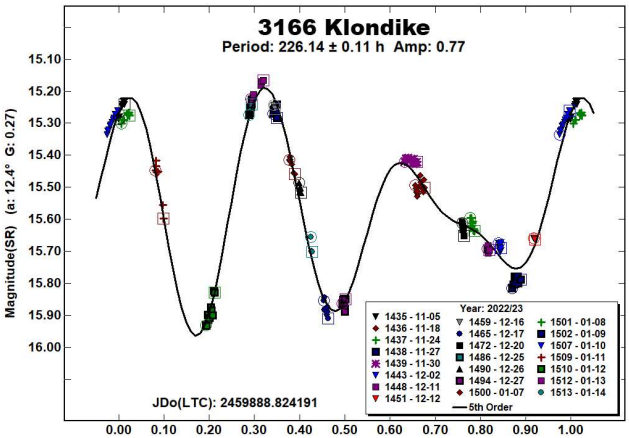

Our period spectrum does not support previously reported periods around 75 or 150 hours (one-third and two-thirds of our period estimate), though those do appear as minor spectral features.

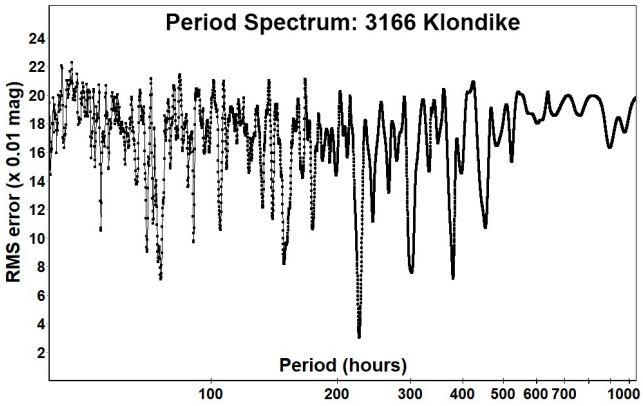

3229 Solnhofen. Our synodic rotational period estimate of 15.332 ± 0.01 h for this inner main-belt asteroid differs from the sole known previous report (11.52 h, Folberth et al., 2012), which is an alias of our result by ½ period per 24 hours. Our Fourier fit RMS error is 16 mmag; our best G value estimate of 0.32 gives much lower fit RMS errors than do fits using MPC's nominal value of 0.15.

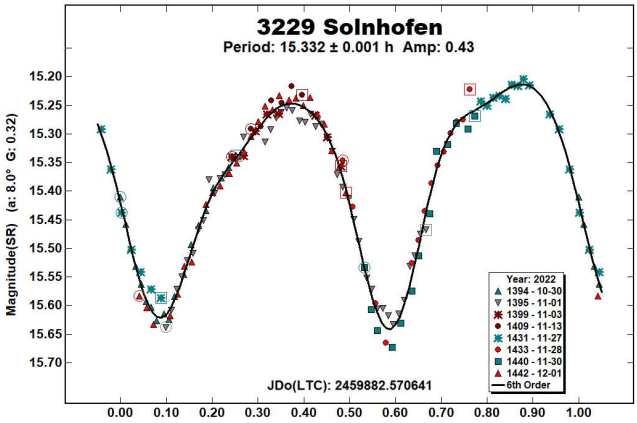

Major signals in our period spectrum appear only at multiples of half our proposed period. The lightcurve shape (especially shape around the maxima), the strongest period spectrum signal, and the relatively high amplitude all support the bimodal interpretation adopted here. The previously reported period of 11.52 h does not appear as major signal in this period spectrum.

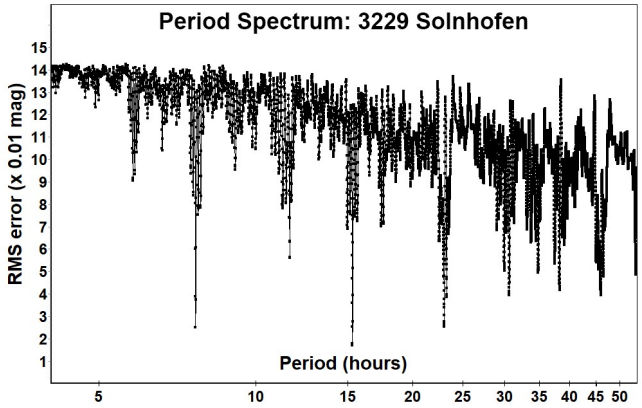

3560 Chenqian. This Eos-family asteroid's 2022 apparition gave a much smaller rotational amplitude (0.05 magnitudes) than previously reported in the LCDB (0.17-0.26). Despite this, we estimate a monomodal-basis rotational period of 18.859 ± 0.007 h, agreeing well with two previous reports (18.79 h, Pligge et al., 2011; 18.8003 h, Ďurech et al., 2020) but disagreeing with one other (12.454 h, Behrend, 2019web). Our RMS error is 10 mmag, using our best G estimate of 0.03.

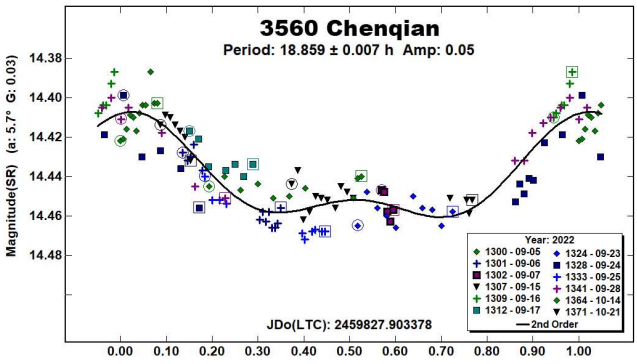

The period spectrum shows no signal at the previously reported period of 12.454 h.

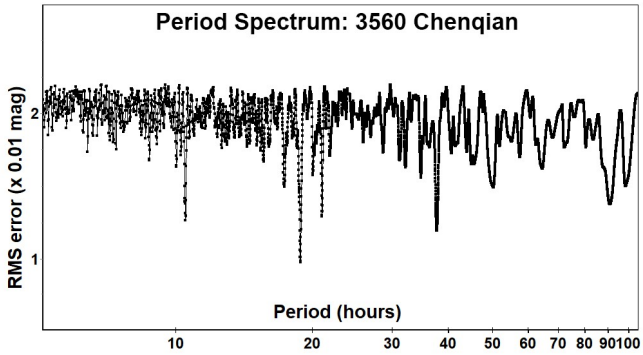

10044 Squyres. No rotational period reports are known for this inner main-belt asteroid. We offer a period estimate of 1.668 ± 0.001 h on a monodal basis from our low signal-to-noise photometric data. Fourier fit RMS error is 25 mmag, about half the measured amplitude. The best G value estimate of 0.45 is of very low confidence, as the exact value made little difference to fit quality.

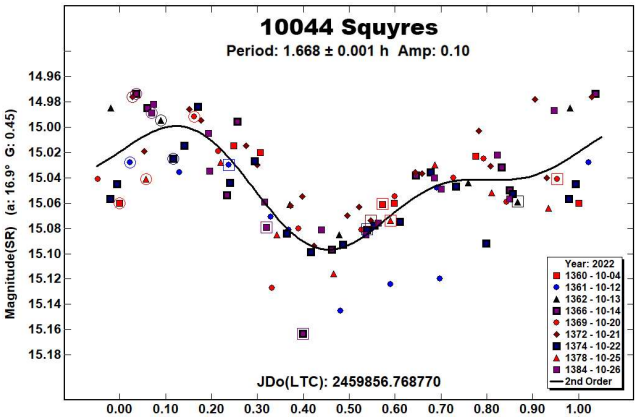

Choosing between monomodal (P=1.668 h) and bimodal (3.336 h) interpretations is not helped by the lightcurve shape, the lightcurve amplitude, or the period spectrum. We report a monomodal period, but a bimodal period is also quite consistent with our data. The current data do appear to rule out periods longer than 3.4 hours. July 2026 offers an especially favorable apparition, visible to both North and South hemispheres, and observations with larger amateur telescopes are encouraged.

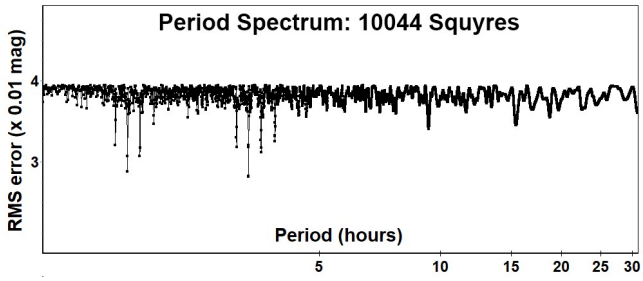

12746 Yumeginga. No previous rotational period reports are known for this Flora asteroid. We report an extraordinary period of 1239.13 ± 2.24 h (bimodal basis) from 25 nights' observations over 10 weeks. The lightcurve displays an exceptional amplitude of 1.33 magnitudes and so is assigned a bimodal interpretation even though the phased lightcurve's halves are similar. We saw no effect of precession ("tumbling"). Fourier fit RMS error is 47 mmag; best G estimate is 0.18.

Our campaign began just after maximum brightness and continued until the asteroid became too faint for the author's equipment (asteroid signal-to-noise ca. 30); despite the campaign's length, it covered only 1.34 rotations, being almost 3 max-min cycles.

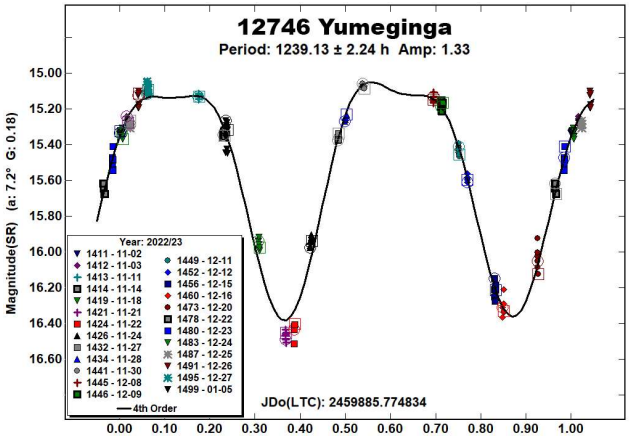

Because this observing campaign was only slightly longer than the proposed period, even longer periods can be only weakly ruled out by the period spectrum itself. However, it hard to imagine any longer period's giving a better bimodal fit to our observation data than that depicted in the phased lightcurve plot above.

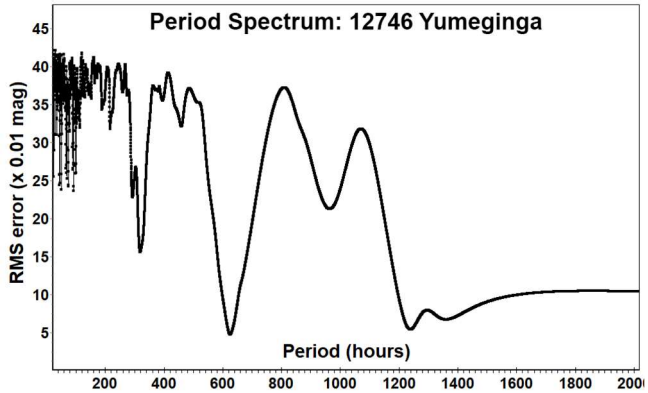

The next favorable apparition in July 2025, with declination -17°, might seem to favor the Southern over the Northern hemisphere, but sky elevation will matter much less for this apparition than for most. That is, given this asteroid's very long period, reliable 4-hour sessions in the Northern Hemisphere will be practically as useful as 9-hour sessions in the Southern. More important than long sessions will be the number of nights observed and length of observing campaigns in months. Getting an early start will be essential.

Acknowledgements

The author thanks all the authors of and contributors to the ATLAS paper (Tonry et al, 2018) for providing openly and without cost the ATLAS refcat2 catalog release. This current work also makes extensive use of the python language interpreter and of several supporting packages (notably: astropy, ccdproc, ephem, matplotlib, pandas, photutils, requests, and statsmodels), all made available openly and without cost.

References

Aznar Macías, A.; Garcerán, A.C.; Mansego, E.A.; Rodriguez, P.B.; Lozano, J.d.H.; Silva, A.F.; Silva, F.S.; Martinez, V.M.; Chiner, O.R.; Porta, D.H. (2016). "Twenty-one Asteroid Lightcurves at Group Observadores de Asteroides (OBAS): Late 2015 to Early 2016." *Minor Planet Bull*. **43**, 257-263.

Aznar Macías, A. (2017). "Lightcurve Analysis for Nine Main-belt Asteroids. Rotation Period and Physical Parameters from APT Observatory Group: 2016 October - December." *Minor Planet Bull*. **44**, 139-141.

Behrend, R. (2004web, 2005web, 2006web, 2007web, 2019web, 2021web). Observatoire de Genève web site. *http://obswww.unige.ch/~behrend/page_cou.html*

Binzel, R.P. (1987). "A photoelectric survey of 130 asteroids." *Icarus* **72**, 135-208.

Brines, P.; Lozano, J.; Rodrigo, O.; Fornas, A.; Herrero, D.; Mas, V.; Fornas, G.; Carreño, A.; Arce, E. (2017). "Sixteen Asteroids Lightcurves at Asteroids Observers (OBAS) - MPPD: 2016 June - November." *Minor Planet Bull*. **44**, 145-149.

Devogèle, M. and 53 colleagues (2017). "Shape and spin determination of Barbarian asteroids." *Astron. Astrophys.* **607**, A119.

Dose, E. (2020). "A New Photometric Workflow and Lightcurves of Fifteen Asteroids." *Minor Planet Bull*. **47**, 324-330.

Dose, E. (2021). "Lightcurves of Nineteen Asteroids." *Minor Planet Bull*. **48**, 69-76.

Ďurech, J.; Tonry, J.; Erasmus, N.; Denneau, L.; Heinze, A.N.; Flewelling, H.; Vančo, R. (2020). "Asteroid models reconstructed from ATLAS photometry." *Astron. Astrophys.* **643**, A59.

Ferrero, A. (2020). "Photometric Lightcurves of Eight Main-Belt Asteroids." *Minor Planet Bull*. **47**, 172-174.

Folberth, J.; Casimir, S.; Dou, Y.; Evans, D.; Foulkes, T.; Haenftling, M.; Kuhn, P.; White, A.; Ditteon, R. (2012). "Asteroid Lightcurve Analysis at the Oakley Southern Sky Observatory: 2011 July - September." *Minor Planet Bull*. **39**, 51-55.

Hanuš, J. and 168 colleagues (2016). "New and updated convex shape models of asteroids based on optical data from a large collaboration network." *Astron. Astrophys.* **586**, A108.

Harris, A.W.; Young, J.W.; Scaltriti, F.; Zappalà, V. (1984a). "Lightcurves and phase relations of the asteroids 82 Alkmene and 444 Gyptis." *Icarus* **57**, 251-258.

Harris, A.W. and 15 colleagues (1984b). "On the maximum amplitude of harmonics of an asteroid lightcurve." *Icarus* **235**, 55-59.

Harris, A.W.; Young, J.W. (1989). "Asteroid lightcurve observations from 1979-1981." *Icarus* **81**, 314-364.

Harris, A.W.; Pravec, P.; Galad, A.; Skiff, B.A.; Warner, B.D.; Vilagi, J.; Gajdos, S.; Carbognani, A.; Hornoch, K.; Kusnirak, P.; Cooney, W.R.; Gross, J.; Terrell, D.; Higgins, D.; Bowell, E.; Koehn, B.W. (2014). "On the maximum amplitude of harmonics on an asteroid lightcurve." *Icarus* **235**, 55-59.

Kryszczyńska, A. and 29 colleagues (2012). "Do Slivan states exist in the Flora family? I. Photometric survey of the Flora region." *Astron. Astrophys.* **546**, A72.

Marciniak, A. and 23 colleagues (2015). "Against the biases in spins and shapes of asteroids." *Planetary Space Sci.* **118**, 256-266.

Marciniak, A. and 42 colleagues (2018). "Photometric survey, modelling, and scaling of long-period and low-amplitude asteroids." *Astron. Astrophys.* **610**, A7.

Martikainen, J.; Muinonen, K.; Penttilä, A.; Cellino, A.; Wang, X.-B. (2021). "Asteroid absolute magnitudes and phase curve parameters from *Gaia* photometry." *Astron. Astrophys.* **649**, A98.

Pál, A.; Szakáts, R.; Kiss, C.; Bódi, A.; Bognár, Z.; Kalup, C.; Kiss, L.L.; Marton, G.; Molnár, L.; Plachy, E.; Sárneczky, K.; Szabó, G.M.; Szabó, R. (2020). "Solar System Objects Observed with TESS - First Data Release: Bright Main-belt and Trojan Asteroids from the Southern Survey." *Ap. J.* **247**, A26.

Pligge, Z.; Monnier, A.; Pharo, J.; Stolze, K.; Yim, A.; Ditteon, R. (2011). "Asteroid Lightcurve Analysis at the Oakley Southern Sky Observatory: 2010 May." *Minor Planet Bull*. **38**, 5-7.

Polakis, T. (2020). "Photometric Observations of Thirty Minor Planets." *Minor Planet Bull*. **47**, 177-184.

Pravec, P.; Wolf, M.; Sarounova, L. (2007web). Ondrejov Asteroid Photometry Project. *https://www.asu.cas.cz/~ppravec/neo.htm*

Sauppe, J.; Torno, S.; Lemke-Oliver, R.; Ditteon, R. (2007). "Asteroid Lightcurve Analysis at the Oakley Observatory – March/April 2007." *Minor Planet Bull*. **34**, 119-122.

Tonry, J.L.; Denneau, L.; Flewelling, H.; Heinze, A.N.; Onken, C.A.; Smartt, S.J.; Stalder, B.; Weiland, H.J.; Wolf, C. (2018). "The ATLAS All-Sky Stellar Reference Catalog." *Astrophys. J.* **867**, A105.

van Gent, H. (1933). "Period, lightcurve and ephemeris of the new asteroid with variable brightness 1931 PH." *Bull. Astron. Institutes Netherlands* **7**, 65-66.

Warner, B.D.; Harris, A.W.; Pravec, P. (2009). "The asteroid lightcurve database." *Icarus* **202**, 134-146. *https://minplanobs.org/MPInfo/php/lcdb.php*

Warner, B.D. (2021). *MPO Canopus* Software, version 10.8.4.11. BDW Publishing. *http://www.bdwpublishing.com*

Waszczak, A.; Chang, C.-K.; Ofek, E.O.; Laher, R.; Masci, F.; Levitan, D.; Surace, J.; Cheng, Y.-C.; Ip, W.-H.; Kinoshita, D.; Helou, G.; Prince, T.A.; Kulkarni, S. (2015). "Asteroid Light Curves from the Palomar Transient Factory Survey: Rotation Periods and Phase Functions from Sparse Photometry." *Astron. J.* **150**, A75.

MAIN-BELT AND TROJAN ASTEROIDS OBSERVED FROM CS3: 2022 OCTOBER-NOVEMBER

Robert D. Stephens
Center for Solar System Studies (CS3)
11355 Mount Johnson Ct., Rancho Cucamonga, CA 91737 USA
rstephens@foxandstephens.com

(Received: 2022 December 16)

CCD photometric observations of three main-belt asteroids and four Jovian Trojans from the L4 cloud were obtained at the Center for Solar System Studies (CS3) from 2022 October-November. Revised periods for 4060 Deipylos from previous oppositions are also reported.

The Center for Solar System Studies (CS3) has nine telescopes which are normally used in program asteroid family studies. The focus is on near-Earth asteroids, Jovian Trojans and Hildas. When it is not the season to study a family, or when a nearly full moon is too close to the family targets being studied, targets of opportunity amongst the main-belt families were selected.

Table I lists the telescopes and CCD cameras that were used to make the observations. Images were unbinned with no filter and had master flats and darks applied. The exposures depended upon various factors including magnitude of the target, sky motion, and Moon illumination.

Telescope	Camera
0.40-m f/10 Schmidt-Cass	FLI Proline 1001E
0.50-m F/8.1 R-C	FLI Proline 1001E

Table I: List of CS3 telescope/CCD camera.

Image processing, measurement, and period analysis were done using *MPO Canopus* (Bdw Publishing), which incorporates the Fourier analysis algorithm (FALC) developed by Harris (Harris et al., 1989). The Comp Star Selector feature in *MPO Canopus* was used to limit the comparison stars to near solar color. Night-to-night calibration was done using field stars from the ATLAS catalog (Tonry et al., 2018), which has Sloan *griz* magnitudes that were derived from the GAIA and Pan-STARR catalogs and are "native" magnitudes of the catalog. Those adjustments are usually ≤ ±0.03 mag. The rare greater corrections may have been related in part to using unfiltered observations, poor centroiding of the reference stars, and not correcting for second-order extinction.

The Y-axis values are ATLAS SR "sky" magnitudes. The two values in the parentheses are the phase angle (a) and the value of *G* used to normalize the data to the comparison stars used in the earliest session. This, in effect, made all the observations seem to be made at a single fixed date/time and phase angle, leaving any variations due only to the asteroid's rotation and/or albedo changes. The X-axis shows rotational phase from -0.05 to 1.05. If the plot includes the amplitude, e.g., "Amp: 0.65", this is the amplitude of the Fourier model curve and *not necessarily the adopted amplitude for the lightcurve*.

For brevity, only some of the previously reported rotational periods may be referenced. A complete list is available at the asteroid lightcurve database (LCDB; Warner et al., 2009).

1143 Odysseus. Odysseus has been observed many times in the past (Stephens and Warner, 2022 and references therein) with most reported periods in the LCDB near 10.1 h. Our period this year is in good agreement with those prior results.

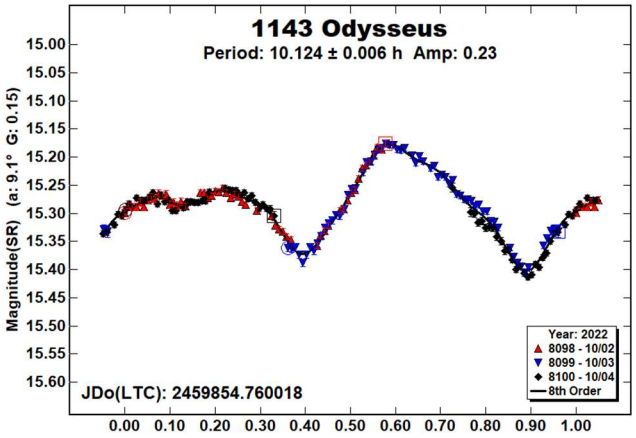

3287 Olmstead. This Mars-crosser has been observed three times in the past. Wisniewski et al. (1997) reported a period of 4.80 h, Warner (2018) reported a period of 4.963 h, and Benishek (2019) reported a period of 4.954 h. Our period this year is in good agreement with the Warner and Benishek results.

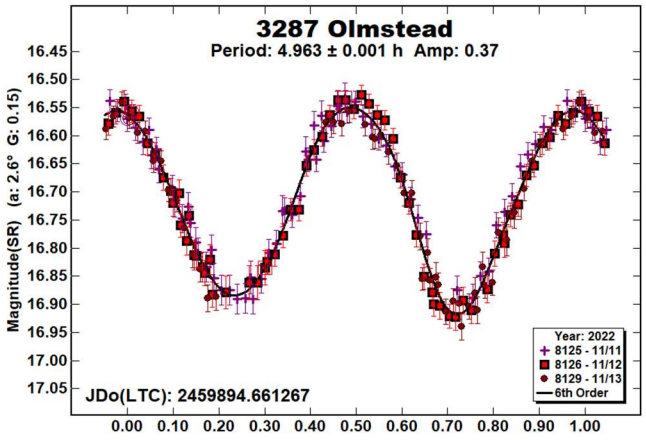

4060 Deipylos. This L_4 Trojan has been observed many times in the past (Stephens and Warner, 2020 and references therein), with most reported periods near 9.3 h. However, that period would not fit the dataset we got this year. The asymmetric lightcurve was a much better fit to a period of 11.486 h. The period spectrum shows a secondary peak near 9.3 h, which is a 5:4 alias of the 11.487 h period.

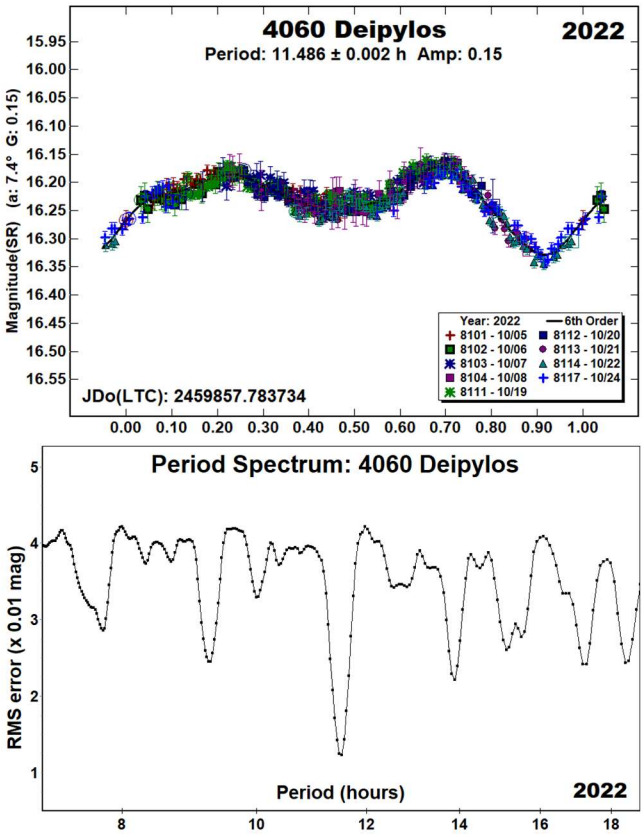

We rephased the periods we found in previous years, many of which showed the 9.3 h period as the dominant period, with a secondary peak near 11.5 h. With the 11.5 h period being nearly commensurate with an Earth's Day, it takes observations spanning two weeks to completely cover a lightcurve. Most of those prior datasets spanned only a week leaving gaps in the lightcurve assuming the 11.5 h period. This is particularly true for the 2017 dataset which has a 40% gap in the lightcurve. Because the 2022 dataset eliminates the possibility of a 9.3 h period, we favor the 11.5 h period for all of the datasets.

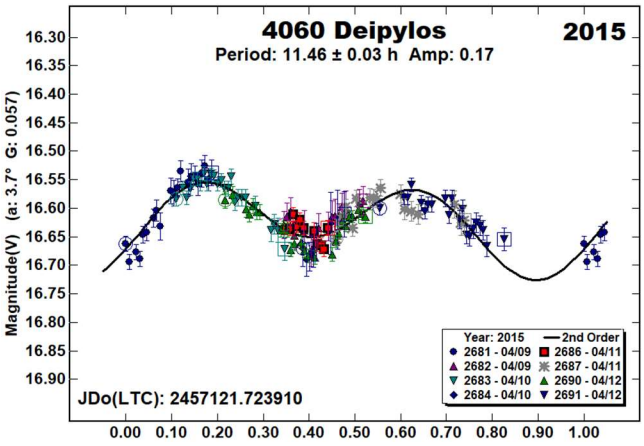

Number	Name	2022/mm/dd	Phase	L_{PAB}	B_{PAB}	Period(h)	P.E.	Amp	A.E.
1143	Odysseus	10/02-10/03	9.1,8.9	55	-1	10.124	0.006	0.23	0.01
3287	Olmstead	11/11-11/13	2.6,3.4	46	-4	4.963	0.001	0.37	0.01
4060	Deipylos	10/06-10/24	7.3,4.5	44	-15	11.486	0.002	0.15	0.01
		2015/04/09-04/12	3.7,3.3	212	12	R11.46	0.03	0.17	0.04
		2016/05/09-05/12	4.1,3.8	242	17	R11.49	0.02	0.15	0.05
		2017/06/30-07/05	3.6,4.1	269	17	R11.75	0.02	0.10	0.05
		2018/08/13-08/19	5.2,6.0	293	14	R11.38	0.03	0.12	0.02
		2019/08/17-08/22	2.0,2.6	318	9	R11.62	0.02	0.13	0.02
4489	Dracius	11/14-11/19	3.9,4.1	45	-17	12.599	0.006	0.22	0.02
5123	Cynus	11/14-11/17	1.1,0.9	55	-4	9.903	0.002	0.49	0.01
7445	Trajanus	11/11-11/13	7.3,8.6	38	0	6.108	0.002	0.79	0.02
10182	Junkobiwaki	10/23-10/31	*1.0,2.8	32	1	4.318	0.003	0.07	0.02

Table II. Observing circumstances and results. RRevised period. The phase angle is given for the first and last date. If preceded by an asterisk, the phase angle reached an extremum during the period. L_{PAB} and B_{PAB} are the approximate phase angle bisector longitude/latitude at mid-date range (see Harris et al., 1984). If more than one line for an asteroid, the first line gives the dominant solution and has a T superscript. Subsequent lines are additional, not alternate, periods. See the text for more details.

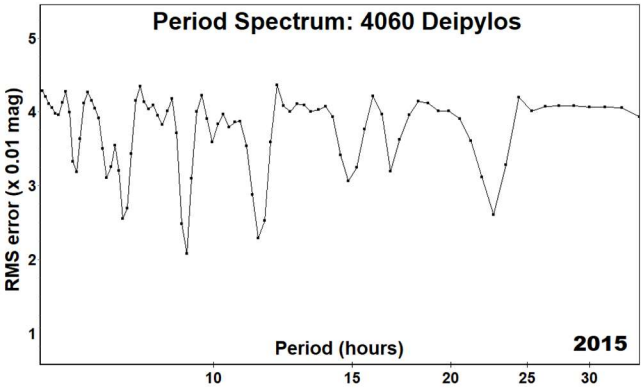

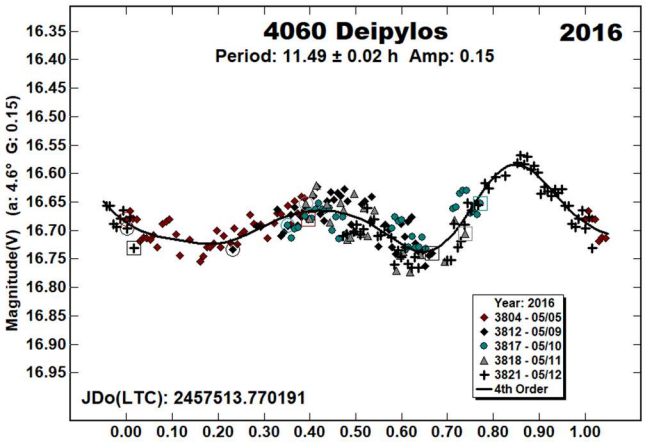

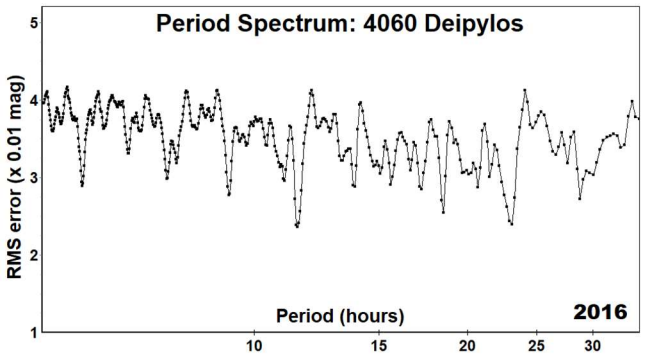

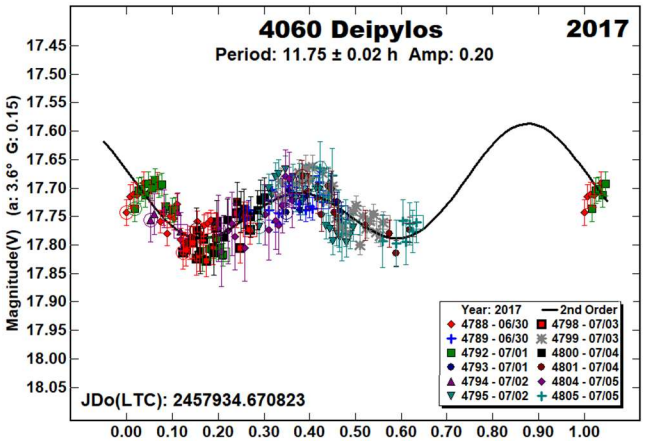

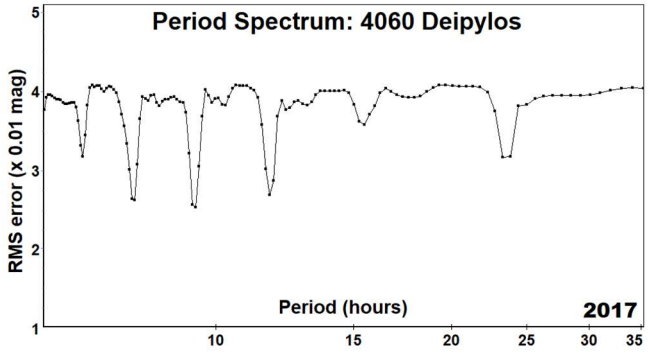

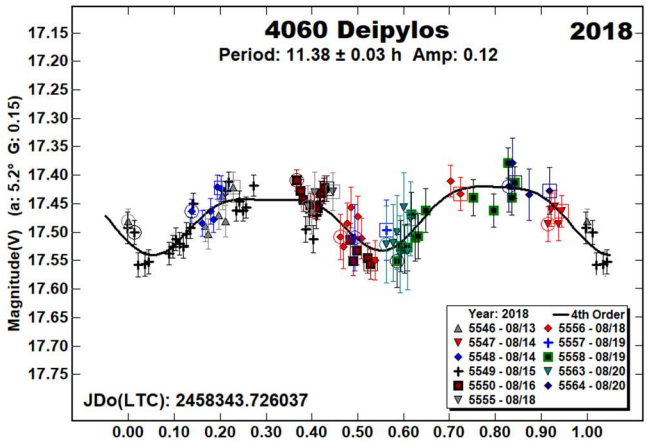

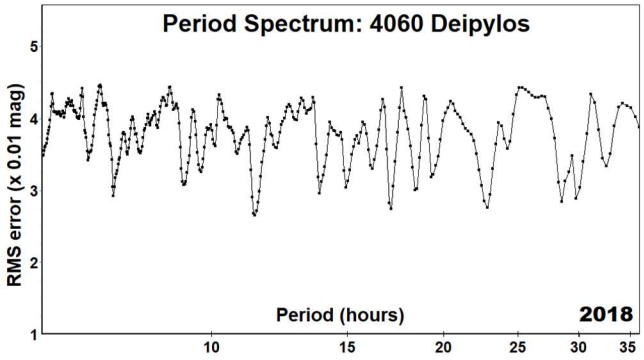

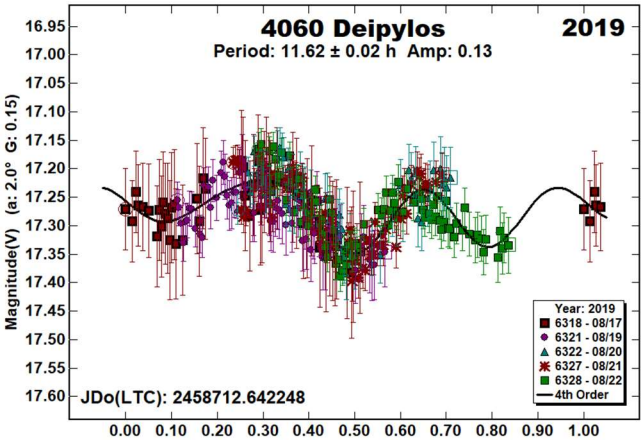

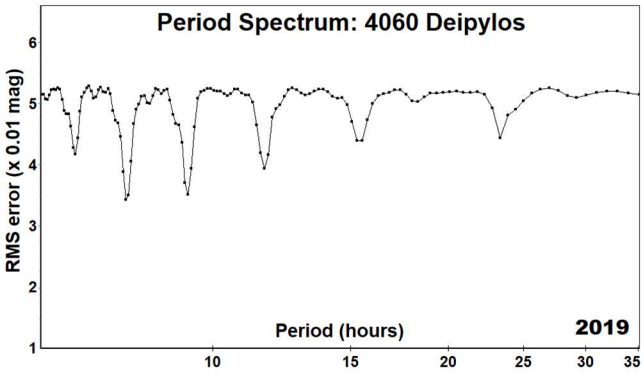

4489 Dracius. Rotational periods for this L_4 Trojan have been found many times in the past (Stephens et al., 2016 and references therein), each time finding a period near 12.58 h. In addition, using sparse data, Ďurech et al. (2019) found a sideral period of 12.58423 h. The result this year is in good agreement with the prior findings.

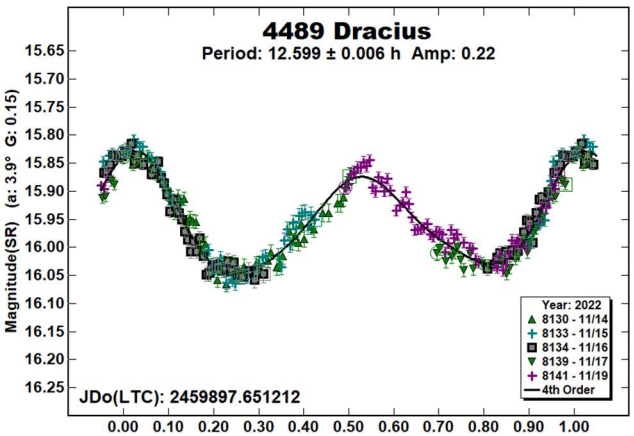

5123 Cynus. A period for this L_4 Trojan has been reported several times in the past. French et al. (2013), Ryan et al. (2017), and Szabó et al. (2017) all found periods near 9.9 h. The result this year is in good agreement with those prior findings.

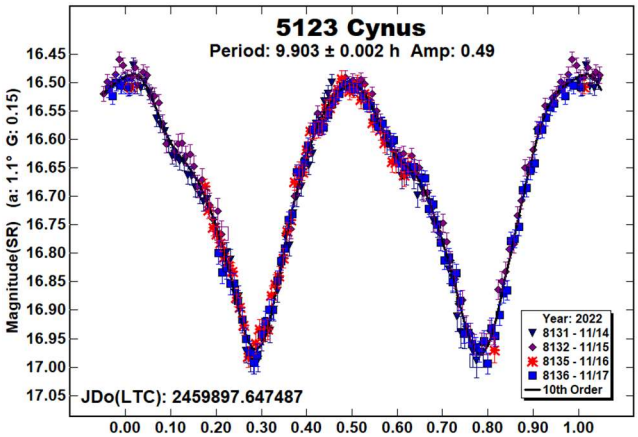

7445 Trajanus. The only previous period reported on the LCDB for this Mars-crosser has been by Durech et al. (2018), who used data from the Lowell Photometric Database and WISE data to find a sidereal period of 6.10802 h. Our period this year is in good agreement with that prior result.

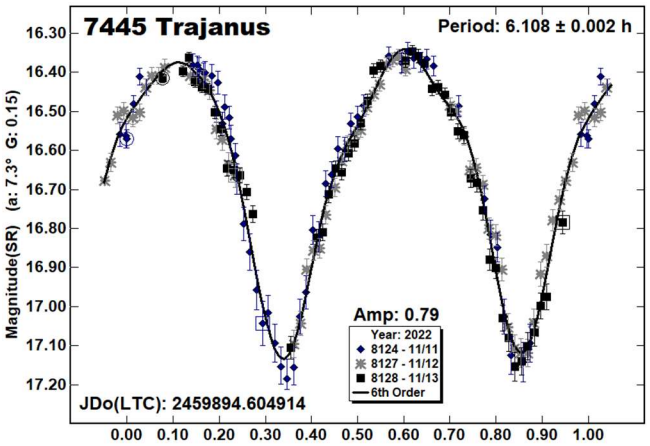

10182 Junkobiwaki. This inner Main-belt asteroid has been observed twice in the past. Pravec et al. (2017web) observed it finding a period of 4.3081 h. Using data from the TESS spacecraft, Pál et al. (2020) found a period of 4.30884 h. Our result this year is in good agreement with those prior results. In none of the results does the amplitude exceed 0.08 mag.

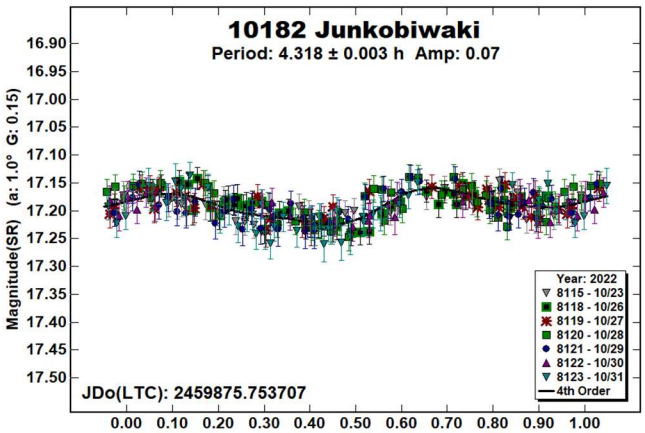

Acknowledgements

This work includes data from the Asteroid Terrestrial-impact Last Alert System (ATLAS) project. ATLAS is primarily funded to search for near earth asteroids through NASA grants NN12AR55G, 80NSSC18K0284, and 80NSSC18K1575; byproducts of the NEO search include images and catalogs from the survey area. The ATLAS science products have been made possible through the contributions of the University of Hawaii Institute for Astronomy, the Queen's University Belfast, the Space Telescope Science Institute, and the South African Astronomical Observatory. The authors gratefully acknowledge Shoemaker NEO Grants from the Planetary Society (2007, 2013). These were used to purchase some of the telescopes and CCD cameras used in this research.

References

Benishek, V. (2019). "Lightcurves and Rotation Periods for Ten Asteroids." *Minor Planet Bul.* **46**, 87-90.

Ďurech, J.; Hanuš, J.; Alí-Lagoa, V. (2018). "Asteroid models reconstructed from the Lowell Photometric Database and WISE data." *Astron. Astrophys.* **617**, A57.

Ďurech, J.; Hanuš, J.; Vančo, R. (2019). "Inversion of asteroid photometry from Gaia DR2 and the Lowell Observatory photometric database." *Astron. Astrophys*. **631**, A2.

French, L.M.; Stephens, R.D.; Coley, D.R.; Wasserman, L.H.; Vilas, F.; La Rocca, D. (2013). "A Troop of Trojans: Photometry of 24 Jovian Trojan Asteroids." *Minor Planet Bull*. **40**, 198-203.

Harris, A.W.; Young, J.W.; Scaltriti, F.; Zappala, V. (1984). "Lightcurves and phase relations of the asteroids 82 Alkmene and 444 Gyptis." *Icarus* **57**, 251-258.

Harris, A.W.; Young, J.W.; Contreiras, L.; Dockweiler, T.; Belkora, L.; Salo, H.; Harris, W.D.; Bowell, E.; Poutanen, M.; Binzel, R.P.; Tholen, D.J.; Wang, S. (1989). "Phase relations of high albedo asteroids: The unusual opposition brightening of 44 Nysa and 64 Angelina." *Icarus* **81**, 365-374.

Pál, A.; Szakáts, R.; Kiss, C.; Bódi, A.; Bognár, Z.; Kalup, C.; Kiss, L.L.; Marton, G.; Molnár, L.; Plachy, E.; Sárneczky, K.; Szabó, G.M.; Szabó, R. (2020). "Solar System Objects Observed with TESS - First Data Release: Bright Main-belt and Trojan Asteroids from the Southern Survey." *Ap. J.* **247**, A26.

Pravec, P.; Wolf, M.; Sarounova, L. (2017web). *http://www.asu.cas.cz/~ppravec/neo.htm*

Ryan, E.L.; Sharkey, B.N.; Woodward, C.E. (2017). "Trojan Asteroids in the Kepler Campaign 6 Field." *Astron. J.* **153**, A116.

Stephens, R.D.; Coley, D.R.; Warner, B.D.; French, L.M. (2016). "Lightcurves of Jovian Trojan Asteroids from the Center for Solar System Studies: L4 Greek Camp and Spies." *Minor Planet Bull*. **43**, 323-331.

Stephens, R.D.; Warner, B.D. (2020). "Lightcurve Analysis of L4 Trojan Asteroids at the Center for Solar System Studies: 2019 July to September." *Minor Planet Bull*. **47**, 43-47.

Stephens, R.D.; Warner, B.D., (2022). "Lightcurve Analysis of L4 Trojan Asteroids at the Center for Solar System Studies: 2021 July to September." *Minor Planet Bull*. **49**, 51-55.

Szabó, G.M.; Pál, A.; Kiss, C.; Kiss, L.L.; Molnár, L.; Hanyecz, O.; Plachy, E.; Sárneczky, K.; Szabó, R. (2017). "The heart of the swarm: K2 photometry and rotational characteristics of 56 Jovian Trojan asteroids." *Astron. Astrophys.* **599**, A44.

Tonry, J.L.; Denneau, L.; Flewelling, H.; Heinze, A.N.; Onken, C.A.; Smartt, S.J.; Stalder, B.; Weiland, H.J.; Wolf, C. (2018). "The ATLAS All-Sky Stellar Reference Catalog." *Astrophys. J.* **867**, A105.

Warner, B.D. (2018). "Asteroid Lightcurve Analysis at CS3-Palmer Divide Station: 2018 April-June." *Minor Planet Bul.* **45**, 380-386.

Warner, B.D.; Harris, A.W.; Pravec, P. (2009). "The Asteroid Lightcurve Database." *Icarus* **202**, 134-146. Updated 2021 Dec. *http://www.minorplanet.info/lightcurvedatabase.html*

Wisniewski, W.Z.; Michalowski, T.M.; Harris, A.W.; McMillan, R.S. (1997). "Photometric Observations of 125 Asteroids." *Icarus* **126**, 395-449.

LIGHTCURVES AND ROTATION PERIODS OF 57 MNEMOSYNE, 645 AGRIPPINA, AND 987 WALLIA

Frederick Pilcher
Organ Mesa Observatory (G50)
4438 Organ Mesa Loop
Las Cruces, NM 88011 USA
fpilcher35@gmail.com

(Received: 2023 January 8)

Synodic rotation periods and amplitudes are found for 57 Mnemosyne 25.316 ± 0.002 h, 0.08 ± 0.01 mag; 645 Agrippina 53.436 ± 0.004 h, 0.18 ± 0.01 mag; 987 Wallia 10.085 ± 0.001 h, 0.14 ± 0.01 mag.

Observations to produce the results reported in this paper were made at the Organ Mesa Observatory with a Meade 35 cm LX200 GPS Schmidt-Cassegrain, SBIG STL-1001E CCD, 20 to 30 second exposures for 57 Mnemosyne, 60 second exposures for 645 Agrippina and 987 Wallia, unguided, clear filter. Image measurement and lightcurve construction were with *MPO Canopus* software with calibration star magnitudes for solar colored stars from the CMC15 catalog reduced to the Cousins R band. Zero-point adjustments of a few ×0.01 magnitude were made for best fit. To reduce the number of data points on the lightcurves and make them easier to read, data points have been binned in sets of 3 with maximum time difference 5 minutes.

57 Mnemosyne. Earlier published periods are by Harris et al. (1992), 12.463 hours; Ditteon and Hawkins (2007), 12.66 hours; Behrend (2016web), 12.64 hours; Behrend (2020web), 12.648 hours. This author (Pilcher, 2019) was unable to fit a lightcurve to a period near 12.5 hours and found a synodic period 25.324 hours with one maximum and minimum per cycle near celestial longitude 197º. This author obtained additional sets of observations (Pilcher, 2020) near celestial longitude 258º, synodic period 25.281 hours with a complex lightcurve; and (Pilcher, 2022) near celestial longitude 331º, synodic period 25.308 hours, again with a complex shape. New observations on 14 nights 2022 Oct. 19 - Nov. 28 provide a fit to an irregular lightcurve with period 25.316 ± 0.002 hours, amplitude 0.08 ± 0.01 magnitudes. A change in the lightcurve shape near rotational phase 0.1 occurred between Oct. 19 and 21 near phase angle 15º and Nov. 27 and 28 near phase angle 6º. A split halves lightcurve for the double period including observations from Oct. 25 to Nov. 28 shows that the two halves are almost identical and rules out the double period. The observations in years 2019, 2020, 2021, and 2022, respectively, indicate consistent rotation periods but very different lightcurve shapes. The differing shapes indicate that the observations were made at different asterocentric latitudes and should be helpful toward future LI modeling.

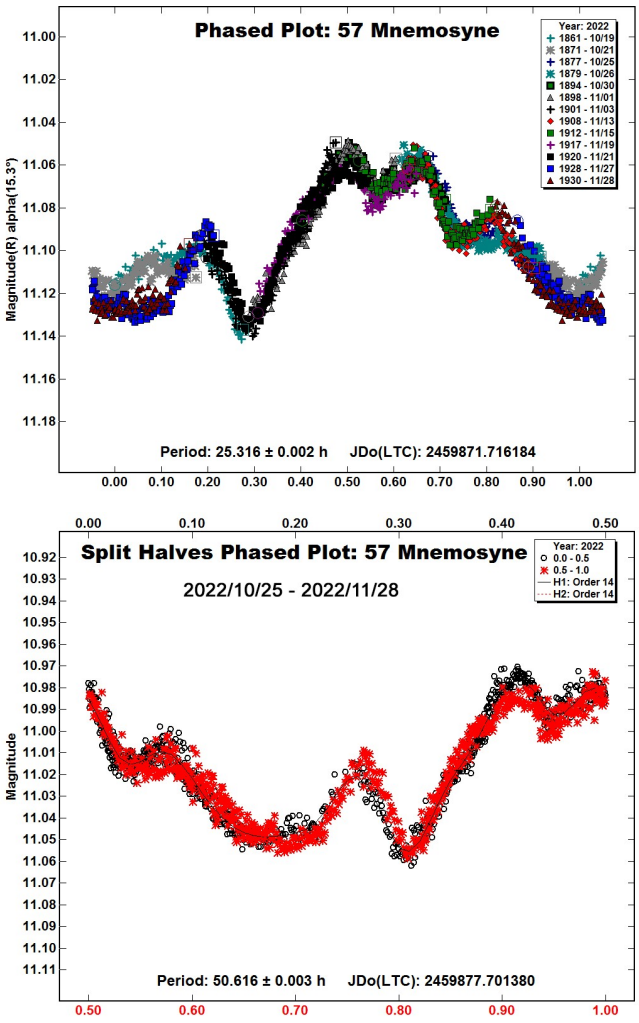

645 Agrippina. Periods published many years ago are by Behrend (2004web), 34.39 h; and Binzel (1987), 32.6 h. Recently published periods are much longer: Pál et al. (2020), 53.7893 h; and Polakis (2019), 54.13 h. New observations on twelve nights 2022 Nov. 14 - Dec. 26 provide a good fit to an irregular lightcurve with period 53.436 ± 0.004 hours, amplitude 0.18 ± 0.01 magnitudes. This value is consistent with the recent publications by Pál et al. and by Polakis. Periods lower than 35 hours can now be definitively ruled out.

Number	Name	2022/mm/dd	Phase	LPAB	BPAB	Period(h)	P.E	Amp	A.E.
57	Mnemosyne	10/19-11/28	15.2, 5.9	66	-13	25.316	0.002	0.08	0.01
645	Agrippina	11/14-12/26	*12.6, 6.1	83	9	53.436	0.004	0.18	0.01
987	Wallia	07/19-08/16	15.2, 3.4	329	0	10.085	0.001	0.14	0.01

Table I. Observing circumstances and results. Pts is the number of data points. The phase angle is given for the first and last date, except that a * denotes a minimum was reached between these dates. LPAB and BPAB are the approximate phase angle bisector longitude and latitude at mid-date range (see Harris *et al.*, 1984).

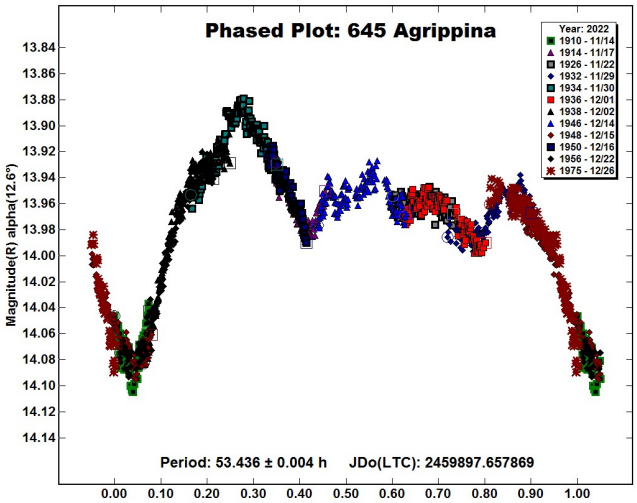

987 Wallia. Previously published periods are by Lagerkvist (1979), >10 h; Cieza et al. (1999), 10.523 h; Behrend (2008web), 10.08 h; Behrend (2011web), 10.0813 h; and Ferrero (2012), 10.082 h. New observations on five nights 2022 July 19 - Aug. 16 provide a good fit to a lightcurve with four unequal maxima and minima per rotational cycle, rotation period 10.085 ± 0.001 hours, amplitude 0.14 ± 0.01 magnitudes, consistent with previously published values.

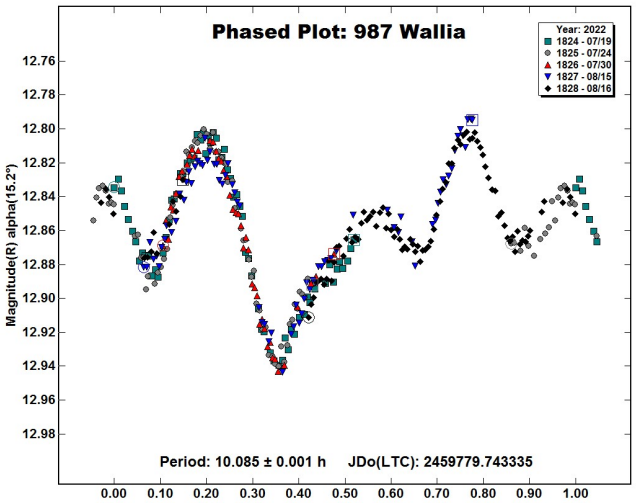

References

Behrend, R. (2004web, 2008web, 2011web, 2016web, 2020web). Observatoire de Geneve web site. *http://*obswww.unige.ch/*~behrend/page_cou.html*.

Binzel, R.P. (1987). "A photoelectric survey of 130 asteroids." *Icarus* **72**, 135-208.

Cieza, L.A.; Ciliberti, L.N.; Iserte, J.A. (2009), *IAPPP Comm.* **74**, 12-23.

Ditteon, R.; Hawkins, S. (2007). "Asteroid lightcurve analysis at the Oakley Observatory - November 2006." *Minor Planet Bull.* **34**, 59-64.

Ferrero, M. (2012). "Lightcurve determination at the Bigmuskie Observatory from 2011 July - December." *Minor Planet Bull.* **39**, 65-67.

Harris, A.W.; Young, J.W.; Scaltriti, F.; Zappala, V. (1984). "Lightcurves and phase relations of the asteroids 82 Alkmene and 444 Gyptis." *Icarus* **57**, 251-258.

Harris, A.W.; Young, J.W.; Dockweiler, T.; Gibson, J.; Poutanen, M.; Bowell, E. (1992). "Asteroid lightcurve observations from 1981." *Icarus* **95**, 115-147.

Lagerkvist, C.-I. (1979). "A lightcurve survey of asteroids with Schmidt telescopes: Observations of nine asteroids during oppositions in 1977." *Icarus* **38**, 106-144.

Pál, A.; Szakáts, R.; Kiss, C.; Bódi, A.; Bognár, Z.; Kalup, C.; Kiss, L.L.; Marton, G.; Molnár, L.; Plachy, E.; Sárneczky, K.; Szabó, G.M.; Szabó, R. (2020). "Solar System Objects Observed with TESS - First Data Release: Bright Main-belt and Trojan Asteroids from the Southern Survey." *Astrophys. J. Suppl. Series* **247**, 26.

Pilcher, F. (2019). "New lightcurves of 50 Virginia, 57 Mnemosyne, 59 Elpis, 444 Gyptis, and 997 Priska." *Minor Planet Bull.* **46**, 445-448.

Pilcher, F. (2020). "Lightcurves and rotation periods of 50 Virginia, 57 Mnemosyne, 58 Concordia, 59 Elpis, 78 Diana, and 529 Preziosa." *Minor Planet Bull.* **47**, 344-346.

Pilcher, F. (2022). "Lightcurves and rotation periods of 57 Mnemosyne and 58 Concordia." *Minor Planet Bull.* **49**, 9-10.

Polakis, T. (2019). "Lightcurve analysis for eleven main-belt minor planets." *Minor Planet Bull.* **45**, 269-273.

ASTEROID LIGHTCURVE ANALYSIS AT THE CENTER FOR SOLAR SYSTEM STUDIES: PALMER DIVIDE STATION 2022 SEPTEMBER-NOVEMBER

Brian D. Warner
Center for Solar System Studies (CS3)
446 Sycamore Ave.
Eaton, CO 80615 USA
brian@MinPlanObs.org

(Received: 2023 January 11)

CCD photometric observations of eight asteroids were made at the Center for Solar System Studies between 2022 September and November. Data analysis showed that at least three objects appeared to have more than one period. The Hungaria-space 2049 Grietje has a dominant period of 41.31 h and two secondary periods of 12.96 h and 19.91 h. Hungaria dynamic family member 5841 Stone shows a secondary period of 20.37 h, along with a well-established primary period of 2.888 h. 6901 Roybishop, another Hungaria-space asteroid, appeared to have a secondary period of 14.302 h, adding to the suspicions raised by observations made by the author in 2008.

CCD photometric observations of eight asteroids were carried out at the Center for Solar System Studies (CS3-PDS) from 2022 September-November as part of an ongoing general study of asteroid rotation periods with a concentration on near-Earth and Hungaria asteroids.

Telescope	Camera
0.30-m *f*/6.3 SCT	SBIG STL-1001E
0.35-m *f*/9.1 SCT (x3)	FLI Microline 1001E
0.50-m *f*/8.1 Ritchey-Chrétien	FLI Proline 1001E

Table I. List of available telescopes and CCD cameras at CS3-PDS. The exact combination for each telescope/camera pair can vary due to maintenance or specific needs.

Table I lists the five telescope/CCD cameras pairs used at CS3-PDS. All the cameras use CCD chips from the KAF 1001 blue-enhanced family and so have essentially the same response. The pixel scales ranged from 1.24-1.60 arcsec/pixel. All lightcurve observations were made with no or a clear filter. The exposures varied depending on the asteroid's brightness.

To reduce the number of times and amounts of adjusting nightly zero-points, the ATLAS catalog r´ (SR) magnitudes (Tonry et al., 2018) are used. Those adjustments are usually ≤ ±0.03 mag. The rare greater corrections may have been related in part to using unfiltered observations, poor centroiding of the reference stars, and not correcting for second-order extinction. Another cause may be selecting what appears to be a single star but is actually an unresolved pair.

The Y-axis values are ATLAS SR "sky" (catalog) magnitudes. The values in the parentheses give the phase angle(s), *a*, along with the value of *G* used to normalize the data to the comparison stars used in the earliest session. This, in effect, adjusts all the observations so that they seem to have been made at a single fixed date/time and phase angle. Presumably, any remaining variations are due only to the asteroid's rotation and/or albedo changes.

There can be up to three phase angles If two, the values are for the first and last night of observations. If three, the middle value is the extrema (maximum or minimum) reached between the first and last observing runs. The X-axis shows rotational phase from -0.05 to 1.05. If the plot includes the amplitude, e.g., "Amp: 0.65," this is the amplitude of the Fourier model curve and *not necessarily the adopted amplitude for the lightcurve*.

For brevity, only some of the previous results are referenced. A more complete listing is in the asteroid lightcurve database (Warner et al., 2009a; "LCDB" from here on).

1103 Sequoia. According to Nesvorny (2015) and Nesvorny et al. (2015), this 8-km asteroid is part of the dynamical Hungaria family, which is named after the largest member, 434 Hungaria. This means that it is one of the remnants of the presumed collision that created a number of asteroids with similar orbital characteristics and taxonomic classification (see Warner et al., 2009b).

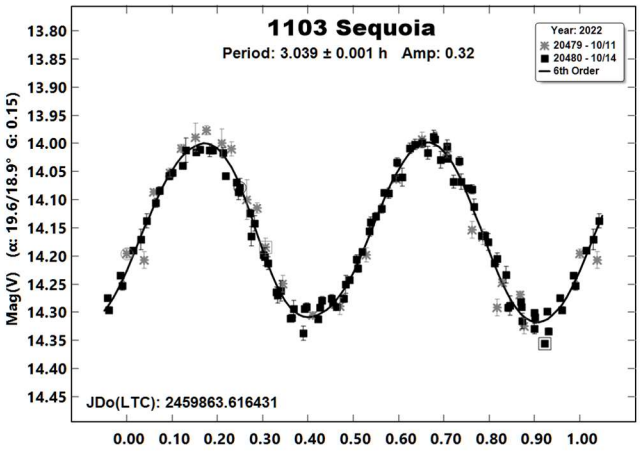

Previous results are all close to 3.04 h, starting with Wisniewski et al. (1997). The asteroid was suspected to be a binary (Warner, 2015e), but no secondary period was given in the only report over the years that raised the possibility of a satellite.

2049 Grietje. The only previous result rated U > 1+ in the LCDB was from Warner (2016), who found P = 8.910 h, A = 0.12 mag. After several false starts, solutions for the two data sets were found that were similar but cannot be said to be in full agreement.

Initially, the 2022 data showed a dominant period of 41.31 h with secondary periods of 12.96 h and 19.91 h. This was suspicious because, first, the solution was significantly different from the 2016 results and, second, because the three periods were harmonically related by

$$1/12.96 - 1/19.91 \cong 1/41.31 \ (\Delta\ 0.003)$$

and so, the search for a different solution set began.

The first step was to revisit the 2016 data to see if they could be fit to the initial results from 2022 without taking excessive liberties when adjusting nightly zero points. In the end, two of the three initial periods could be extracted, but only after dropping about 30% of the nightly sessions. So much forcing of the data to fit those periods ("curving a fit" instead of "fitting a curve") meant that a new theory (alternate periods) needed to be pursued. The result is reflected in the period spectrum, which shows stronger solutions somewhat close to the 2016 results.

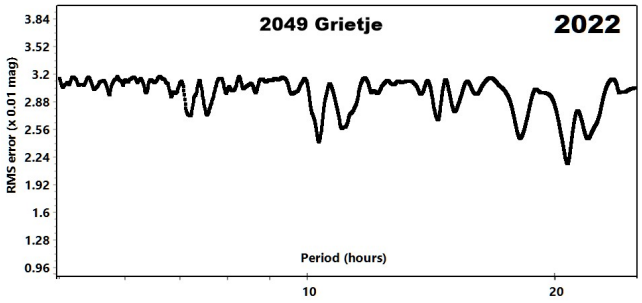

Going back to the 2016 data, the comp star catalog magnitudes were checked and most found to be accurate. However, two sessions had unresolvable discrepancies and so were dropped from new analysis. This led to a monomodal lightcurve with P = 9.56 h, or about 0.6 hours longer than the original result. Given the low amplitude (0.06 mag), a bimodal solution was not assured (Harris et al., 2014). An alternate solution, with bimodal lightcurve, has a period of 19.09 h.

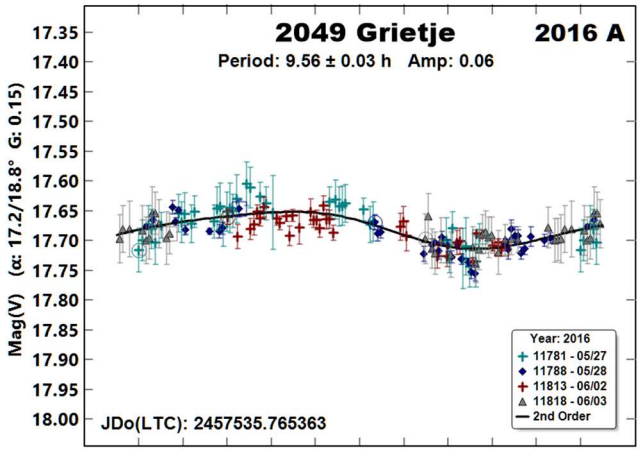

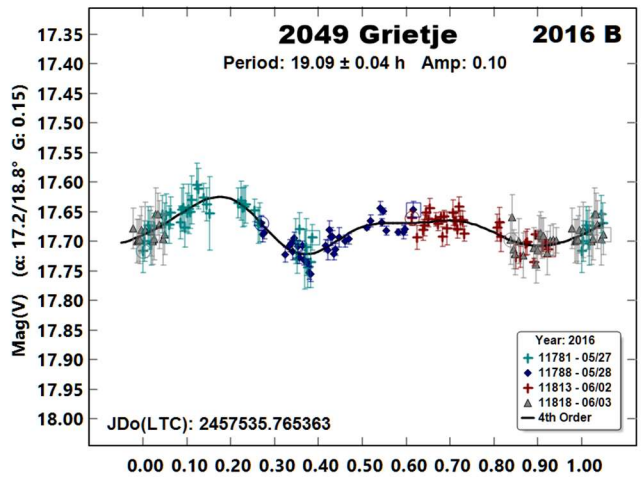

Returning to the 2022 data, a period search near the revised 2016 results found a good fit to a monomodal lightcurve with a period of 10.34 h, or 1.4 hours more than the original solution and about 0.8 hours more than the revised period. The secondary period from the 2022 data is almost 1.6 hours longer than in 2016 (revised).

None of the revised/new periods can be considered secure because of the combination of low amplitudes and poor coverage of the lightcurves, i.e., number of data points, limited date range compared to the periods, and a significant gap in one case. At best, future observers will know that finding a reliable solution for this asteroid will require careful work, some luck, and, better yet, a collaboration involving observers widely-distributed in longitude.

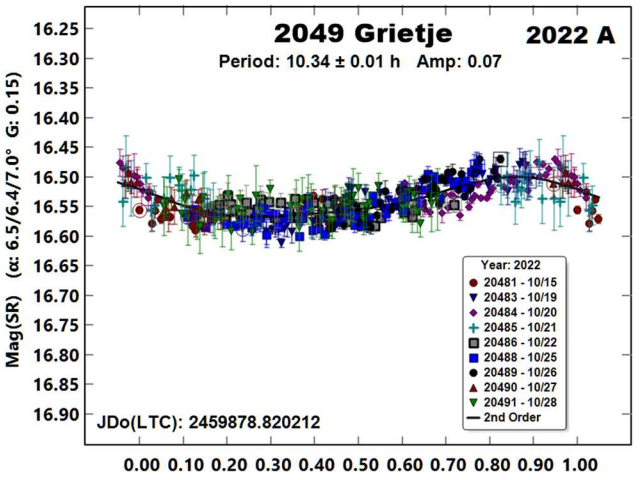

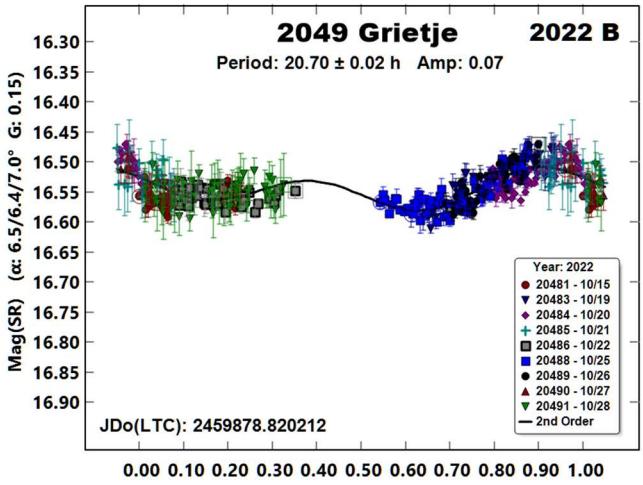

5439 Couturier. The only previous result found in the LCDB was from Dahlgren et al. (1998) who estimated the period to be about 50 h and amplitude of 0.47 mag. The period found from the 2022 data was about 220 h.

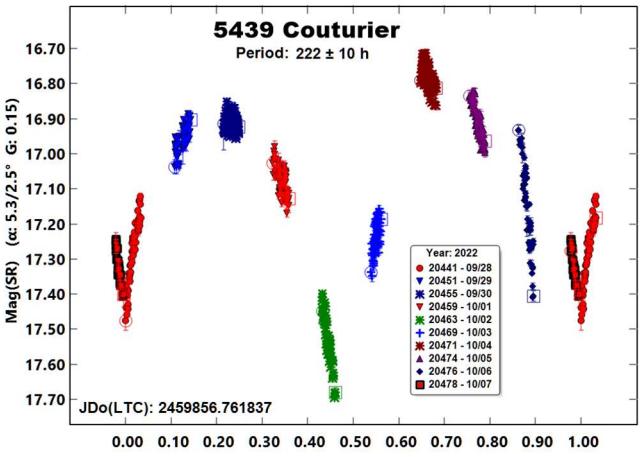

With what appear to be very long periods, there is the possibility that the period is much shorter due the observing window "sliding" slowly across a lightcurve that has a period that is nearly commensurate with an Earth-day. In this case, the raw plot of the data (not shown but nearly identical to the phased plot) that was built using observing runs that exceded six hours appears to eliminate the possibility of a period shorter than reported here.

5841 Stone. Five previous results from the author (Warner, 2007; 2010; 2013; 2015b; 2015c) did not report signs of a secondary period. The "NoSub" plot gives a strong indication of there being one. A dual-period search using *MPO Canopus* found a primary period in close agreement with previous results as well as an ill-defined lightcurve with a period of 20.37 h.

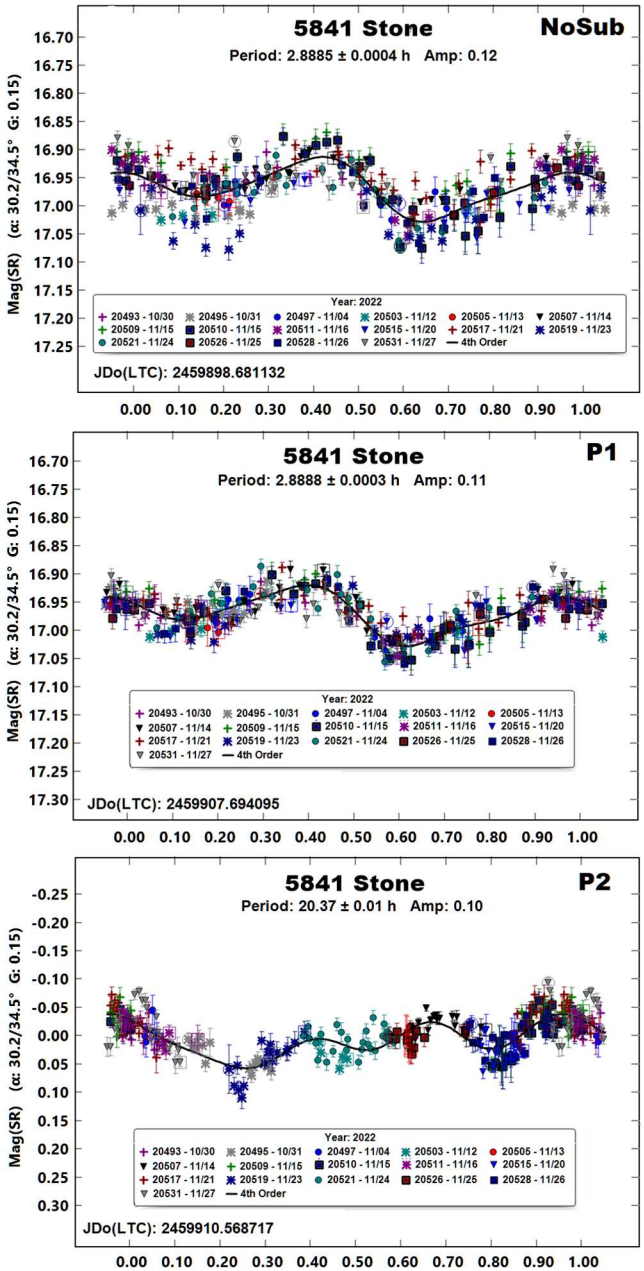

Unfortunately, additional observations could not be made to help confirm these results. The asteroid, a member of the Hungaria dynamical family, should be observed at future apparitions and, with an unprejudiced eye, the data analyzed for signs of a satellite.

6901 Roybishop. Warner (2009) reported that observations made in 2008 August showed possible signs of a satellite, i.e., a lightcurve with a period of 17.157 h and apparent mutual events that led to an estimated effective satellite-to-primary diameter ratio of > 0.19.

The 2022 data showed a putative primary period of 4.4608 h, which is in good agreement with previous results. The secondary lightcurve had a much larger amplitude (0.11 mag) than in the earlier result but a period about three hours shorter.

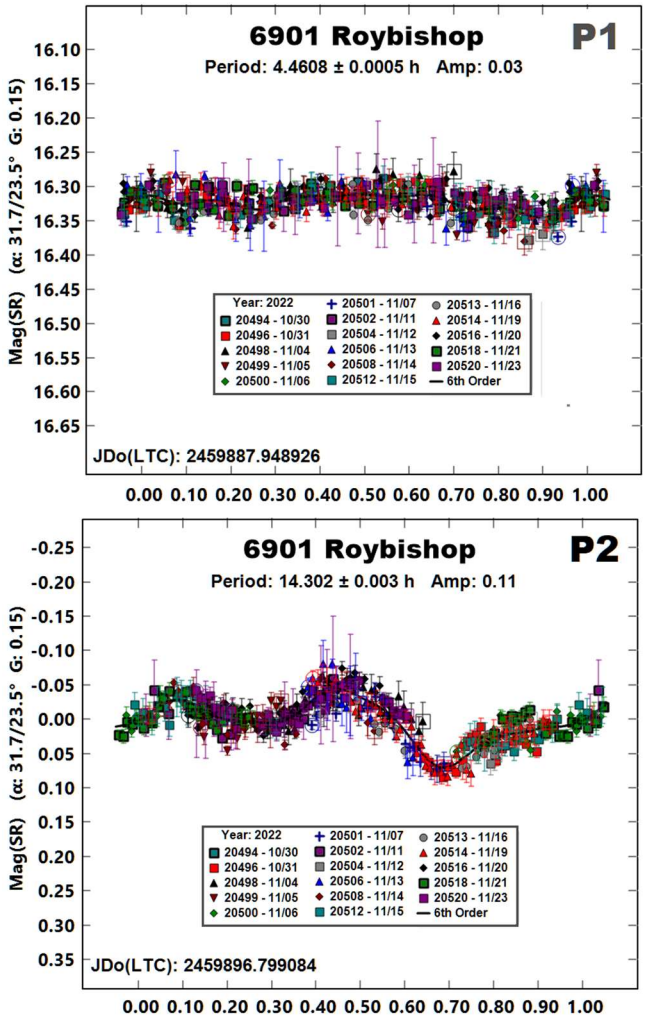

The two secondary periods have an almost exact 6:5 ratio. Given the greater confidence in the 2022 result, the period of 14.302 h is adopted for this paper. Even so, the shape of the lightcurve is not easily interpreted for an estimate of the effective diameter ratio. A *rough guess* of 0.04 mag for the shallower "event" does yield a ratio of Ds/Dp ≥ 0.19, the same as determined from the 2008 observations.

Number	Name	2022/mm/dd	Phase	L_{PAB}	B_{PAB}	Period(h)	P.E.	Amp	A.E.	Grp
1103	Sequoia	10/11-10/11	19.5	26	26	3.039	0.001	0.32	0.01	H
2049	Grietje	10/15-10/28	*6.5,7.0	29	-6	[A]10.34	0.01	0.07	0.01	H
						20.70	0.02	0.07	0.01	
		2016/05/24-06/03	17.2,18.8	242	26	[A]9.56	0.03	0.06	0.01	
						19.09	0.04	0.10	0.01	
5439	Couturier	09/28-10/07	5.3,2.5	21	1	222	10	0.90	0.05	HIL
5841	Stone	10/30-11/27	30.3,34.5	309	13	[P]2.8888	0.0003	0.11	0.01	H
						20.37	0.01	0.10	0.02	
6901	Roybishop	10/30-11/21	31.7,24.4	87	18	[P]4.4608	0.0005	0.04	0.01	H
						14.302	0.003	0.11	0.02	
22070	2000 AN106	09/30-10/05	12.6,11.4	40	-16	11.5	0.01	0.60	0.03	HIL
85713	1998 SS49	10/03-10/05	33.4,33.3	49	-3	[D]2.831	0.002	0.24	0.02	NEA
						5.331	0.006	0.11	0.01	
		2014/09/26-10/01	35.6,35.9	49	-3	[P]2.680	0.002	0.24	0.02	
						14.27	0.03	0.03	0.01	
		2014/11/20-11/24	86.4,96.8	115	23	[P]2.258	0.002	0.06	0.01	
						13.98	0.02	0.05	0.01	
523823	2015 BG311	11/23-11/27	24.9,25.1	42	1	80.4	0.5	1.15	0.1	NEA

Table II. Observing circumstances and results. [A]Preferred period of an ambiguous solution. [P]Rotation period of the putative primary in a binary system. The second line is the presumed orbital period of the satellite. [D]Dominant period of a multi-period solution. Subsequent lines are additional, not alternate, periods. The phase angle is given for the first and last date. If preceded by an asterisk, the phase angle reached an extremum during the period. LPAB and BPAB are the approximate phase angle bisector longitude/latitude at mid-date range (see Harris et al., 1984).

(22070) 2000 AN106. There were no previously reported periods found in the LCDB. Analysis of the data from the 2022 observations led to a period very close to being commensurate with an Earth-day. Fortunately, the individual observations sessions covered almost half the adopted period and, more important, the relatively low phase angle and large amplitude virtually assured a bimodal lightcurve (Harris et al., 2014).

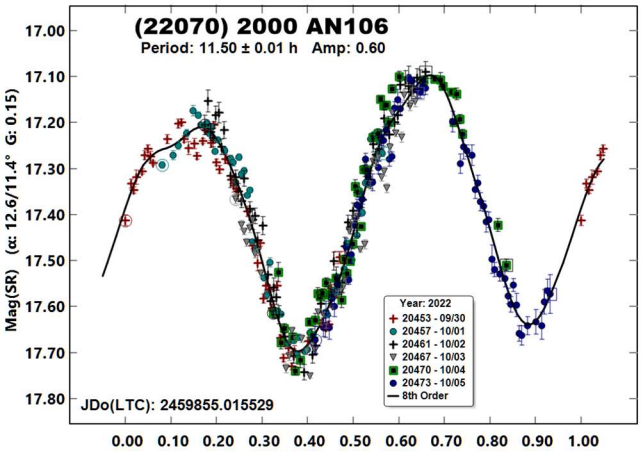

(85713) 1998 SS49. There were three sets of results found in the LCDB: Warner (2015a; 5.370 h), Warner (2015d; 5.66 h), and Vaduvescu et al. (2017; 5.398 h).

Using the 2022 data, a solution near 5.3 h was found, but the period spectrum showed different more strongly-favored periods. Following that guide, a period of about 3.3 h was found and adopted. However, it's best to check previous data sets to see if they could be fit to the new result. They could not. Instead, the three data sets led to the possibility of the asteroid being binary.

2014 November Revisited

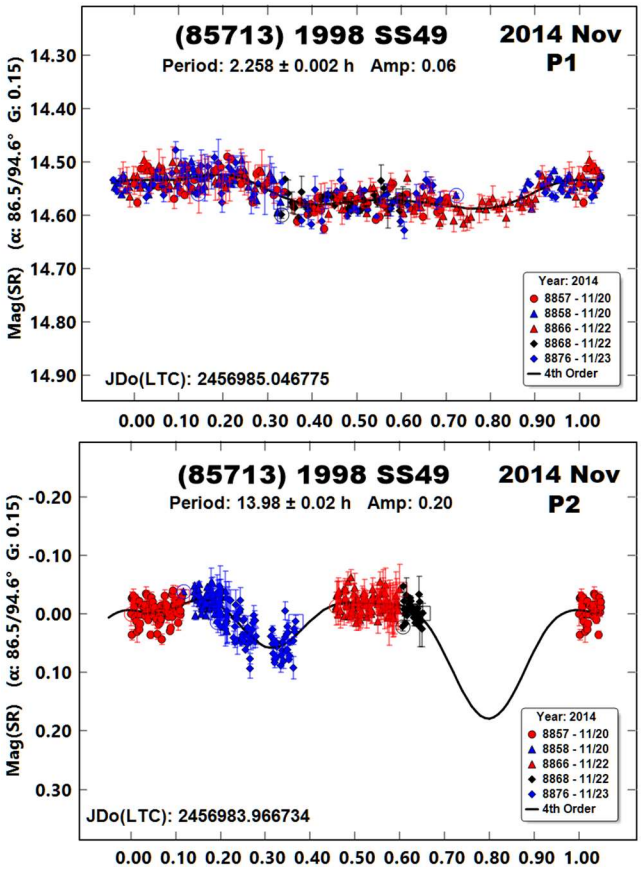

On the face of it, the most compelling case was that based on the work from 2014 November. However, as with all observations, the large phase angles could have introduced strong shadowing effects; those can often lead the analysis down a false path. Even so, the "primary" period of 2.258 h, combined with the estimated size of 2 km, made the asteroid a good candidate for being binary. This was supported by a typical secondary period of about 14 h and a lightcurve, with liberal interpretation, that resembled one for an elongated satellite and, possibly, non-total mutual events.

2014 September Data Revisited: The single-period analysis of data from 2014 September appeared to show signs of a second period and so, using the results from 2014 September as a guide, a dual-period search was made with *MPO Canopus*.

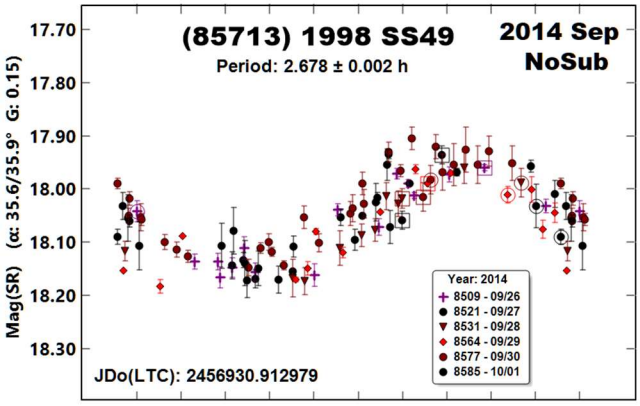

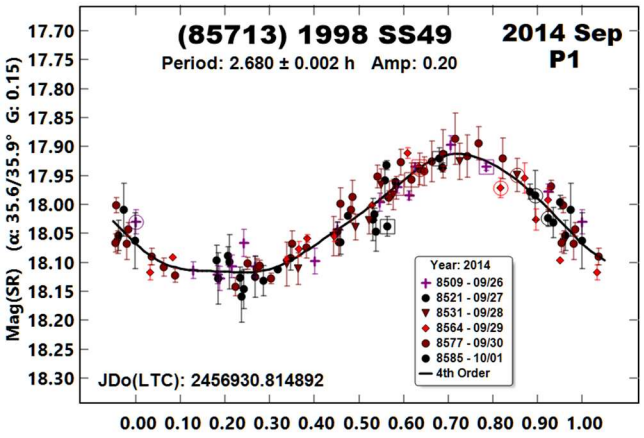

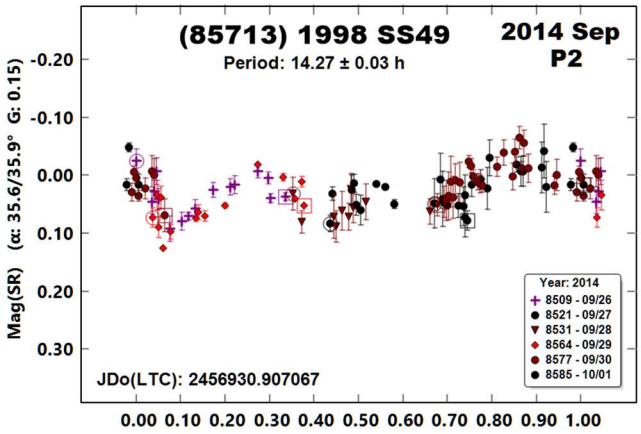

Again, a very liberally interpreted secondary period was found that was similar to the September results. However, the primary period was significantly longer and the amplitude much larger. This seems contrary to the expected decrease in amplitude with decreasing phase angle (Zappala et al., 1990) but, given the large phase angles, this might be attributed to decreasing shadowing effects.

Back to the Future: Re-analysis of 2022 October data: The period spectrum from the 2022 data analysis shows that a period near 6.6 h was the most dominant, but this led to a lightcurve with coverage gaps that were signs of a *fit by exclusion*, which is when the Fourier analysis finds a "better" solution by minimizing the number of overlapping data points in the phased lightcurve. The period spectrum has lower-confidence solutions near the two primary periods found from the 2014 data.

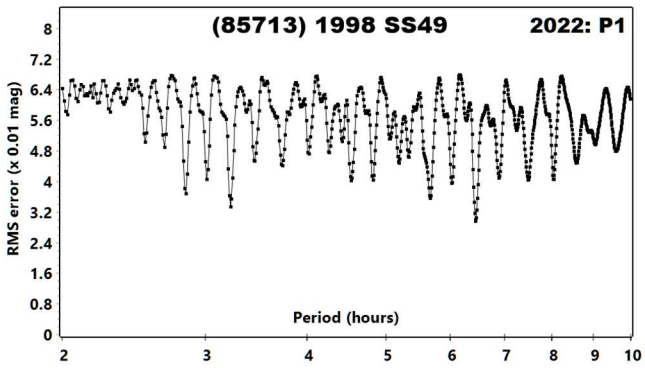

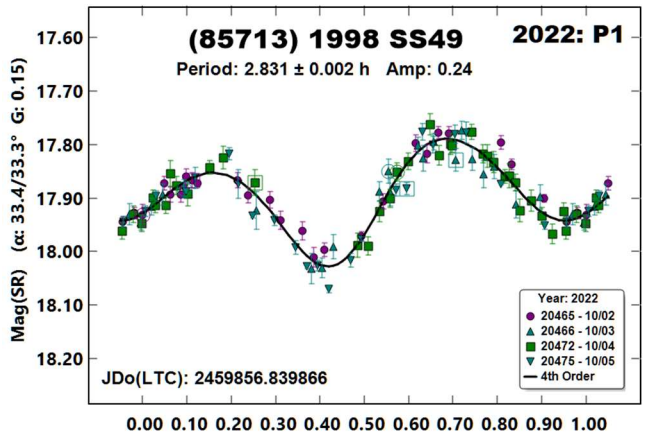

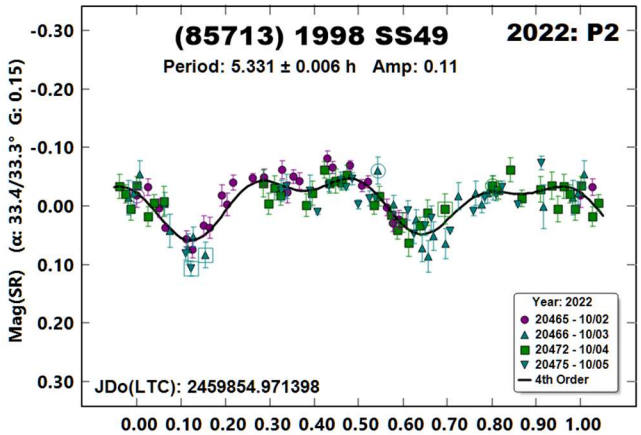

The strongest signal was for a period at 2.831 h. This produced a bimodal lightcurve with an amplitude of 0.24 mag. Even with the somewhat large phase angles near 33°, the amplitude makes a good argument for a bimodal lightcurve (Harris et al., 2014).

The derived secondary period leaves much to be desired, though its lightcurve, if the period were not known, could easily be interpreted as a nearly-spheroidal satellite undergoing mutual events. Further complicating matters is that the primary and secondary periods have a close to integral ratio if extending out 30-40 and 60+ rotations of the shorter period. In other words, one period might be a complicated harmonic of the other.

The lack of agreement among the results is likely due to not having enough data. Even though the 2014 November data set had more than 300 data points, it covered a span of only three days. The solution seemed obvious, or at least reasonably secure, at the time but the small diameter and being an NEA should have prompted more extended observations.

This is not always easy: the target may be observable for only a short time or, as the large change in amplitude and lightcurve shape during the 2014 observations show, finding a secure solution becomes far more complicated. One might wonder how many binary, tumbling, or otherwise interesting objects have been overlooked by crossing a false finish line.

(523823) 2015 BG311. There were no previous period entries in the 2021 December version of the LCDB. The estimated size is only 240 meters. Given that and the apparently long period of almost 3.5 days, the chances that the asteroid is tumbling are good (Pravec et al., 2005; 2014). The slight misfits of the data to the derived lightcurve appear to confirm some low-level of tumbling.

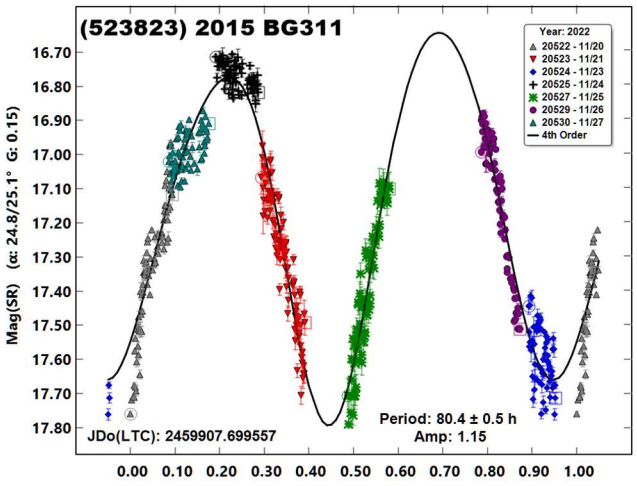

Acknowledgements

This work includes data from the Asteroid Terrestrial-impact Last Alert System (ATLAS) project. ATLAS is primarily funded to search for near earth asteroids through NASA grants NN12AR55G, 80NSSC18K0284, and 80NSSC18K1575; byproducts of the NEO search include images and catalogs from the survey area. The ATLAS science products have been made possible through the contributions of the University of Hawaii Institute for Astronomy, the Queen's University Belfast, the Space Telescope Science Institute, and the South African Astronomical Observatory.

The author gratefully acknowledges a Shoemaker NEO Grants from the Planetary Society (2007). This was used to purchase some of the equipment used in this research.

References

Dahlgren, M.; Lahulla, J.F.; Lagerkvist, C.-I.; Lagerros, J.; Mottola, S.; Erikson, A.; Gonano-Beurer, M.; Di Martino, M. (1998). "A Study of Hilda Asteroids. V. Lightcurves of 47 Hilda Asteroids." *Icarus* **133**, 247-285.

Harris, A.W.; Young, J.W.; Scaltriti, F.; Zappala, V. (1984). "Lightcurves and phase relations of the asteroids 82 Alkmene and 444 Gyptis." *Icarus* **57**, 251-258.

Harris, A.W.; Pravec, P.; Galad, A.; Skiff, B.A.; Warner, B.D.; Vilagi, J.; Gajdos, S.; Carbognani, A.; Hornoch, K.; Kusnirak, P.; Cooney, W.R.; Gross, J.; Terrell, D.; Higgins, D.; Bowell, E.; Koehn, B.W. (2014). "On the maximum amplitude of harmonics on an asteroid lightcurve." *Icarus* **235**, 55-59.

Nesvorny, D. (2015). "Nesvorny HCM Asteroids Families V3.0." NASA Planetary Data Systems, id. EAR-A-VARGBET-5-NESVORNYFAM-V3.0.

Nesvorny, D.; Broz, M.; Carruba, V. (2015). "Identification and Dynamical Properties of Asteroid Families." In *Asteroids IV* (P. Michel, F. DeMeo, W.F. Bottke, R. Binzel, Eds.). Univ. of Arizona Press, Tucson, also available on astro-ph.

Pravec, P.; Harris, A.W.; Scheirich, P.; Kušnirák, P.; Šarounová, L.; Hergenrother, C.W.; Mottola, S.; Hicks, M.D.; Masi, G.; Krugly, Yu.N.; Shevchenko, V.G.; Nolan, M.C.; Howell, E.S.; Kaasalainen, M.; Galád, A.; Brown, P.; Degraff, D.R.; Lambert, J.V.; Cooney, W.R.; Foglia, S. (2005). "Tumbling asteroids." *Icarus* **173**, 108-131.

Pravec, P.; Scheirich, P.; Durech, J.; Pollock, J.; Kusnirak, P.; Hornoch, K.; Galad, A.; Vokrouhlicky, D.; Harris, A.W.; Jehin, E.; Manfroid, J.; Opitom, C.; Gillon, M.; Colas, F.; Oey, J.; Vrastil, J.; Reichart, D.; Ivarsen, K.; Haislip, J.; LaCluyze, A. (2014). "The tumbling state of (99942) Apophis." *Icarus* **233**, 48-60.

Tonry, J.L.; Denneau, L.; Flewelling, H.; Heinze, A.N.; Onken, C.A.; Smartt, S.J.; Stalder, B.; Weiland, H.J.; Wolf, C. (2018). "The ATLAS All-Sky Stellar Reference Catalog." *Astrophys. J.* **867**, A105.

Vaduvescu, O.; Aznar, A.M.; Tudor, V.; Predatu, M.; and 30 colleagues (2017). "The EURONEAR Lightcurve Survey of Near Earth Asteroids." *Earth, Moon, and Planets* **120**, 41-100.

Warner, B.D. (2007). "Asteroid Lightcurve Analysis at the Palmer Divide Observatory - June-September 2006." *Minor Planet Bull.* **34**, 8-10.

Warner, B.D. (2009). "Asteroid Lightcurve Analysis at the Palmer Divide Observatory: 2008 May-September." *Minor Planet Bull.* **36**, 7-13.

Warner, B.D.; Harris, A.W.; Pravec, P. (2009a). "The Asteroid Lightcurve Database." *Icarus* **202**, 134-146. Updated 2021 Dec. *http://www.minorplanet.info/lightcurvedatabase.html*

Warner, B.D.; Harris, A.W.; Vokrouhlický, D.; Nesvorný, D.; Bottke, W.F. (2009b). "Analysis of the Hungaria asteroid population." *Icarus* **204**, 172-182.

Warner, B.D. (2010). "Asteroid Lightcurve Analysis at the Palmer Divide Observatory: 2009 September-December." *Minor Planet Bull*. **37**, 57-64.

Warner, B.D. (2013). "Asteroid Lightcurve Analysis at the Palmer Divide Observatory: 2013 January-March." *Minor Planet Bull*. **40**, 137-145.

Warner, B.D. (2015a). "Near-Earth Asteroid Lightcurve Analysis at CS3-Palmer Divide Station: 2014 June-October." *Minor Planet Bull*. **42**, 41-53.

Warner, B.D. (2015b). "Asteroid Lightcurve Analysis at CS3-Palmer Divide Station: 2014 June-October." *Minor Planet Bull*. **42**, 54-60.

Warner, B.D. (2015c). "Asteroid Lightcurve Analysis at CS3-Palmer Divide Station: 2014 October-December." *Minor Planet Bull*. **42**, 108-114.

Warner, B.D. (2015d). "Near-Earth Asteroid Lightcurve Analysis at CS3-Palmer Divide Station: 2014 October-December." *Minor Planet Bull*. **42**, 115-127.

Warner, B.D. (2015e). "Two New Binaries and Continuing Observations of Hungaria Group Asteroids." *Minor Planet Bull*. **42**, 132-136.

Warner, B.D. (2016). "Asteroid Lightcurve Analysis at CS3-Palmer Divide Station: 2016 April-July." *Minor Planet Bull.* **43**, 300-304.

Wisniewski, W.Z.; Michalowski, T.M.; Harris, A.W.; McMillan, R.S. (1997). "Photometric Observations of 125 Asteroids." *Icarus* **126**, 395-449.

Zappala, V.; Cellini, A.; Barucci, A.M.; Fulchignoni, M.; Lupishko, D.E. (1990). "An anlaysis of the amplitude-phase relationship among asteroids." *Astron. Astrophys*. **231**, 548-560.

LIGHTCURVE ANALYSIS FOR SIX MAIN-BELT ASTEROIDS

Fernando Huet
Observatorio Polop (Z93)
Apdo. 61 03520 Polop (SPAIN)
fhuet@me.com

Gonzalo Fornas
Centro Astronómico del Alto Turia (J57)
Asociación Valenciana de Astronomía (AVA) SPAIN

Alvaro Fornas
Centro Astronómico del Alto Turia (J57)
Asociación Valenciana de Astronomía (AVA) SPAIN

(Received: 2023 Jan 7)

Photometric observations of six main-belt asteroids were obtained from 2022 August 3 to December 31. We derived the following rotational periods: 940 Rockefellia 6.834 ± 0.006 h, 1399 Teneriffa 2.829 ± 0.001 h, 1543 Bourgeois 41.163 ± 0.016 h, 5076 Lebedev-Kumach 3.341 ± 0.003 h, 6025 Naotosato 27.016 ± 0.009 h, and (20602) 1999 RC198 7.304 ± 0.005 h.

We report on the photometric analysis result for six main-belt asteroids. This work was done from Observatorio Polop MPC Z93 (Alicante) and from the Astronomical Center Alto Turia (CAAT), with the MPC code J57, located in Aras de los Olmos, Valencia, both operated by members of the Valencian Astronomy Association (AVA) (*http://www.astroava.org*). This database shows graphic results of the data (lightcurves), with the plot phased to a given period.

Observatory	Telescope	CCD
Polop Z93	SC 8"	SBIG ST8300
C.A.A.T. J57	43 cm DK	SBIG STXL-11002

Table I. List of instruments used for the observations.

We managed to obtain a number of accurate and complete lightcurves. Observations were concentrated on asteroids with no reported period and those where the reported period was poorly established and needed confirmation. All the targets were selected from the Collaborative Asteroid Lightcurve (CALL) website at (*http://www.minorplanet.info/call.html*) and Minor Planet Center (*http://www.minorplanet.net*). The Asteroid Lightcurve Database (LCDB; Warner et al., 2009) was consulted to locate previously published results.

Images were calibrated in *MaximDL* and measured using *MPO Canopus* (Bdw Publishing) with a differential photometry technique. The comparison stars were restricted to near solar-color to avoid introducing color dependencies, especially at larger air masses. The lightcurves give the synodic rotation period. The amplitude (peak-to-peak) that is shown is that for the Fourier model curve and not necessarily the true amplitude.

Number	Name	mm/dd	Pts	Phase	L_{PAB}	B_{PAB}	Period(h)	P.E.	Amp	A.E.	Grp
904	Rockefellia	2022 12/28-12/31	274	9.70,10.47	81.7	-17.7	6.834	0.006	0.11	0.02	MB-O
1399	Teneriffa	2022 10/01-11/19	204	13.7,17.84	29.5	-7.3	2.829	0.001	0.18	0.02	MB-I
1543	Bourgeois	2022 08/04-08/19	1,242	8.67,9.34	319	9.5	41.163	0.016	0.16	0.02	MB-M
5076	Lebedev-Kumach	2022 11/18-11/25	340	8.3,8.66	59.6	-11.4	3.341	0.003	0.05	0.01	MB-I
6025	Naotosato	2022 08/15-09/04	928	3.32,5.68	329.3	8.5	27.016	0.009	0.43	0.05	MB-O
20602	1999 RC198	2022 12/25-12/27	287	8.3,8.04	104.2	14.6	7.304	0.005	0.64	0.05	MB-O

Table II. Observing circumstances and results. Pts is the number of data points. The Phase angle values are for the first and last date. L_{PAB} and B_{PAB} are the approximate phase angle bisector longitude and latitude at mid-date range (see Harris *et al.*, 1984). Grp is the asteroid family/group (Warner *et al.*, 2009). MB-I/O: Main-belt inner/outer.

(904) Rockefellia. This main-belt asteroid (outer) was discovered on 1918 October 29 by German astronomer Max Wolf at the Heidelberg-Königstuhl State Observatory. It measures approximately 59 kilometers (37 miles) in diameter. It was named after American philanthropist and oil industrialist John D. Rockefeller (1839-1937). We made observations on 2022 Dec 28 to 31. We derived a rotation period of 6.836 ± 0.006 h and an amplitude of 0.11 mag. This is consistent with previous results: Dose (2022), Polakis (2018), and Polakis (2020).

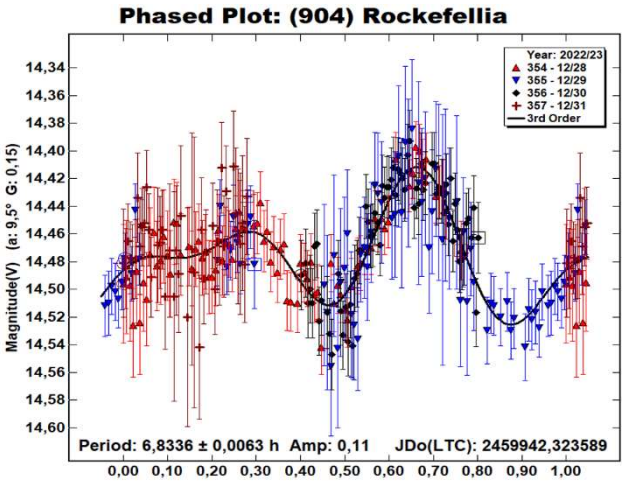

(1399) Teneriffa. This main-belt asteroid was discovered on 1936 August 23 by K. Reinmuth at Heidelberg. Its name derives from Tenerife, the largest and most populous island of the Canary Islands. We made observations on 2022 Oct 1-2 and Nov 19. From our data we derive a rotation period of 2.2829 ± 0.001 h and an amplitude of 0.18 mag. This is consistent with Waszczak et al. (2015), who got a 2.692 h period.

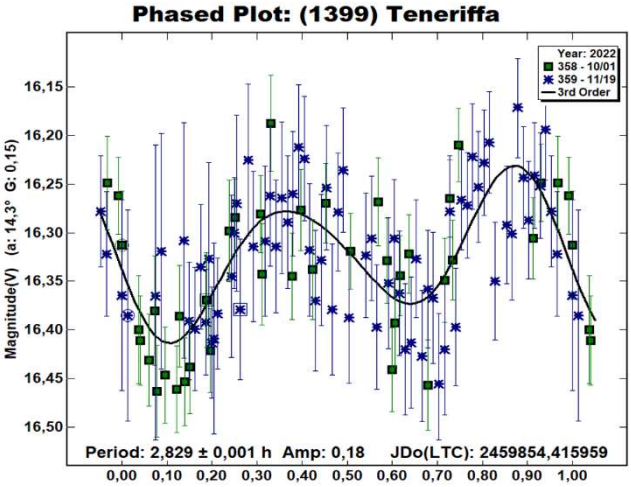

(1543) Bourgeois. This main-belt asteroid (middle) was discovered on 1941 September 2 by E. Delporte at the Uccle observatory. We made observations on 2022 Aug 4 to 19. From our data we derive a rotation period of 41.163 ± 0.016 h and an amplitude of 0.18 mag. Behrend (2005web) found a period of 2.48 h with incomplete data (U=1).

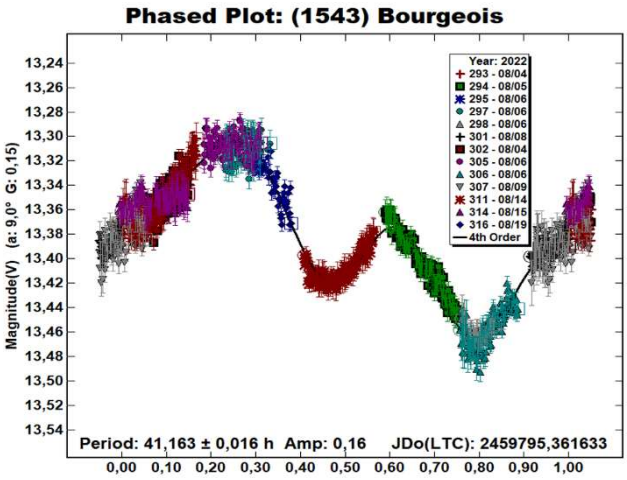

(5076) Lebedev-Kumach. This main-belt asteroid (inner) was discovered on 1973 September 23 by L. I. Chernykh at the Crimean Astrophysical Observatory. We made observations on 2022 Nov 18-25. From our data we derive a rotation period of 3.341 ± 0.003 h and an amplitude of 0.05 mag. Warner (2014) found a period of 3.219 h and Fauerbach and Fauerbach (2019) found 3.215 h.

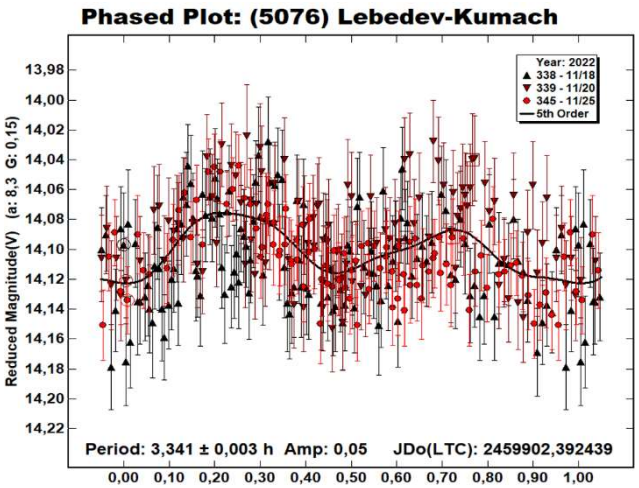

(6025) Naotosato. This main-belt asteroid (outer) was discovered on 1992 December 30 by T. Urata at Oohira Observatory, Japan. We made observations on 2022 Aug 15 to Sep 4. From our data we derive a rotation period of 27.016 ± 0.009 h and an amplitude of 0.43 mag. Behrend (2006web) found a period of 10 h with incomplete data (U=1), which is not consistent with our observations.

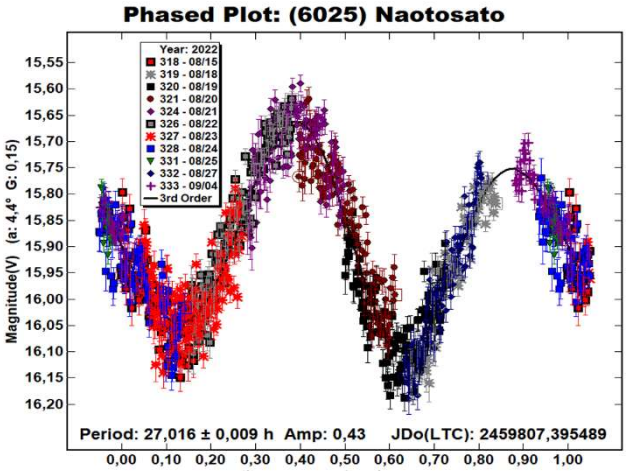

(20602) 1999 RC198. This main-belt asteroid (outer) of the MEL category was discovered on 1999 September 8 at the LINEAR observatory, Socorro, USA. We made observations on 2022 Dec 25-27. From our data we derive a rotation period of 7.3038 ± 0.0038 h and an amplitude of 0.64 mag. Durech et al. (2019) and Pál et al. (2020) found a period of 7.361 h and 7.305 h respectively, both of which agree with our observations.

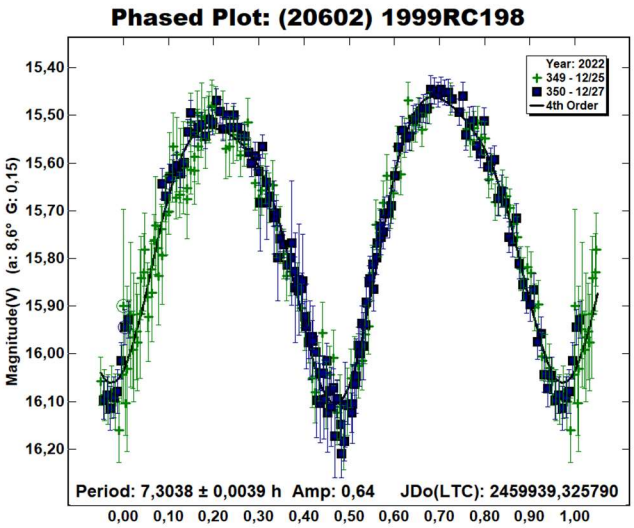

Acknowledgements

We would like to express our gratitude to Brian Warner for supporting the CALL web site and his suggestions.

References

Behrend, R. (2005web; 2006web). Observatoire de Geneve web site. *http://obswww.unige.ch/~behrend/page_cou.html*

Dose, E.V. (2020). "Lightcurves of Seven Asteroids." *Minor Planet Bull.* **49**, 44-47.

Durech, J.; Hanus, J.; Vanco, R. (2019). "Inversion of asteroid photometry from Gaia DR2 and the Lowell Observatory photometric database." *Astron. Astrophys.* **631**, A2.

Fauerbach, M.; Fauerbach, M. (2019). "Rotational Period Determination for Asteroids 755 Quintilla, 1830 Pogson, 5076 Lebedev-Kumach, and (29153) 1998 SY2." *Minor Planet Bull.* **46**, 138-139.

Harris, A.W.; Young, J.W.; Scaltriti, F.; Zappala, V. (1984). "Lightcurves and phase relations of the asteroids 82 Alkmene and 444 Gyptis." *Icarus* **57**, 251-258.

Pál, A.; Szakáts, R.; Kiss, C.; Bódi, A.; Bognár, Z.; Kalup, C.; Kiss, L.L.; Marton, G.; Molnár, L.; Plachy, E.; Sárneczky, K.; Szabó, G.M.; Szabó, R. (2020). "Solar System Objects Observed with TESS - First Data Release: Bright Main-belt and Trojan Asteroids from the Southern Survey." *Ap. J. Suppl. Ser*. **247**, id. 26.

Polakis, T. (2018). "Lightcurve Analysis for Eleven Main-belt Asteroids." *Minor Planet Bull*. **45**, 269-273.

Polakis, T. (2020). "Photometric Observations of Twenty-Seven Minor Planets." *Minor Planet Bull.* **47**, 314-321.

Warner, B.D.; Harris, A.W.; Pravec, P. (2009). "The Asteroid Lightcurve Database." *Icarus* **202**, 134-146. Updated 2021 Dec. *http://www.minorplanet.info/lightcurvedatabase.html*

Warner, B.D. (2014). "Near-Earth Asteroid Lightcurve Analysis at CS3-Palmer Divide Station: 2013 June-September." *Minor Planet Bull*. **41**, 41-47.

Waszczak, A.; Chang, C.-K.; Ofek, E.O.; Laher, R.; Masci, F.; Levitan, D.; Surace, J.; Cheng, Y.-C.; Ip, W.-H.; Kinoshita, D.; Helou, G.; Prince, T.A.; Kulkarni, S. (2015). "Asteroid Light Curves from the Palomar Transient Factory Survey: Rotation Periods and Phase Functions from Sparse Photometry." *Astron. J.* **150**, A75.

COLLABORATIVE ASTEROID PHOTOMETRY FROM UAI: 2022 OCTOBER-DECEMBER

Lorenzo Franco
Balzaretto Observatory (A81), Rome, ITALY
lor_franco@libero.it

Alessandro Marchini
Astronomical Observatory, DSFTA - University of Siena (K54)
Via Roma 56, 53100 - Siena, ITALY

Marco Iozzi
HOB Astronomical Observatory (L63)
Capraia Fiorentina, ITALY

Gianni Galli
GiaGa Observatory (203), Pogliano Milanese, ITALY

Nico Montigiani, Massimiliano Mannucci
Osservatorio Astronomico Margherita Hack (A57)
Florence, ITALY

Giulio Scarfi
Iota Scorpii Observatory (K78), La Spezia, ITALY

Alessandro Coffano, Wladimiro Marinello
Osservatorio Serafino Zani (130), Lumezzane (BS), ITALY

Andrea Mattei
San Marco Astronomical Observatory (L78), Salerno, ITALY

Nello Ruocco
Osservatorio Astronomico Nastro Verde (C82), Sorrento, ITALY

Giorgio Baj
M57 Observatory (K38), Saltrio, ITALY

(Received: 2023 January 12)

Photometric observations of eight asteroids were made in order to acquire lightcurves for shape/spin axis modeling. The synodic period and lightcurve amplitude were found for 58 Concordia, 397 Vienna, 929 Algunde, 1589 Fanatica, 1660 Wood, 1756 Giacobini, (85713) 1998 SS49, 2015 RN35. We also found color indices for 58 Concordia and 397 Vienna.

Collaborative asteroid photometry was done inside the Italian Amateur Astronomers Union (UAI; 2022) group. The targets were selected mainly in order to acquire lightcurves for shape/spin axis modeling. Table I shows the observing circumstances and results.

The CCD observations of eight asteroids were made in 2022 October-December using the instrumentation described in Table II. Lightcurve analysis was performed at the Balzaretto Observatory with *MPO Canopus* (Warner, 2021). All the images were calibrated with dark and flat frames and converted to standard magnitudes using solar colored field stars from CMC15 and ATLAS catalogues, distributed with *MPO Canopus*. For brevity, the following citations to the asteroid lightcurve database (LCDB; Warner et al., 2009) will be summarized only as "LCDB".

58 Concordia is a Ch-type (Bus and Binzel, 2002) middle main-belt asteroid. Collaborative observations were made over four nights. The period analysis shows a synodic period of $P = 9.894 \pm 0.002$ h with an amplitude $A = 0.08 \pm 0.03$ mag. The period is close to the previously published results in the LCDB. Multiband photometry was made by N. Montigiani and M. Mannucci (A57) on 2022 October 29. We found the color indices (B-V) = 0.70 ± 0.03; (V-R) = 0.34 ± 0.03, consistent with a C-type asteroid (Shevchenko and Lupishko, 1998).

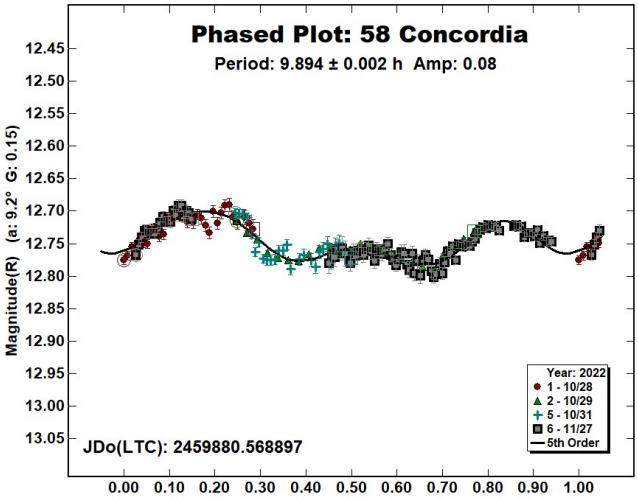

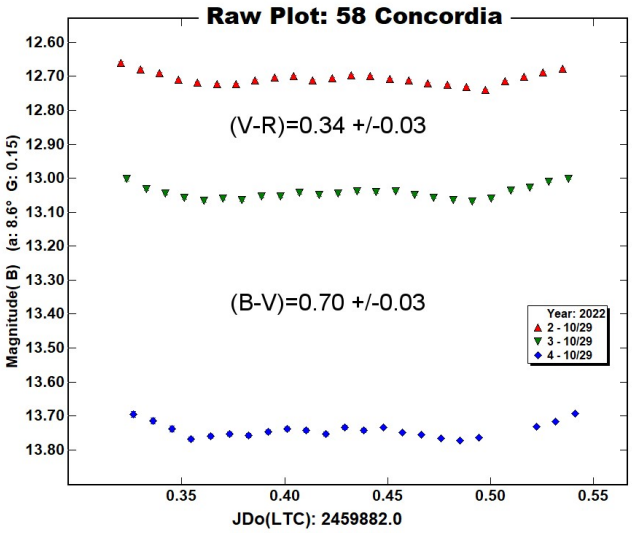

397 Vienna is a K-type (Bus and Binzel, 2002) middle main-belt asteroid. Collaborative observations were made over seven nights. The period analysis shows a synodic period of $P = 15.470 \pm 0.001$ h with an amplitude $A = 0.17 \pm 0.03$ mag. The period is close to the previously published results in the LCDB. Multiband photometry was made by G. Scarfi (K78) on 2022 October 29. We found the color index (V-R) = 0.45 ± 0.02, consistent with a S-type asteroid (Shevchenko and Lupishko, 1998).

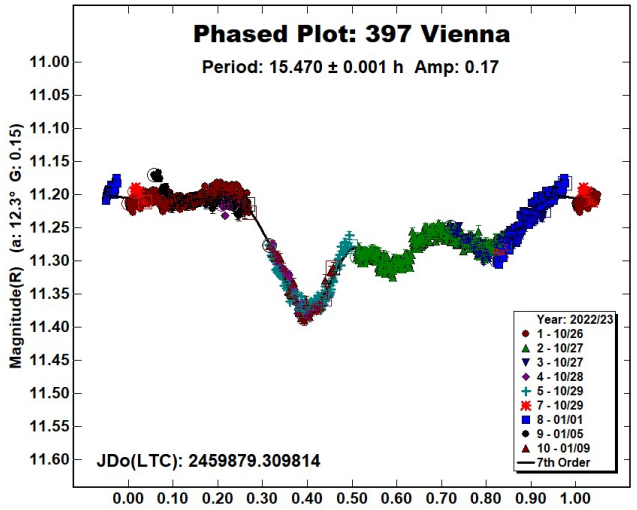

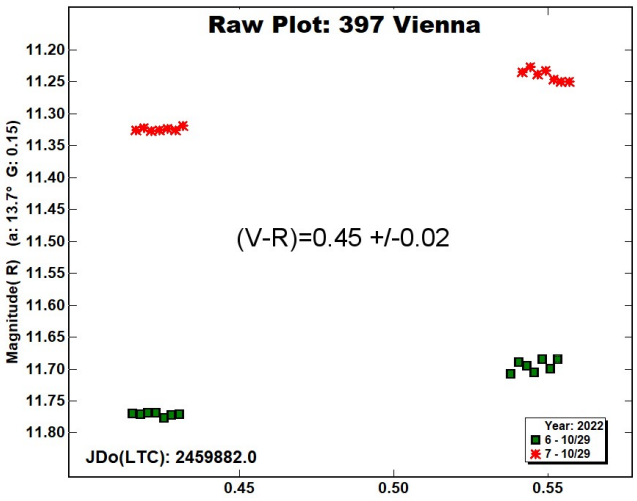

929 Algunde is a S-type (Bus and Binzel, 2002) inner main-belt asteroid. Collaborative observations were made over five nights. The period analysis shows a synodic period of $P = 3.3101 \pm 0.0001$ h with an amplitude $A = 0.12 \pm 0.03$ mag. The period is close to the previously published results in the LCDB.

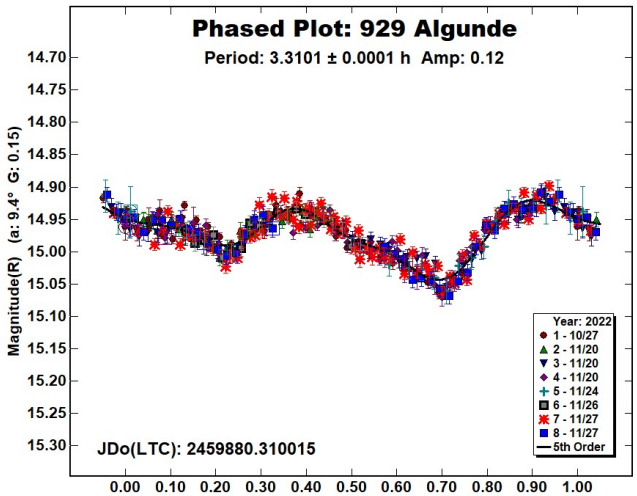

1589 Fanatica is a medium albedo inner main-belt asteroid. Collaborative observations were made over four nights. We found a synodic period of $P = 2.5815 \pm 0.0001$ h with an amplitude $A = 0.18 \pm 0.04$ mag. The period is close to the previously published results in the LCDB.

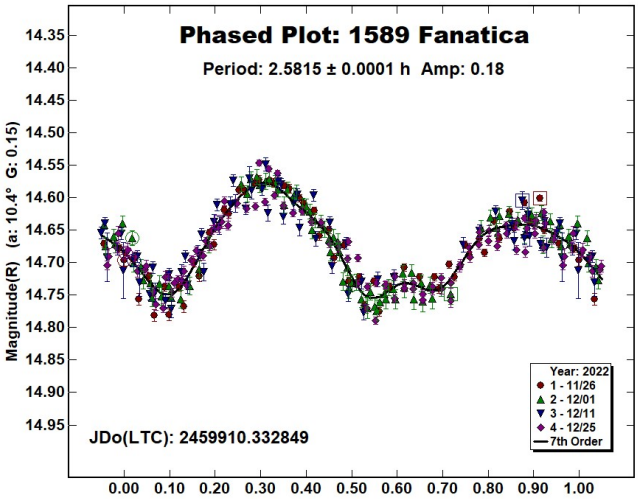

1660 Wood is a S-type (Bus and Binzel, 2002) inner main-belt asteroid. Observations were made over three nights by A. Marchini (K54). We found a synodic period of $P = 6.816 \pm 0.004$ h with an amplitude $A = 0.11 \pm 0.03$ mag. The period is close to the previously published results in the LCDB.

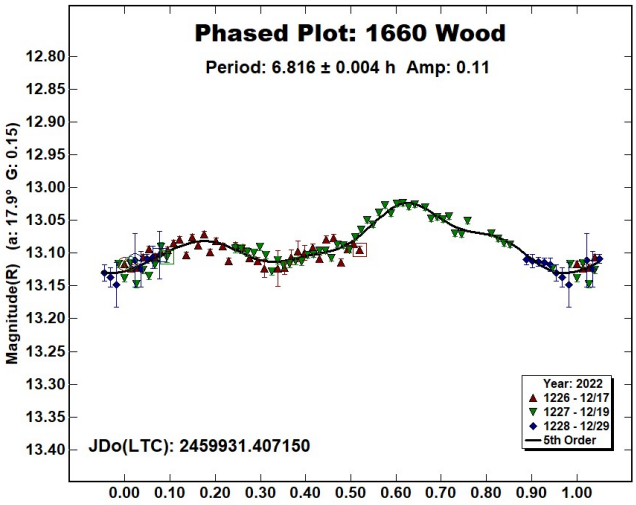

1756 Giacobini is a medium albedo middle main-belt asteroid. Observations were made over three nights by M. Iozzi (L63). We found a synodic period of $P = 3.854 \pm 0.001$ h with an amplitude $A = 0.22 \pm 0.04$ mag. The period is close to the previously published results in the LCDB.

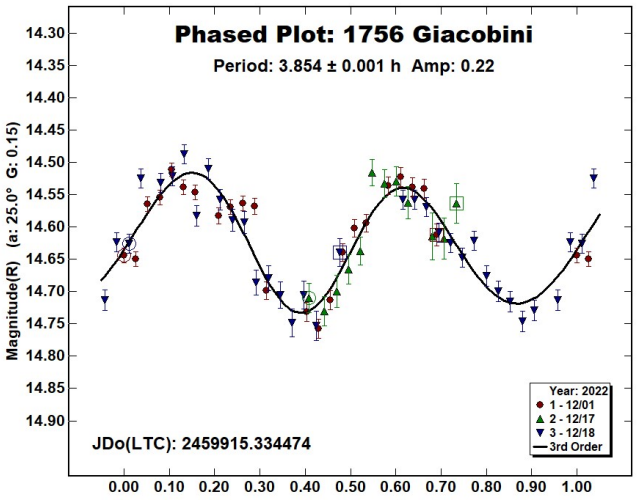

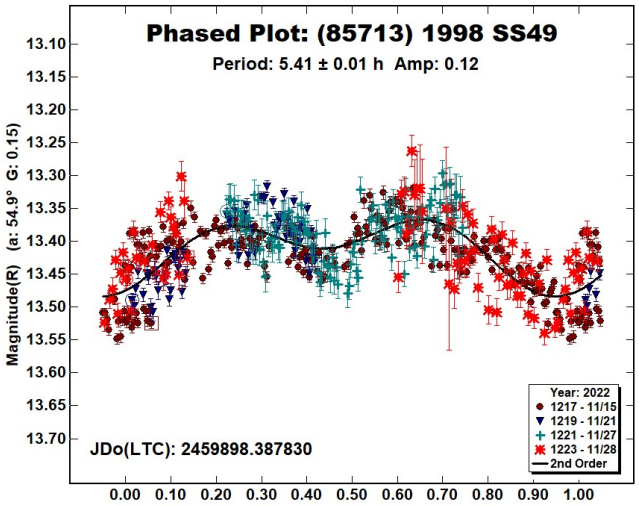

(85713) 1998 SS49 is a low albedo Apollo near-Earth asteroid classified as Potentially Hazardous Asteroid (PHA). Observations were made over four nights by A. Marchini (K54). We found a synodic period of P = 5.41 ± 0.01 h with an amplitude A = 0.12 ± 0.08 mag. The period is close to the previously published results in the LCDB.

2015 RN35 is an Apollo near-Earth asteroid. Collaborative observations were made over two nights, in the following few days to its close approach to the Earth. We found a bimodal solution with a synodic period of P = 0.3193 ± 0.0001 h and an amplitude A = 0.63 ± 0.30 mag. For this asteroid none period were found in

Number	Name	2022-23 mm/dd	Phase	L_{PAB}	B_{PAB}	Period(h)	P.E.	Amp	A.E.	Grp
58	Concordia	10/28-11/27	*8.9, 4.9	56	-6	9.894	0.002	0.08	0.03	MB-M
397	Vienna	10/26-01/09	12.3, 28.1	23	4	15.470	0.001	0.17	0.03	MB-M
929	Algunde	10/27-11/27	*9.3, 6.0	53	0	3.3101	0.0001	0.12	0.03	MB-I
1589	Fanatica	11/26-12/25	*10.3, 5.0	84	-1	2.5815	0.0001	0.18	0.04	MB-I
1660	Wood	12/17-12/29	17.8, 21.4	81	-26	6.816	0.004	0.11	0.03	MB-I
1756	Giacobini	12/01-12/18	25.0, 28.2	27	6	3.854	0.001	0.22	0.04	MB-M
85713	1998 SS49	11/15-11/28	54.9, 100.9	100	24	5.41	0.01	0.12	0.08	NEA
	2015 RN35	12/18-12/19	31.0, 31.2	101	-7	0.3193	0.0001	0.64	0.30	NEA

Table I. Observing circumstances and results. The first line gives the results for the primary of a binary system. The second line gives the orbital period of the satellite and the maximum attenuation. The phase angle is given for the first and last date. If preceded by an asterisk, the phase angle reached an extrema during the period. L_{PAB} and B_{PAB} are the approximate phase angle bisector longitude/latitude at mid-date range (see Harris et al., 1984). Grp is the asteroid family/group (Warner et al., 2009).

Observatory (MPC code)	Telescope	CCD	Filter	Observed Asteroids (#Sessions)
Astronomical Observatory of the University of Siena(K54)	0.30-m MCT f/5.6	SBIG STL-6303e(bin 2x2)	Rc,C	397(1), 929(3), 58(1), 1660(3), 1589(1), 857713(4)
HOB Astronomical Observatory (L63)	0.20-m SCT f/6.0	ATIK 383L+	Rc,C	397(2), 1756(3). 58(2), 2015 RN35(1)
GiaGa Observatory (203)	0.36-m SCT f/5.8	MORAVIAN G2-3200	Rc	397(1), 929(2)
Osservatorio Astronomico Margherita Hack (A57)	0.35-m SCT f/8.3	SBIG ST10XME (bin 2x2)	B,V, Rc	929(1), 58(1), 1589(1)
Iota Scorpii(K78)	0.40-m RCT f/8.0	SBIG STXL-6303e (bin 2x2)	V,Rc	397(1), 1589(1)
Osservatorio Serafino Zani (130)	0.40-m RCT f/5.8	SBIG ST8 XME (bin 2x2)	C	397(2)
San Marco Astronomical Observatory (L78)	0.25-m RCT f/8.0	ATIK 383L+ (bin 2x2)	C	397(1), 2015 RN35(1)
Osservatorio Astronomico Nastro Verde (C82)	0.35-m SCT f/6.3	SBIG ST10XME (bin 2x2)	C	1589(1), 2015 RN35(1)
M57 (K38)	0.35-m RCT f/5.5	SBIG STT1603ME	Rc	397(1)

Table II. Observing Instrumentations. MCT: Maksutov-Cassegrain, NRT: Newtonian Reflector, RCT: Ritchey-Chretien, SCT: Schmidt-Cassegrain.

the LCDB. Some discrepancies in the lightcurve could indicate the presence of a tumbling nature.

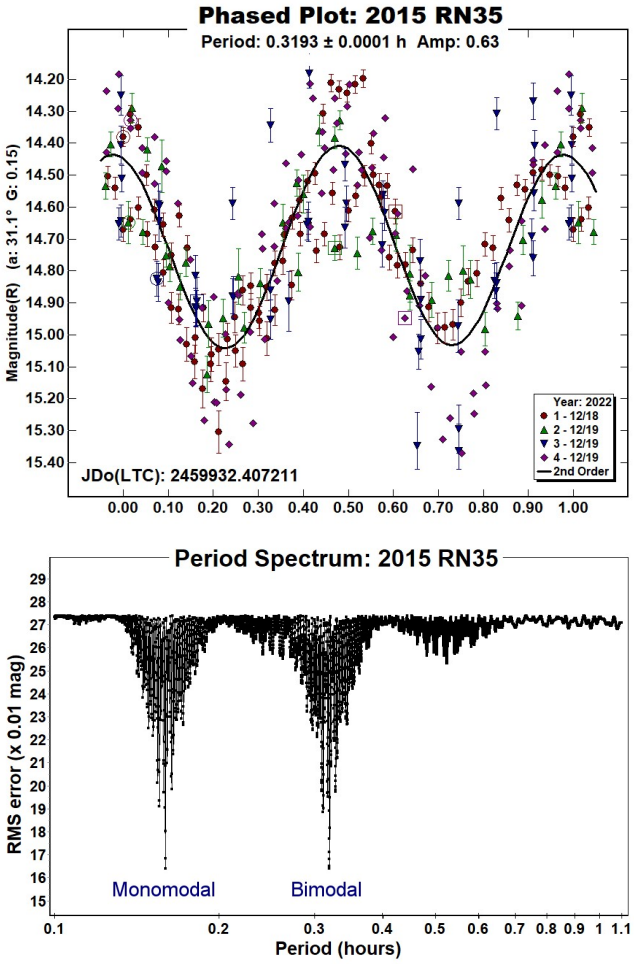

References

Bus, S.J.; Binzel, R.P. (2002), "Phase II of the Small Main-Belt Asteroid Spectroscopic Survey - A Feature-Based Taxonomy." *Icarus* **158**, 146-177.

Harris, A.W.; Young, J.W.; Scaltriti, F.; Zappala, V. (1984). "Lightcurves and phase relations of the asteroids 82 Alkmene and 444 Gyptis." *Icarus* **57**, 251-258.

Shevchenko, V.G.; Lupishko, D.F. (1998). "Optical properties of Asteroids from Photometric Data." *Solar System Research*, **32**, 220-232.

UAI (2022). "Unione Astrofili Italiani" web site. *https://www.uai.it*

Warner, B.D.; Harris, A.W.; Pravec, P. (2009) "The asteroid lightcurve database." *Icarus* **202**, 134-146. Updated 2023 January. *https://minplanobs.org/alcdef/index.php*

Warner, B.D. (2021). MPO Software, MPO Canopus v10.8.5.0. Bdw Publishing. *http://minorplanetobserver.com*

LIGHTCURVE PHOTOMETRY OPPORTUNITIES: 2023 APRIL-JUNE

Brian D. Warner
Center for Solar System Studies (CS3)
446 Sycamore Ave.
Eaton, CO 80615 USA
brian@MinPlanObs.org

Alan W. Harris
Center for Solar System Studies (CS3)
La Cañada, CA 91011-3364 USA

Josef Ďurech
Astronomical Institute
Charles University
18000 Prague, CZECH REPUBLIC
durech@sirrah.troja.mff.cuni.cz

Lance A.M. Benner
Jet Propulsion Laboratory
Pasadena, CA 91109-8099 USA
lance.benner@jpl.nasa.gov

We present lists of asteroid photometry opportunities for objects reaching a favorable apparition and have no or poorly-defined lightcurve parameters. Additional data on these objects will help with shape and spin axis modeling using lightcurve inversion. The "Radar-Optical Opportunities" section includes a list of potential radar targets as well as some that might be in critical need of astrometric data.

We present several lists of asteroids that are prime targets for photometry and/or astrometry during the period 2023 April through June. The "Radar-Optical Opportunities" section provides an expanded list of potential NEA targets, many of which are planned or good candidates for radar observations.

In the first three sets of tables, "Dec" is the declination and "U" is the quality code of the lightcurve. See the latest asteroid lightcurve data base (LCDB from here on; Warner et al., 2009) documentation for an explanation of the U code:

http://www.minorplanet.info/lightcurvedatabase.html

The ephemeris generator on the MinorPlanet.info web site allows creating custom lists for objects reaching V ≤ 18.0 during any month in the current year and up to five years in the future, e.g., limiting the results by magnitude and declination, family, and more.

https://www.minorplanet.info/php/callopplcdbquery.php

We refer you to past articles, e.g., Warner et al. (2021a; 2021b) for more detailed discussions about the individual lists and points of advice regarding observations for objects in each list.

Once you've obtained and analyzed your data, it's important to publish your results. Papers appearing in the *Minor Planet Bulletin* are indexed in the Astrophysical Data System (ADS) and so can be referenced by others in subsequent papers. It's also important to make the data available at least on a personal website or upon request. We urge you to consider submitting your raw data to the ALCDEF database. This can be accessed for uploading and downloading data at

http://www.alcdef.org

The database contains almost 10.2 million observations for 24,075 objects (as of 2022 October 5), making it one of the more useful sources for raw data of *dense* time-series asteroid photometry.

Lightcurve/Photometry Opportunities

Objects with U = 3- or 3 are excluded from this list since they will likely appear in the list for shape and spin axis modeling. Those asteroids rated U = 1 or have only a lower limit on the period, should be given higher priority over those rated U = 2 or 2+. On the other hand, do not overlook asteroids with U = 2/2+ on the assumption that the period is sufficiently established. Regardless, do not let the existing period influence your analysis since even highly-rated result have been proven wrong at times. Note that the lightcurve amplitude in the tables could be more or less than what's given. Use the listing only as a guide.

All objects are reaching one of their five brightest apparitions from 1995-2050. Bold text indicates a near-Earth asteroid (NEA).

		Brightest			LCDB Data		
Number	Name	Date	Mag	Dec	Period	Amp	U
2388	Gase	04 02.5	15.0	-8	26.3	0.48	1
7676	1995 WN8	04 02.5	15.9	+10	21.61	0.19	2+
23552	1994 NB	04 03.3	15.8	+37	3.629	0.36-0.45	2
21946	1999 VD138	04 05.4	15.9	-17	2.141	0.06	1
7116	Mentall	04 08.4	16.0	+4	6.489	0.11	2+
3666	Holman	04 09.4	16.0	-4	35.531		2-
5606	Muramatsu	04 09.9	15.3	-3	4.91	0.06	2
5702	Morando	04 09.9	15.6	-12	9.5	0.62	2+
4137	Crabtree	04 10.0	15.8	-10	13.662	0.25	1+
3138	Ciney	04 12.4	15.4	-12	113	0.48-0.56	2+
4993	Cossard	04 12.5	15.9	-6	48.26		2-
5549	Bobstefanik	04 15.2	16.0	-19	3.18	0.16	2
1030	Vitja	04 17.0	14.1	-3	7.749	0.21-0.35	2
4033	Yatsugatake	04 24.9	15.6	-11	5.691		2-
5073	Junttura	04 27.0	15.2	-18	6.1	0.13	1+
2856	Roser	04 27.3	15.4	-19	13.73	0.49	2+
1039	Sonneberga	04 27.8	14.6	-14	34.2	0.41	2
5826	Bradstreet	04 29.9	15.7	-11	5.55	0.54-0.63	2
6139	Naomi	04 30.6	15.3	-31	21.35	0.20	2+
11828	Vargha	05 01.3	16.0	-28	10.518	0.53	2
3316	Herzberg	05 05.7	15.9	-11	9.6	0.1	1
12424	1995 VM	05 05.7	16.0	-8	173.772	0.81-1.05	2
40429	1999 RL27	05 09.5	15.6	-23	430	0.81	2-
1462	Zamenhof	05 10.0	14.9	-18	10.4	0.15-0.30	2
5877	Toshimaihara	05 11.4	16.0	+2	8.91	0.09	2
23080	1999 XH100	05 13.6	15.9	-6	3.063	0.17	2
6193	Manabe	05 15.2	15.4	-35	3.244	0.13	2
11129	Hayachine	05 16.6	15.9	-19	17.6	0.22	2-
10846	1995 AW2	05 17.1	15.8	-21	4.685	0.09	2
1574	Meyer	05 18.9	14.8	-22	12.64	0.12-0.19	2
67681	2000 SH293	05 24.6	15.2	-17	19.847	0.53-0.57	2
4085	Weir	05 25.4	15.1	-19	14.602	0.18-0.39	2
1753	Mieke	05 26.5	14.9	-23	8.8	0.2	2
5238	Naozane	05 30.3	15.4	-18	88.775	0.25	2
7611	Hashitatsu	06 10.3	15.6	-16	9.806	0.17	2
4644	Oumu	06 10.7	15.2	-37	84.24	0.59	2
5916	van der Woude	06 11.5	15.0	-22	5.855	0.09	2
49389	1998 XS20	06 12.2	15.4	-39	7.138	0.41	2
17430	1989 KF	06 14.8	15.7	-23	2.227	0.08	1
11597	1995 KL1	06 16.7	15.6	-55	127.695	0.40	2
4058	Cecilgreen	06 16.8	15.4	-30	7.34	0.15-0.25	2
467336	**2002 LT38**	**06 19.2**	**15.2**	**-6**	**21.8**	**1.16**	**2+**
3563	Canterbury	06 21.4	15.3	-23	15.553	0.61	2
42273	2001 QO245	06 21.7	15.6	-22	19.01	0.24	2+
7289	Kamegamori	06 22.7	15.8	-34	3.831	0.73	2
6234	Sheilawolfman	06 22.9	15.3	-32	11.784	0.75	2
9065	1993 FN1	06 23.3	15.6	-9	3.064	0.19	2
7124	Glinos	06 25.1	15.4	-24	29.31	0.42	2
30800	1989 ST	06 26.3	15.6	-27	2.74	0.12-0.14	2
2880	Nihondaira	06 27.8	14.2	-34	17.97	0.22-0.75	2
1582	Martir	06 28.0	15.1	-24	12.372	0.31-0.46	2
6499	Michiko	06 29.8	15.5	-33	6.004	0.57-0.74	2
2259	Sofievka	06 30.0	13.8	-24	31.6	0.10-0.11	2
2127	Tanya	06 30.7	15.4	-20	7.854	0.18-0.40	2

Low Phase Angle Opportunities

The Low Phase Angle list includes asteroids that reach very low phase angles ($\alpha < 1°$). The "α" column is the minimum solar phase angle for the asteroid. Getting accurate, calibrated measurements (usually V band) at or very near the day of opposition can provide important information for those studying the "opposition effect." Use the on-line query form for the LCDB to get more details about a specific asteroid.

https://www.minorplanet.info/php/callopplcdbquery.php

The best chance of success comes with covering at least half a cycle a night, meaning periods generally < 16 h, when working objects with low amplitude. Objects with large amplitudes and/or long periods are much more difficult for phase angle studies since, for proper analysis, the data must be reduced to the average magnitude of the asteroid for each night. Refer to Harris et al. (1989) for the details of the analysis procedure.

As an aside, it is arguably better for physical interpretation (e.g., *G* value versus albedo) to use the maximum light rather than mean level to find the phase slope parameter (*G*), which better models the behavior of a spherical object of the same albedo, but it can produce significantly different values for both *H* and *G* versus using average light, which is the method used for values listed by the Minor Planet Center. Using and reporting the results of both methods can provide additional insights into the physical properties of an asteroid.

The International Astronomical Union (IAU) has adopted a new system, H-G_{12}, introduced by Muinonen et al. (2010). It will be some years before H-G_{12} becomes widely used, and hopefully not until a discontinuity flaw in the G_{12} function has been fixed. This discontinuity results in false "clusters" or "holes" in the solution density and makes it impossible to draw accurate conclusions.

We strongly encourage obtaining data as close to 0° as possible, then every 1-2° out to 7°, below which the curve tends to be non-linear due to the opposition effect. From 7° out to about 30°, observations at 3-6° intervals should be sufficient. Coverage beyond 50° or so is not generally helpful since the H-G system is best defined with data from 0-30°.

It's important to emphasize that all observations should (must) be made using high-quality catalogs to set the comparison star magnitudes. These include ATLAS, Pan-STARRS, SkyMapper, and Gaia2/3. Catalogs such as CMC-15, APASS, or the MPOSC from *MPO Canopus* have too high of significant systematic errors.

Also important is that that there are sufficient data from each observing run such that their location can be found on a combined, phased lightcurve derived from two or more nights obtained *near the same phase angle.* If necessary, the magnitudes for a given run should be adjusted so that they correspond to mid-light of the combined lightcurve. This goes back to the H-G system being based on average, not maximum or minimum light.

The asteroid magnitudes are brighter than in others lists because higher precision is required and the asteroid may be a full magnitude or fainter when it reaches phase angles out to 20-30°.

Num	Name	Date	α	V	Dec	Period	Amp	U
874	Rotraut	04	04.0	0.32	14.0	-5	14.297	0.24 0.29 3-
126	Velleda	04	10.7	0.16	12.5	-8	5.367	0.07 0.22 3
102	Miriam	04	13.4	0.33	13.8	-10	23.613	0.04 0.14 3
162	Laurentia	04	21.0	0.33	12.3	-11	11.869	0.28 0.37 3
158	Koronis	04	28.6	0.45	13.2	-15	14.218	0.28 0.43 3
168	Sibylla	05	01.2	0.45	13.1	-13	47.009	0.16 3
74	Galatea	05	02.9	0.75	13.4	-13	17.268	0.06 0.16 3
32	Pomona	05	04.1	0.20	10.4	-15	9.448	0.13 0.33 3
33	Polyhymnia	05	10.8	0.61	12.6	-19	18.608	0.12 0.25 3
245	Vera	05	11.9	0.36	12.9	-17	14.38	0.26 3
266	Aline	05	12.3	0.53	13.2	-20	13.018	0.07 0.10 3
150	Nuwa	05	19.3	0.55	12.8	-18	8.135	0.08 0.31 3
215	Oenone	05	22.0	0.56	13.1	-22	27.937	0.18 0.20 3
423	Diotima	05	23.1	0.82	11.3	-18	4.775	0.05 0.20 3
19	Fortuna	05	26.7	0.51	10.9	-20	7.443	0.23 0.30 3
937	Bethgea	05	29.4	0.34	13.3	-21	7.539	0.12 0.19 3
91	Aegina	05	30.6	0.99	12.7	-24	6.025	0.12 0.27 3
441	Bathilde	06	02.0	0.19	12.6	-23	10.446	0.08 0.20 3
897	Lysistrata	06	05.1	0.84	12.9	-24	11.34	0.11 0.14 3-
774	Armor	06	07.0	0.36	12.1	-22	25.194	0.11 0.34 3
104	Klymene	06	07.3	0.61	13.6	-25	8.984	0.26 0.3 3
76	Freia	06	13.4	0.62	13.5	-21	9.973	0.05 0.33 3
243	Ida	06	15.8	0.51	13.9	-25	4.634	0.45 0.86 3
20	Massalia	06	16.4	0.38	10.0	-22	8.098	0.17 0.27 3
146	Lucina	06	17.6	0.32	11.5	-24	18.557	0.08 0.15 3
171	Ophelia	06	22.9	0.20	13.0	-23	6.665	0.14 0.46 3
431	Nephele	06	27.0	0.39	12.6	-22	13.530	0.03 0.23 3
86	Semele	06	30.0	0.44	13.3	-25	16.634	0.10 0.18 3
2259	Sofievka	06	30.0	0.25	13.8	-24	31.6	0.10 0.11 2

Shape/Spin Modeling Opportunities

Those doing work for modeling should contact Josef Ďurech at the email address above. If looking to add lightcurves for objects with existing models, visit the Database of Asteroid Models from Inversion Techniques (DAMIT) web site.

https://astro.troja.mff.cuni.cz/projects/damit/

Additional lightcurves could lead to the asteroid being added to or improving one in DAMIT, thus increasing the total number of asteroids with spin axis and shape models.

Included in the list below are objects that:

1. Are rated U = 3– or 3 in the LCDB.
2. Do not have reported pole in the LCDB Summary table.
3. Have at least three entries in the Details table of the LCDB where the lightcurve is rated U ≥ 2.

The caveat for condition #3 is that no check was made to see if the lightcurves are from the same apparition or if the phase angle bisector longitudes differ significantly from the upcoming apparition. The last check is often not possible because the LCDB does not list the approximate date of observations for all details records. Including that information is an on-going project.

With the wide use of sparse data from the surveys for modeling that produces hundreds of statistically valid poles and shapes, the need for data for main-belt objects is not what it used to be. The best use of observing time might be to concentrate on near-Earth asteroids, or on asteroids where the only period was derived from sparse data, which can help eliminate alias periods. The latter targets are usually flagged with an 'S' on the LCDB summary line. Regardless, it's a good idea to visit the DAMIT site and see what it has, if anything, on the target(s) you've picked for observations.

Objects in **bold** text are at a favorable apparition. Those in italic text are near-Earth objects.

		Brightest			LCDB Data		
Num	Name	Date	Mag	Dec	Period	Amp	U
49	Pales	04 01.0	13.0	-8	20.705	0.17-0.19	3
735	Marghanna	04 03.6	14.9	+7	20.625	0.11-0.13	3
2535	Hameenlinna	04 05.3	14.6	-4	3.231	0.07-0.11	3
3397	**Leyla**	**04 10.3**	**15.3**	**-3**	**3.098**	**0.29-0.40**	**3**
2575	Bulgaria	04 10.6	14.9	-15	8.605	0.43-0.62	3
126	Velleda	04 10.8	12.4	-8	5.367	0.07-0.22	3
102	Miriam	04 13.4	13.8	-10	23.613	0.04-0.14	3
7965	Katsuhiko	04 18.5	14.9	-55	5.39	0.26-0.50	3
1929	Kollaa	04 19.2	15.3	-3	2.989	0.20-0.22	3
2602	**Moore**	**04 23.5**	**15.1**	**-4**	**3.467**	**0.15-0.34**	**3**
1139	Atami	04 23.8	15.2	-13	27.446	0.19-0.45	3
5175	**Ables**	**04 30.0**	**15.1**	**-24**	**2.686**	**0.05-0.33**	**3**
284	Amalia	05 01.3	12.3	-18	8.545	0.13-0.18	3
1071	Brita	05 04.0	14.5	-14	5.817	0.12-0.23	3
294	Felicia	05 04.9	14.6	-7	10.423	0.19-0.24	3
177	Irma	05 06.1	14.3	-18	13.856	0.24-0.37	3
6249	Jennifer	05 06.5	15.2	-13	4.957	0.06-0.55	3
4417	Lecar	05 08.1	15.3	-28	3.176	0.17-0.38	3
3680	Sasha	05 08.7	15.5	-21	5.815	0.30-0.35	3
554	Peraga	05 10.6	12.7	-22	13.713	0.11-0.28	3
194386	***2001 VG5***	***05 11.3***	***14.7***	***-51***	***6.38***	***0.38-0.77***	***3***
266	Aline	05 12.4	13.1	-20	13.018	0.07-0.10	3
3443	Leetsungdao	05 18.3	15.1	+2	3.439	0.23-0.47	3
2460	Mitlincoln	05 19.1	15.3	-14	3.007	0.03-0.20	3
200	Dynamene	05 19.9	12.8	-30	37.394	0.06-0.10	3
1015	Christa	05 22.4	14.3	-9	11.23	0.12-0.20	3-
1717	Arlon	05 23.1	15.3	-31	5.148	0.06-0.12	3
1120	Cannonia	05 24.9	15.0	-14	3.816	0.15-0.21	3
947	Monterosa	05 26.5	14.4	-24	5.164	0.08-0.23	3-
1587	Kahrstedt	05 30.2	15.4	-33	7.971	0.12-0.24	3
348	May	06 02.1	13.8	-17	7.381	0.14-0.16	3
2195	Tengstrom	06 02.4	15.3	-18	2.821	0.17-0.45	3
5452	**1937 NN**	**06 02.6**	**14.0**	**-33**	**3.256**	**0.37-0.50**	**3**
357	Ninina	06 03.4	13.9	-3	35.983	0.11-0.24	3
547	Praxedis	06 08.6	14.5	-1	9.105	0.04-0.12	3
1166	Sakuntala	06 08.9	13.0	-3	6.292	0.24-0.40	3
1005	Arago	06 09.6	15.3	-49	8.789	0.22-0.25	3
3248	Farinella	06 10.0	15.3	-38	6.675	0.12-0.25	3
1700	Zvezdara	06 12.2	15.5	-31	9.114	0.10-0.14	3
1041	Asta	06 13.2	15.0	-31	7.978	0.12-0.16	3
4148	McCartney	06 13.2	15.3	-32	20.737	0.14-0.27	3
504	Cora	06 14.7	13.5	-15	7.587	0.15-0.27	3
1817	**Katanga**	**06 15.6**	**12.8**	**-18**	**8.481**	**0.22-0.30**	**3**
414	Liriope	06 16.7	14.9	-18	11.005	0.10-0.16	3
15491	1999 CW85	06 17.7	15.3	-33	3.902	0.10-0.13	3
1242	Zambesia	06 19.0	14.8	-38	17.315	0.11-0.24	3
109	Felicitas	06 22.3	13.8	-35	13.191	0.06-0.17	3
431	Nephele	06 27.1	12.6	-22	13.53	0.03-0.23	3

Radar-Optical Opportunities

Table I below gives a list of near-Earth asteroids reaching maximum brightness for the current quarter-year based on calculations by Warner. We switched to this presentation in lieu of ephemerides for reasons outlined in the 2021 October-December opportunities paper (Warner et al., 2021b), which centered on the potential problems with ephemerides generated several months before publication.

The initial list of targets started using the planning tool at

https://www.minorplanet.info/php/callopplcdbquery.php

where the search was limited to near-Earth asteroids only that were V ≤ 18 for at least part of the quarter.

The list was then filtered to include objects that might be targets for the Goldstone radar facility or, if it were still operational, the Arecibo radar. This was based on the calculated radar SNR using

http://www.naic.edu/~eriverav/scripts/index.php

Num	Name	H	Diam	BDate	BMag	BDec	Period	AMn	AMx	U	A	G	Notes
436774	**2012 KY3**	**18.47**	**0.600**	**04 16.4**	**14.2**	**-83**					**2200**	**640**	
1862	Apollo	16.11	1.780	04 19.1	15.1	-2	3.065	0.15	1.15	3	-	-	Data to refine YORP See LCDB for numerous periods.
	2006 HV5	**19.7**	**0.307**	**04 24.5**	**15.4**	**59**					**10750**	**3000**	**PHA**
488453	**1994 XD**	**19.3**	**0.412**	**06 10.6**	**13.5**	**38**	**2.7365**		**0.08**	**3-**	**7600**	**2200**	**Binary (Benner et al. 2005)**
452334	**2001 LB**	**21.06**	**0.182**	**06 11.6**	**16.5**	**-26**					**12**		
	2020 DB5	**19.3**	**0.410**	**06 15.0**	**13.9**	**-43**					**1610**	**460**	**PHA**
152685	1998 MZ	19.3	0.403	06 19.0	16.9	-18					7		
467336	**2002 LT38**	**20.6**	**0.225**	**06 19.2**	**15.2**	**-6**	**21.8**		**1.16**	**2+**	**480**	**140**	**PHA/NHATS Warner (2017)**

Table I. A list of near-Earth asteroids reaching brightest in 2023 April-June. PHA: potentially hazardous asteroid. NHATS: Near-Earth Object Human Space Flight Accessible Targets Study. Diameters are based on p_V = 0.20. The Date, V, and Dec columns are the mm/dd.d, approximate magnitude, and declination when at brightest. Amp is the single or range of amplitudes. The A and G columns are the approximate SNRs for an assumed full-power Arecibo (not operational) and Goldstone radars. The references in the Notes column are those for the reported periods and amplitudes.

and assuming a rotation period of 4 hours (2 hours if $D \leq 200$ m) if a period was not given in the asteroid lightcurve database (LCDB; Warner et al., 2009). The SNR values are estimates only and assume that the radar is fully functional.

If an asteroid was on the list but failed the SNR test, we checked if it might be a suitable target for radar and/or photometry sometime through 2050. If so, it was kept on the list to encourage physical and astrometric observations during the current apparition. In most of those cases, the SNR values in the "A" and "G" columns are not for the current quarter but the year given in the Notes column. If a better apparition is forthcoming through 2050, the Notes column in Table I contains SNR values for that time.

The final step was to cross-reference our list with that found on the Goldstone planned targets schedule at

http://echo.jpl.nasa.gov/asteroids/goldstone_asteroid_schedule.html

In Table I, objects in bold text are on the Goldstone proposed observing list as of early 2022 October.

It's important to note that the final list in Table I is based on *known* targets and orbital elements when it was prepared. It is common for newly discovered objects to move in or out of the list. We recommend that you keep up with the latest discoveries by using the Minor Planet Center observing tools.

In particular, monitor NEAs and be flexible with your observing program. In some cases, you may have only 1-3 days when the asteroid is within reach of your equipment. Be sure to keep in touch with the radar team (through Benner's email or their Facebook or Twitter accounts) if you get data. The team may not always be observing the target but your initial results may change their plans. In all cases, your efforts are greatly appreciated.

For observation planning, use these two sites

MPC: *http://www.minorplanetcenter.net/iau/MPEph/MPEph.html*
JPL: *http://ssd.jpl.nasa.gov/?horizons*

Cross-check the ephemerides from the two sites just in case there is discrepancy that might have you imaging an empty sky.

About YORP Acceleration

Near-Earth asteroids are particularly sensitive to YORP acceleration. YORP (Yarkovsky-O'Keefe-Radzievskii-Paddack; Rubincam, 2000) is the asymmetric thermal re-radiation of sunlight that can cause an asteroid's rotation period to increase or decrease. High precision lightcurves at multiple apparitions can be used to model the asteroid's *sidereal* rotation period and see if it's changing.

It usually takes four apparitions to have sufficient data to determine if the asteroid rotation rate is changing under the influence of YORP. This is why observing an asteroid that already has a well-known period remains a valuable use of telescope time. It is even more so when considering the BYORP (binary-YORP) effect among binary asteroids that has stabilized the spin so that acceleration of the primary body is not the same as if it would be if there were no satellite.

The Quarterly Target List Table

The Table I columns are

Num	Asteroid number, if any.
Name	Name assigned by the MPC.
H	Absolute magnitude from MPCOrb.
Dkm	Diameter (km) assuming $p_V = 0.2$.
Date	Date (mm dd.d) of brightest magnitude.
V	Approximate V magnitude at brightest.
Dec	Approximate declination at brightest.
Period	Synodic rotation period from summary line in the LCDB summary table.
Amp	Amplitude range (or single value) of reported lightcurves.
U	LCDB U (solution quality) from 1 (probably wrong) to 3 (secure).
A	Approximate SNR for Arecibo (if operational and at full power).
G	Approximate SNR for Goldstone radar at full power.
Notes	Comments about the object.

"PHA" is a potentially hazardous asteroid. NHATS is for "Near-Earth Object Human Space Flight Accessible Targets Study." Presume that that astrometry and photometry have been requested to support Goldstone observations. The sources for the rotation period are given in the Notes column. If none are qualified with a specific period, then the periods from multiple sources were in general agreement. Higher priority should be given to those where the current apparition is the last one V ≤ 18 through 2050 or several years to come.

References

Benner, L.A.M.; Nolan, M.C.; Ostro, S.J.; Giorgini, J.D.; Margot, J.L.; Magri, C. (2005). "1994 XD." *IAUC* **8563**.

Harris, A.W.; Young, J.W.; Bowell, E.; Martin, L.J.; Millis, R.L.; Poutanen, M.; Scaltriti, F.; Zappala, V.; Schober, H.J.; Debehogne, H.; Zeigler, K.W. (1989). "Photoelectric Observations of Asteroids 3, 24, 60, 261, and 863." *Icarus* **77**, 171-186.

Muinonen, K.; Belskaya, I.N.; Cellino, A.; Delbò, M.; Levasseur-Regourd, A.-C.; Penttilä, A.; Tedesco, E.F. (2010). "A three-parameter magnitude phase function for asteroids." *Icarus* **209**, 542-555.

Rubincam, D.P. (2000). "Radiative Spin-up and Spin-down of Small Asteroids." *Icarus* **148**, 2-11.

Warner, B.D. (2017). "Near-Earth Asteroid Lightcurve Analysis at CS3-Palmer Divide Station: 2016 July-September." *Minor Planet Bul*. **44**, 22-36.

Warner, B.D.; Harris, A.W.; Pravec, P. (2009). "The Asteroid Lightcurve Database." *Icarus* **202**, 134-146. Updated 2021 Dec. *http://www.minorplanet.info/lightcurvedatabase.html*

Warner, B.D.; Harris, A.W.; Durech, J.; Benner, L.A.M. (2021a). "Lightcurve Photometry Opportunities" 2021 January-March." *Minor Planet Bull.* **48**, 89-97.

Warner, B.D.; Harris, A.W.; Durech, J.; Benner, L.A.M. (2021b). "Lightcurve Photometry Opportunities" 2021 October-December." *Minor Planet Bull.* **48**, 406-410.

IN THIS ISSUE

This list gives those asteroids in this issue for which physical observations (excluding astrometric only) were made. This includes lightcurves, color index, and H-G determinations, etc. In some cases, no specific results are reported due to a lack of or poor-quality data. The page number is for the first page of the paper mentioning the asteroid. EP is the "go to page" value in the electronic version.

Number	Name	EP	Page
57	Mnemosyne	49	162
58	Concordia	60	173
128	Nemesis	4	117
397	Vienna	60	173
478	Tergeste	38	151
603	Timandra	8	121
622	Esther	34	147
645	Agrippina	49	162
783	Nora	34	147
879	Ricarda	34	147
904	Rockefellia	57	170
929	Algunde	60	173
960	Birgit	34	147
960	Birgit	38	151
987	Wallia	49	162
1048	Feodosia	34	147
1103	Sequoia	51	164
1143	Odysseus	44	157
1399	Teneriffa	5	118
1399	Teneriffa	57	170
1497	Tampere	12	125
1543	Bourgeois	34	147
1543	Bourgeois	38	151
1543	Bourgeois	57	170
1589	Fanatica	29	142
1589	Fanatica	60	173
1636	Porter	29	142
1660	Wood	60	173
1690	Mayrhofer	38	151
1756	Giacobini	29	142
1756	Giacobini	60	173
1780	Kippes	38	151
1857	Parchomenko	29	142
1946	Walraven	38	151
2035	Stearns	34	147
2049	Grietje	51	164
2052	Tamriko	34	147
2085	Henan	38	151
2151	Hadwiger	29	142
2243	Lonnrot	1	114
2243	Lonnrot	29	142
2243	Lonnrot	34	147
2820	Iisalmi	29	142
3166	Klondike	38	151
3180	Morgan	29	142
3229	Solnhofen	38	151
3287	Olmstead	44	157
3382	Cassidy	29	142
3385	Bronnina	29	142
3560	Chenqian	38	151
4060	Deipylos	44	157
4338	Velez	29	142
4376	Shigemori	7	120
4376	Shigemori	34	147
4429	Chinmoy	34	147
4489	Dracius	44	157
4497	Taguchi	29	142
4538	Vishyanand	34	147
5076	Lebedev-Kumach	57	170
5123	Cynus	44	157
5439	Couturier	51	164
5841	Stone	51	164
6025	Naotosato	57	170
6363	Doggett	29	142
6901	Roybishop	51	164
7357	1995 UJ7	29	142
7445	Trajanus	44	157
8548	Sumizihara	29	142
10044	Squyres	38	151
10182	Junkobiwaki	44	157
11671	1998 BG4	3	116
12746	Yumeginga	38	151
20602	1999 RC198	57	170
22070	2000 AN106	51	164
50379	2000 CB89	29	142
65803	Didymos	15	128
70411	1999 SF3	29	142
85713	1998 SS49	51	164
85713	1998 SS49	60	173
86829	2000 GR146	15	128
161989	Cacus	15	128
523823	2015 BG311	51	164
	2003 EM1	18	131
	2008 EZ7	18	131
	2011 EY11	18	131
	2011 MD	18	131
	2012 FP35	18	131
	2015 RN35	60	173
	2016 GP221	18	131
	2017 TE5	18	131
	2018 SM1	18	131
	2018 ST1	18	131
	2021 LO2	18	131
	2022 TG	18	131
	2022 TG1	13	126
	2022 TG1	18	131
	2022 UR4	13	126
	2022 VL1	18	131
	2022 WG5	18	131

THE MINOR PLANET BULLETIN (ISSN 1052-8091) is the quarterly journal of the Minor Planets Section of the Association of Lunar and Planetary Observers (ALPO, http://www.alpo-astronomy.org). Current and most recent issues of the *MPB* are available on line, free of charge from:

https://mpbulletin.org/

The Minor Planets Section is directed by its Coordinator, Prof. Frederick Pilcher, 4438 Organ Mesa Loop, Las Cruces, NM 88011 USA (fpilcher35@gmail.com). Robert Stephens (rstephens@foxandstephens.com) serves as Associate Coordinator. Dr. Alan W. Harris (MoreData! Inc.; harrisaw@colorado.edu), and Dr. Petr Pravec (Ondrejov Observatory; ppravec@asu.cas.cz) serve as Scientific Advisors. The Asteroid Photometry Coordinator is Brian D. Warner (Center for Solar System Studies), Palmer Divide Observatory, 446 Sycamore Ave., Eaton, CO 80615 USA (brian@MinorPlanetObserver.com).

The Minor Planet Bulletin is edited by Professor Richard P. Binzel, MIT 54-410, 77 Massachusetts Ave, Cambridge, MA 02139 USA (rpb@mit.edu). Brian D. Warner (address above) is Associate Editor. Assistant Editors are Dr. David Polishook, Department of Earth and Planetary Sciences, Weizmann Institute of Science (david.polishook@weizmann.ac.il) and Dr. Melissa Hayes-Gehrke, Department of Astronomy, University of Maryland (mhayesge@umd.edu). The *MPB* is produced by Dr. Pedro A. Valdés Sada (psada2@ix.netcom.com).

Effective with Volume 50, the *Minor Planet Bulletin* is an electronic-only journal; print subscriptions are no longer available. In addition to the free electronic download of the *MPB* as noted above, electronic retrieval of all *Minor Planet Bulletin* articles (back to Volume 1, Issue Number 1) is available through the Astrophysical Data System:

http://www.adsabs.harvard.edu/

Authors should submit their manuscripts by electronic mail (rpb@mit.edu). Author instructions and a Microsoft Word template document are available at the web page given above. All materials must arrive by the deadline for each issue. Visual photometry observations, positional observations, any type of observation not covered above, and general information requests should be sent to the Coordinator.

* * * * *

The deadline for the next issue (50-3) is April 15, 2023. The deadline for issue 50-4 is July 15, 2023.

This page intentionally blank